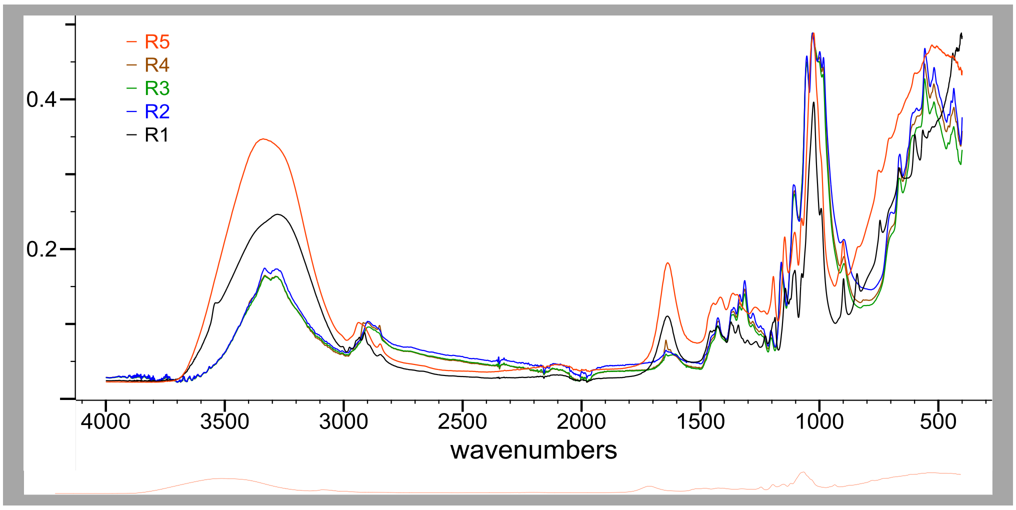

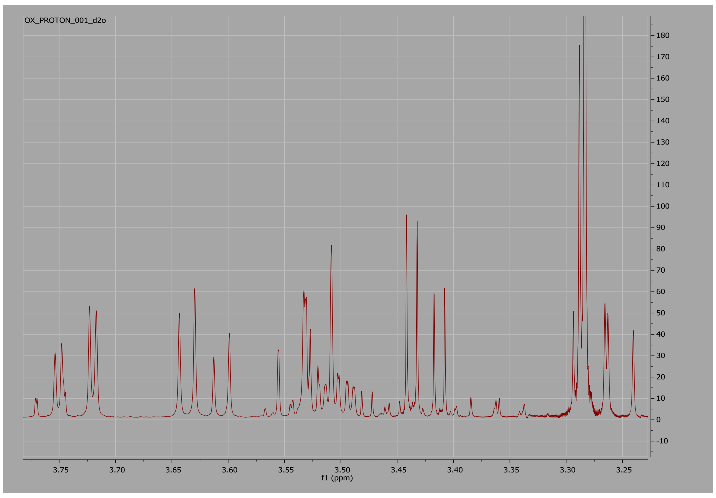

TEMPO Mediated Electrochemical Oxidation of Cellulose

Towards sustainable recycling of textile fibres

Master's thesis in Materials Chemistry and Nanotechnology

LISA ÅKERLUND

Department of Chemistry and Chemical Engineering
CHALMERS UNIVERSITY OF TECHNOLOGY
SP: Technical Research Institute of Sweden
Gothenburg, Sweden 2015

TEMPO mediated Electrochemical Oxidation of Cellulose

Towards sustainable recycling of textile fibres

LISA ÅKERLUND

Department of Chemistry and Chemical Engineering
CHALMERS UNIVERSITY OF TECHNOLOGY
Gothenburg, Sweden 2015

TEMPO mediated Electrochemical Oxidation of Cellulose
Towards sustainable recycling of textile fibres
LISA ÅKERLUND

Department of Chemistry and Chemical Engineering
Chalmers University of Technology
SE-412 96 Gothenburg
Sweden
Telephone + 46 (0)31-772 1000

Cover:
Top figure shows an FT-IR spectra that can be found on page 46.
Bottom figure shows an NMR spectra that can be found on page 35.

Reproservice
Gothenburg, Sweden 2015

Sammanfattning

Det ofullständiga kretslopp, vilket den nuvarande användningen av bomullsbaserade textilier utgör, är ett resultat av de betingelser som krävs för att lösa upp fibrerna. Antingen kan toxiska lösningsmedel användas, vilket är ett dåligt val när miljövänliga processer är önskvärda, eller joniska vätskor, vilka i dagsläget är dyra eftersom en stor mängd i förhållande till cellulosan krävs för att de skall fungera. Förutom upplösningen finns det även andra problem i återvinningsprocessen. Dessa är *nedbrytning av fibrer* på grund av användning, vilket kräver upplösning följt av våtspinning för att fibrerna skall återfå sin styrka[1], *heterogena material,* då bomullstyger ofta består av blandmaterial innehållandes t.ex. elastan och polyester, och slutligen innehållet av *tillsatsämnen*, från exempelvis tryck som måste avlägsnas, vilka alla är svåra utmaningar för att en fullständig återvinningsprocess skall uppnås.

För att få bukt med dessa problem behövs utveckling av en ny återvinningsmetod för cellulosafibrer där toxiska kemikalier undviks. Dessutom behöver kvaliteten på återvunna fibrer förbättras får att de skall återfå maximal kommersiell potential. Återvunna bomullsfibrer är åtråvärda i textilindustrin som ett billigt och miljövänligt material men det finns även stor potential inom andra områden, såsom inom produktion av nanocellulosa för diverse ändamål, exempelvis för vävnader och implantat eftersom ren cellulosa är biokompatibel och kan användas i kroppen.

I detta arbete har en TEMPO-medierad elektrokemisk process undersökts med målet att tillverka oxiderade material från cellulosa och cellulosalika substrat. En elektrokemisk uppsättning med ett tre-elektrodsystem användes tillsammans med ett program för att köra *amperometri (i-t kurva)*. Körningarna var mellan 1 och 24 timmar och potentialen som användes var 0,5-0,7 V. Som jämförelse utfördes standardexperiment med TEMPO-oxidation där halider användes som hjälpoxidanter. Resultaten från de senare experimenten visade inte på högre oxidation än med den elektrokemiska metoden. Vidare har resultaten analyserats med fast- och vätskefas-NMR, FT-IR och XPS. Oxidationstoppar hittades för prov som oxiderats under 24 timmar. Reaktionen behöver dock optimeras.

Abstract

The non-existent, closed loop, recycling of cellulosic textile fibres is a result of the problematic conditions needed to dissolve the fibres. The use of either toxic organic solvents, which are a bad choice for environmental reasons, or expensive ionic liquids (ILs), needed in large amount for the cellulose to be dissolved, are both choices far from perfect. Apart from the problematic dissolving, *fibre degradation* due to wear (which requires dissolving followed by wet spinning to regain its strength)[1], *heterogenous materials*, since cotton fabric is often mixed with other fibres such as elastane and polyester, and the *removal of additives,* which often are present in textile products (such as in prints and mixed fabric), are all challenging problems to solve.

To address stated problems, development of a novel recycling method for cellulosic textile fibres, without using harmful chemicals in any substantial amount, is needed. Further, the quality of recycled fibres needs to be improved in order for the fibres to regain full commercial potential. Recycled cotton fibres are eligible in the textile industry and are also of potential use within new areas, such as material for production of nanocellulosic materials, e.g. for tissue/implants since pure cellulose is biocompatible.

In this thesis, a TEMPO-mediated electrochemical process has been investigated with the aim of producing oxidized materials from cellulose or cellulose-like substrates. A three-electrode setup with an *amperometric i-t curve* program was used. The runs were between 1h and 24 h and the potential was set at 0.5-0.7 V. For comparison, a standard TEMPO-mediated oxidation was performed, using halides as cooxidants. Results were analyzed using solid- and liquid state NMR, FT-IR and XPS. For samples electrochemically oxidized during 24h, oxidation products were found, but the setup needs to be further investigated for optimization and the reaction conditions need to be longer to approach optimal conditions. The standard TEMPO-mediated oxidation did not result in higher oxidation than the electrochemical oxidation, with a conclusion that both reactions were performed too weak.

Acknowledgements

My supervisor Hanna de la Motte – For giving me the opportunity of performing this thesis.

My examiner Maria Abrahamsson – for giving me support and encouragement in critical stages of the work.

All my co-workers at Chalmers – For the warm and friendly atmosphere who makes me sad to leave this place! And not to forget, the occasional hallway dancing when energy levels are down.

Victor – For always believing in me.

Lisa Åkerlund, Gothenburg 2015

Contents

Introduction 1

Background 1

Motivation...1

Scope 2

Theory 3

Cellulose 3

Methyl-α-D-Glucopyranoside (MGP) 5

Oxidation methods 5

TEMPO 6

Activation of cellulose 8

Electrochemistry 8

Methods for preparation, characterization and analysis 10

Theoretical background to electrochemical reactions with electrolysis............10

Nuclear Magnetic Resonance Spectroscopy, NMR 13

Flash Chromatography...14

Infrared Spectroscopy, IR...16

X-ray Photoelectron Spectroscopy, XPS 17

Experimental 19

Materials 19

Experimental 1st part: TEMPO mediated electrochemical oxidation of cotton and MGP...21

Flash Chromatography...22

Experimental 2nd part: Revised setup of TEMPO mediated electrochemical oxidation of four substrates...22

Experimental 3rd part: TEMPO-mediated oxidation 23

Results 24

Optimizing experimental setup 24

Results from i-t voltammetry...26

Electrochemical experiments: 1st part 27

Electrochemical oxidation of different substrates 29

Short summary of electrolysis 30

Results from characterization methods....................30
  NMR....................31
FT-IR....................43
  Short summary of FT-IR characterization....................45
XPS....................46
  Short summary of XPS-characterization....................49
Discussion....................50
  NMR....................52
  FT-IR....................52
  XPS....................53
Conclusions....................54
Outlook....................56
References....................57

Appendix I: Electrochemical experiments

Appendix II: Liquid state NMR

List of abbreviations

DP	Degree of polymerization
MGP	Methyl-α-D-glucopyranoside
DMSO	Dimethyl sulfoxide
TEMPO	2,2,6,6-tetramethylpiperidine-1-oxyl
Mediator	“A chemical agent which carries out a process or reaction” or ”a protein that enhance and activate the functions of other proteins”
DCM	Dichloromethane
NMR	Nuclear Magnetic Resonance
TLC	Thin Layer Chromatography
FT-IR	Fourier Transformed Infrared Spectroscopy
XPS	X-ray Photoelectron Spectroscopy

Introduction

Background

This thesis is connected to two larger research projects; *MISTRA Future Fashion* and *Increased reactivity and applications for recycled cotton textiles by electrochemical oxidation techniques* (financed by Formas). MISTRA Future Fashion aims for a sustainable fashion industry and is divided into eight projects and this thesis belongs to subproject 5: *reuse, recycling and end of life issues* (of textiles). The focus on recycling seeks to develop and improve the conversion of textile fibres into new valuable materials. Existing methods are insufficient both by environmental- and economical standards, which makes it an important field of study.

Motivation

Cellulose is nature's most abundant macromolecule, being the structural component of plant cells. This natural resource has for long been used for fuel, clothing, paper, building materials and recently also in chemical and medical applications[2,3]. A large source to natural cellulose is cotton. The cotton industry has an annual production of 26 million tonnes[4] requiring 4 % ot the total cultivated area and as much as 11 % of the total pesticides used[5]. Additionally, this industry requires a massive amount of freshwater and energy. As the world population is growing, fibre demand continues to increase, which leads to several dilemmas; higher demand for cultivated land in food production, increased fresh water demand for drinking water and the energy consumption giving rise to CO_2-emissions which on long term decrease both the area possible for growing crops on and the accessible sources of fresh water.

With an increasing demand for cotton fibres, the improved recycling, quality and manageability of cellulose are extremely important factors for maintaining the fibres utility, improving its value and minimizing the effect on the planet. The status of these factors may have great impact on the cellulose based industries future as well as on the high consumption of energy- and water resources that cotton production is responsible for. By replacing new grown cotton with recycled textiles many of the stated problems could be revised.

Western countries need not be concerned about basic levels of *Maslows hierarchy of needs*. Environmental issues can therefore be allowed into consideration. In the search for how to bring about a green economy, recycling has recently become more trendy and is given a lot of interest in media. However, the common behaviour of wearing fashion goods for a single season after which it is classified as “out” is still predominant, and fibre to fibre (or *cradle to cradle*) recycled fashion would be a necessary contribution towards a modern and sustainable society. If we continue to use an unnecessary amount of resources that is not needed for our survival, how will it end up in 80 years’ time when world population is thought to have doubled[6]?

If the processability of cellulose would become easier, there is great potential to get a cheap and abundant source of natural fibres. Recyclable, high quality cellulosic materials have unlimited application areas if we can overcome stated barriers.

The above statements are all reasons for why I chose to do my master thesis work on trying to find an environmentally friendly way to recycle one of the most important natural resources from our planet; cellulose.

Scope

The main goal of this thesis was to develop a setup to achieve environmentally friendly electrochemical oxidation of cellulose, with a future goal of producing high quality recycled fibres. The questions I wanted to answer was:

How can environmentally friendly oxidation of cellulose be achieved?

And:

What is needed for the oxidation to be performed by electrochemistry?

Oxidation of cellulose converts hydroxyl groups to carbonyl or carboxyl groups, such as aldehydes and carboxylic acids. These groups increase the reactivity of cellulose fibres, which highly facilitates further processing. Additionally, enhanced reactivity makes it easier to crosslink the polymer, which increases its strength, or to perform defibrillation for production of other materials, such as nanocellulose.

Theory

Starting with an introduction to the main character of this thesis, cellulose, this chapter will further present available oxidation methods. Finally, analytical tools used for characterization of the substrates used in this work and their oxidized products will be explained briefly.

Cellulose

Cellulose is a polysaccharide, indispensable for plant cell walls by providing strength and structure. It is also the most abundant macromolecule of this planet, making up for more than 50 % of all available biomass. This biopolymer consists of glucose units connected by strong β(1→4)-glycosidic bond, which makes the chains straight and facilitates close packing between them, resulting in a high degree of crystallinity.[7]

The cellulose chains, which are between 3000-15000 units long for naturally occuring cellulose and shorter for man-made ones, are interconnected by different types of forces: hydrogen bonds, van der Waal forces and hydrophobic interactions, which all provide strength to the microfibrillar structure. These structures in turn constitute cell walls, which further constructs a plant or tree (Figure 1).[7]

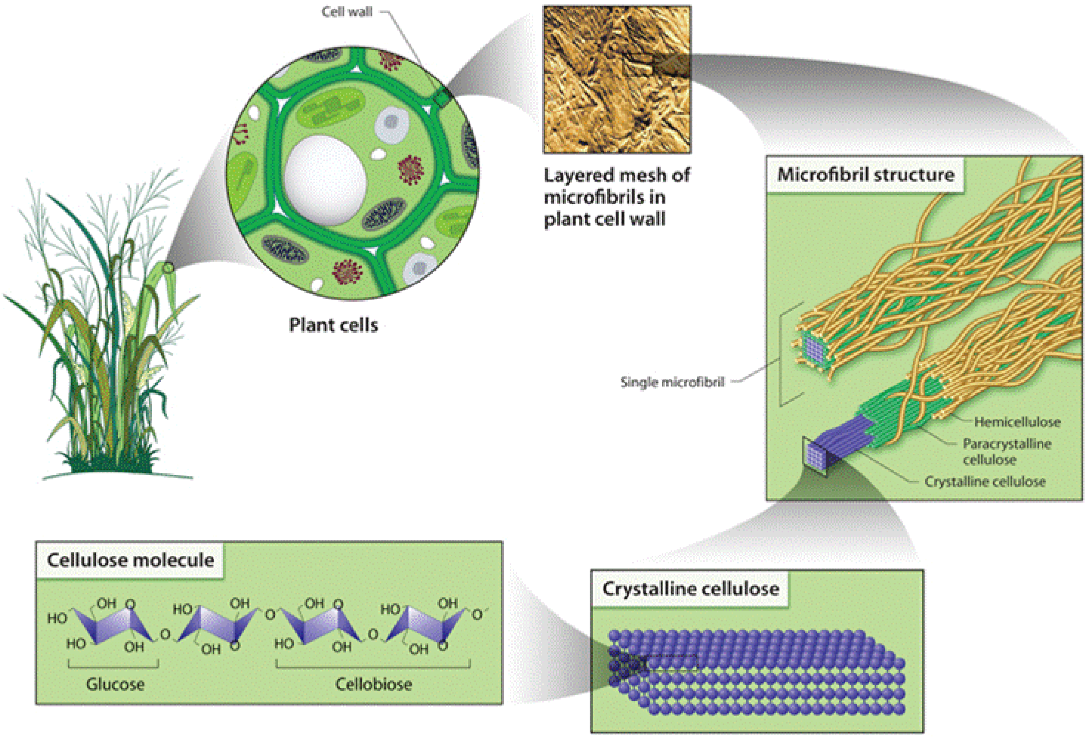

Figure 1: Schematic picture of cellulose and how it is structured. Adapted with permission from U.S. Department of Energy Genomic Science program (http://genomicscience.energy.gov).

The only primary hydroxyl group of a glucose unit is found on carbon 6 (C6 in Figure 2), which has a higher reactivity than remaining hydroxyls[8]. Oxidation of hydroxyls can introduce new functionalities in the form of aldehydes and carboxylic acids. These groups facilitate further processing by introducing charge to the polymer chains. By the addition of negative charge, hydrogen bonds can be broken and electrostatic repulsion between the chains are introduced. This will lead to easier separation of the fibers. Separation is an essential step in the case of forming nanocellulose[9] and will decrease the amount of energy otherwise needed.

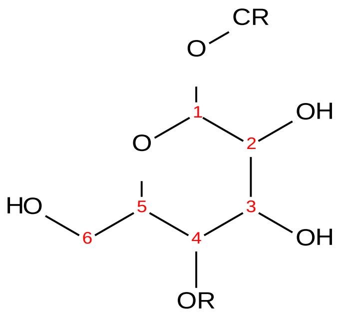

Figure 2: A schematic picture of bondings and numbering of carbons in a glycosidic polysaccharide.

Methyl-α-D-Glucopyranoside (MGP)

The monosaccaride Methyl-α-D-Glucopyranoside (MGP), seen in Figure 3**,** represents a monomeric unit of cellulose and was therefore used as a model system in this work. Just as for cellulose, the only primary hydroxyl group is found on C6. Simplified, cellulose and MGP are assumed to exhibit similar properties but with higher reactivity for MGP due to its smaller size. Additionally, it is easier to characterize MGP since it is soluble in water.

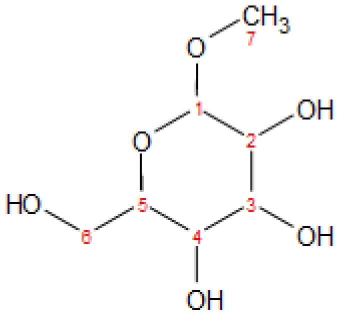

Figure 3: Schematic picture of MGP considering bondings and numbering of carbons.

Oxidation methods

To activate cellulose for further quality upgrade in the recycling process, various catalysts can be used to oxidize the C6-hydroxyl group, forming aldehydes and carboxylic acids. A potential method for the scope of this thesis must be mild, as not to depolymerize the cellulosic chains, and be acceptable in a green perspective.[3]

Previously, stoichiometric amounts of hazardous oxidants have been applied for oxidation of secondary alcohols. Examples of these oxidants are Cr(VI)-reagents[10] and toxic salts of Ru or Mn[11]. Other examples are *Dess Martin reagents*[12], which uses hypervalent iodine, and the *Swern oxidation*[12] in which stoichiometric amounts of DMSO is consumed. Although currently used methods are far better than these, with O_2 or H_2O_2[13,14] as main oxidant only producing water as by-product, they still rely on use of catalytic amounts of co-oxidants, including transition metal complexes such as (apart from previously mentioned) V-, Cu, Os-, Mn- and Co- based[15], to accommodate the reaction.[1,16]

TEMPO

TEMPO (2,2,6,6-tetramethylpiperidine-1-oxyl) and its derivatives[17] are relatively stable and bulky radicals that have been shown in several studies to selectively oxidize primary alcohols[18,19,20]. The radicals mediate a reaction after first being activated, by e.g. a co-catalyst in a catalytic pathway as the one seen in Figure 4.

Cellulose has only one primary hydroxyl group, positioned on the C6-carbon, as seen in Figure 2. Since cellulose is often highly crystalline, containing both inter- and intramolecular hydrogen bonds, it can be difficult for reagents to reach into and open up its structure.

TEMPO can operate under mild conditions, regarding temperature and pH. Optimal settings for the most stable reaction conditions are basic pH[21] with applied external cooling as not to decompose[22], though it has also been used under acidic conditions[23]. Further, TEMPO needs to be activated into its oxidized form to be able of acting as a mediator in a reaction. This has previously been achieved by use of halogen species (see reaction scheme in Figure 4), such as sodium bromide together with sodium hypochlorite, a drawback when green chemistry is desired[16]. On the other hand the reaction is often fast, can be performed under acidic or basic conditions, and only a catalytic amount of TEMPO is needed. Selective oxidation[24,25] of the primary C6 hydroxyl goup has been successfully performed even without loss of cellulose crystallinity, which is an advantage for many applications[9]**.** Additionally, TEMPO can be recovered in the system and used as a mediator for several cycles, as have been shown in several studies[3].

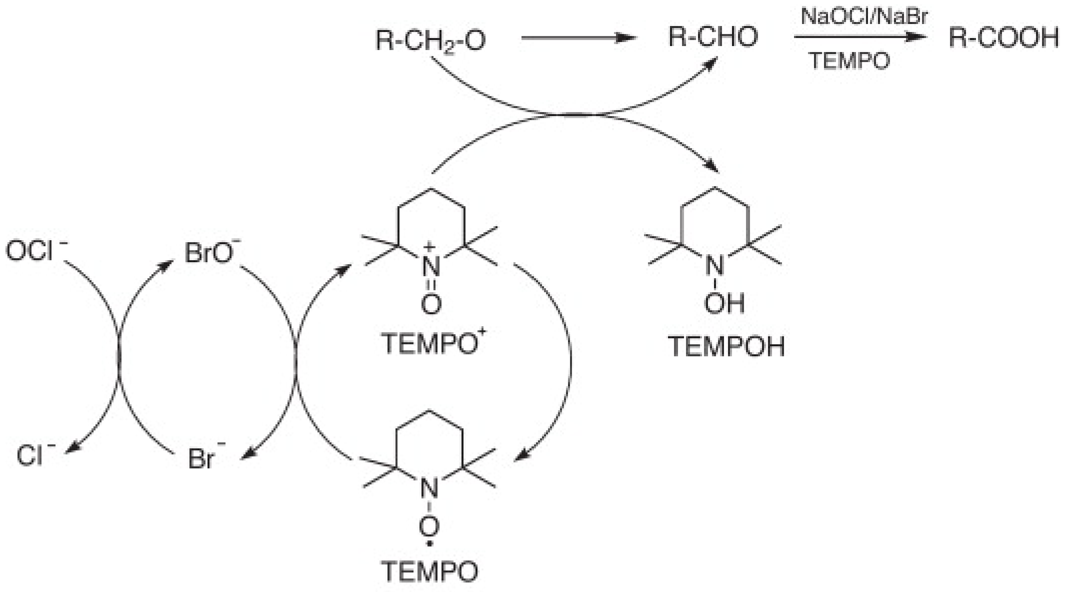

Figure 4: TEMPO-mediated oxidation. Reproduced from reference 33, with permission from Elsevier.

For this study, TEMPO will be in focus as an environmentally acceptable candidate to mediate the oxidation of cellulose.

Immobilized TEMPO

There is one additional concern about using TEMPO as mediator in oxidation reactions: Although regeneration of TEMPO has been reported, this relatively small sized molecule can still make separation and recovery difficult when a green chemical process is the main goal. As of today, extraction with toxic solvents such as DCM, is often applied. To facilitate the recycling, oligomeric structures referred to as immobilized TEMPO has been proposed. Some different variants of immobilization have been tried such as sol-gel entrapment[26] and anchoring onto silica support. [16,27,28,29]

One approach of immobilization is Polymer-Immobilized Piperidinyl Oxyl (PIPO), which is derived from the commercially available Chimassorb® 944[29], a chemical commonly used as stabilizer and light absorber in plastics. PIPO has shown an increased activity compared to its predecessor[29], resulting in no need for the bromide co-oxidant**.** Additionally, the heterogeneous catalyst has proved easy to regenerate. [30,31,32,33]

O_2 variants

As oxygen is readily available and often produces water as a byproduct, it is an interesting oxidant to investigate. Molecular oxygen, below a temperature of 100 °C[34], has been shown to generate the oxoammonium ion from TEMPO, hence activating it for further oxidation. Another approach was using Mn/Co as catalysts together with molecular oxygen in 40 °C to perform oxidation of alcohols[35]. In table 4 of *Modern Oxidation Methods*, Backvall compare these results with the enzymatically catalysed reaction using molecular oxygen and laccase. In the laccase system, only 25 °C were needed, though reaction times were long (24h)[36]. Other studies using laccase together with TEMPO and its derivatives as mediators have been performed under similar conditions, with ambient temperature but long reaction time and moderate yield[23,37]. Other approaches for oxidation of alcohols have been using Ru or Cu complexes together with molecular oxygen and TEMPO or PIPO for a recyclable catalytic system[30,38,39].[16]

Activation of cellulose

To enhance the dissolution and activation of cellulose, different sources of energy can be introduced into the system**.** Microwave treatment [40], ultrasound irradiation[41,42,43], electron beam irradiation[44] and electrochemistry, which will be further introduced in the next chapter, are examples of energy sources that have been applied for enhancing cellulosic dissolution or activation. [45]

Electrochemistry

Electricity is defined as the movement of charged particles. In the context of electrochemistry, electricity is applied to facilitate chemical reactions by enabling electron transfer between species. This reaction is known as a redox reaction since oxidation and reduction must take place at the same time, at the anode and cathode respectively. Applying a potential can therefore facilitate a reaction, by providing activation energy, which when applied for previously non-electrochemical reactions may enable removal of unwanted toxic or expensive reagents.[46]

Electrochemical activation of Tempo

To avoid halide-based reagents, activation of TEMPO by electrochemical oxidation has been proposed as a greener alternative. Some successful results have been reported, though with long reaction times (48h) and substantial depolymerization[9]. 4-acetamido-TEMPO, a variant of TEMPO, showed slightly better results, especially concerning depolymerization[25,47].

In an oxidation process, TEMPO reacts to its oxoammonium ion (TEMPO+) by a one electron reaction. TEMPO+ then oxidizes the primary C6 OH-group on cellulose, generating a carbonyl or carboxyl group and subsequently TEMPO+ is converted into its corresponding hydroxylamine, TEMPOH. TEMPOH is then reoxidized to form the oxoammonium ion. The electrolyte works as a reducing base for the alcohol. A membrane can be applied to separate oxidized cellulose from the counter electrode where it could otherwise be reduced.[25,48,49] A water based buffer solution is often used and the optimal pH is a compromize between the levels tolerable for, in the case of this thesis, the cellulosic substrate not to degrade, and the optimal level for TEMPO, being a compromise of good stability and high activity[50,51].

A reaction scheme of TEMPO-mediated electrochemical oxidation of cellulosic substrates is found in Figure 5. In this illustration a membrane is applied for separation of the counter electrode, to not reduce either TEMPO or cellulose.

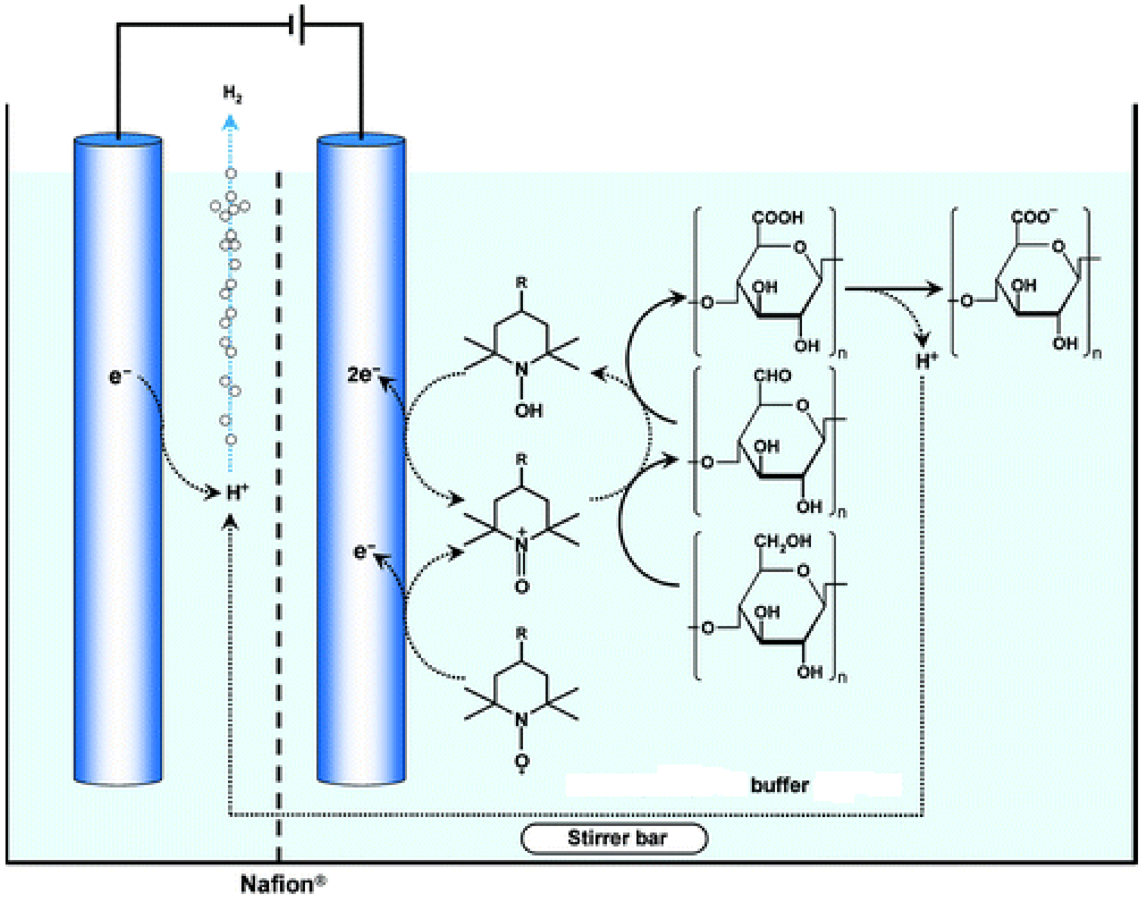

Figure 5: Schematic picture of TEMPO-mediated electrochemical oxidation of cellulose. Reproduced from reference 47, with permission from The American Chemical Society.

Methods for preparation, characterization and analysis

To characterize the substrates and their oxidation products, different methods can be used depending on which type of information is sought. Since the scope of this work was to oxidize hydroxyl groups into carboxylic groups, determination of functionality rather than focusing on structural changes has been in focus. With this in mind the methods chosen for characterization studies are NMR, FT-IR and XPS, which are all presented later in this chapter. But first, a theoretical insight to the nature of electrochemical reactions, focusing on electrolysis, is presented.

Theoretical background to electrochemical reactions with electrolysis

Faradaic processes are when a chemical reaction is caused by electron transfer. This is performed by applying a potential between two electrodes, as depicted in Figure 5.

A potentiostat is normally used to control the potential of a reaction by adjusting the current. If a potential is too low for a redox reaction to occur (meaning no current will flow between the electrodes), other processes can still take place such as adsorption and desorption. These are called non-faradaic processes and they can also occur simultaneously with faradaic processes. The non-faradaic processes works like capacitors. A capacitor is charged (q) when a potential (E) is applied, until its energy storage capacity, the capacitance (C), is fulfilled by equation: [46]

$$q/E = C$$

In electrochemical cells, this phenomenon is present at the electrode-solution interface. This interface consists of two layers of opposite charge, one on the metal (q^M) and one in the solution (q^S): [46]

$$q^M = -q^S.$$

The charges can be expressed as charge densities (σ^M) by relation to the electrode area (A), and is often expressed in $\mu C/cm^2$: [46]

$$\sigma^M = q^M/A$$

The *electrical double layer* consists of all charged species at the metal-solution interface and is characterized by a double-layer capacitance (C_d), which is dependent on the potential over the cell. The double layer typically consists of an inner layer closest to the electrode and with specifically adsorbed species, and an outer layer consisting of nonspecifically adsorbed species interacting by long-range electrostatic forces. The outer layer is extended by agitation into the bulk, therefore it is also called the diffuse layer. The double layer structure is important for electrochemical processes since a drop of effective potential can be seen when species travels through the diffuse layer towards an electrode. This affects reaction rates and results in that a higher potential than the one calculated is needed to pursue a reaction. [46]

There are four major factors that affect the rate of an electrode reaction. These factors are detailed in Figure 6 below, together with solutions to how they can be governed. The first factor, mass transfer, is the flow of reactants and products to and from the electrodes, which is important for reacting species to meet, hence stirring and closeness of electrodes are controlling functions. The second factor is electron transfer, relying on electron diffusion and adsorption on the surface of the electrodes, which increase by an increase in potential. Relying on the electron transfer, the third factor is chemical reactions, which is governed by knowing and controlling the rate determining step. The fourth factor is non-faradaic processes taking place at the electrodes. This factor can inhibit mass transfer and electrode transfer by blocking electrode surface area. A higher potential might then be needed to pursue a reaction, and/or a change in solution composition to avoid e.g. crystallizing species.

Factor	**Solution**
Mass transfer	Increase stirring, maintain short distance between electrodes
Electron transfer	Increase potential, increase electrode surface area
Homogenous or heterogenous chemical reactions, ensued by electron transfer	Concentration changes of certain reactants, increase the energy of the system (by e.g. temperature or potential increase)
Non-faradaic processes, such as adsorption (which if on the electrode will affect the reaction, hence inhibit the function of the process), desorption and crystallization	Increase potential, alter solution composition

Figure 6: Factors affecting reaction rate in electrolysis.

Electrolysis methods

To pursue an electrochemical reaction, a potentiostat, controlling the voltage over the electrodes, is often used together with a programmed technique. Which technique is used depends on what you want to see or do. To start with, *Cyclic Voltammetry*, CV, is often applied to see how the current responds to a cyclic potential sweep and this will show the oxidation and reduction potentials. In a programmed *Amperometric it-curve*, the potential is set (e.g. after what was seen to be the oxidizing potential of CV) and the current will change by time, depending on how much reactants that can be oxidized. Two ways of deciding when an electrolysis reaction is to be stopped, is to either use a pre-set time or to stop the reaction when a certain amount of current has been consumed in the system, which is the calculated total amount of current needed for a reaction to be fulfilled.

Nuclear Magnetic Resonance Spectroscopy, NMR

Nuclear Magnetic Resonance Spectroscopy (NMR) has been applied for structure determination in organic chemistry since the 1960s. This technique is used for mapping the bonds in an organic molecule by applying a magnetic field and electromagnetic irradiation. Only nuclei with internal spins can be used, such as ^{1}H and ^{13}C each having a spin of ½, which makes them behave like magnets. This property cause nuclei to align with an external magnetic field (B). Depending on its own field, the nuclei will be parallel or antiparallel to this external field, with the parallel orientation often lower in energy (which makes it favoured). If a specific energy is applied that corresponds to the energy difference between two spin states, energy will be absorbed by the nuclei and this will induce a spin flip to the orientation higher in energy. The energy needed depends on the field strength and is introduced by electromagnetic irradiation.[52,53]

Each type of nuclei have a specific resonance frequency related to the strength of an applied field. For example a previously common field strength of 2.35 Tesla results in a resonance frequency of 100 MHz for ^{1}H and 25.14 MHz for ^{13}C. An instrument with this field strength is referred to as a 100 MHz system. Today instruments with stronger field strengths, like 300-800 MHz, are more common, resulting in higher sensitivity and resolution as well as shorter acquisition time than when applying weaker field strengths. [52,53]

The nucleus in a molecule is surrounded by electrons having their own magnetic fields, which affects the nucleus such that it experiences a lower effective field. This phenomena is called shielding and it results in that same type of nucleus but with varying surroundings will give rise to different resonance frequencies and could therefore be distinguished from each other. This is referred to as a chemical shift and applies for some thousand Hz around the standard resonance area.[52,53]

Apart from chemical shifts, peaks can also show multiplet structures, referred to as splitting. The split of a peak is due to interactions with neighboring nuclei and the grade of a multiplet depends on how many neighboring nuclei that couples to it. Additionally, stiffness in a molecule can result in that for example two protons on the same position are closer or further from different neighbours. This results in different shifts, which for a doublet would result in a double doublet. Example on different shifts can be seen in Figure 7.

Different nuclei-coupling results in specific distances between the peaks in a multiplet and is referred to as the coupling constant, J. This constant makes it possible to distinguish which peaks that belong to the same nuclei and to which neighboring nuclei it couples to. By using NMR in this way it is possible to distinguish if the C6 hydroxyl group has formed a carboxylic group or an aldehyde, since their spins are distinct and the position will display coupling effects.[52,53]

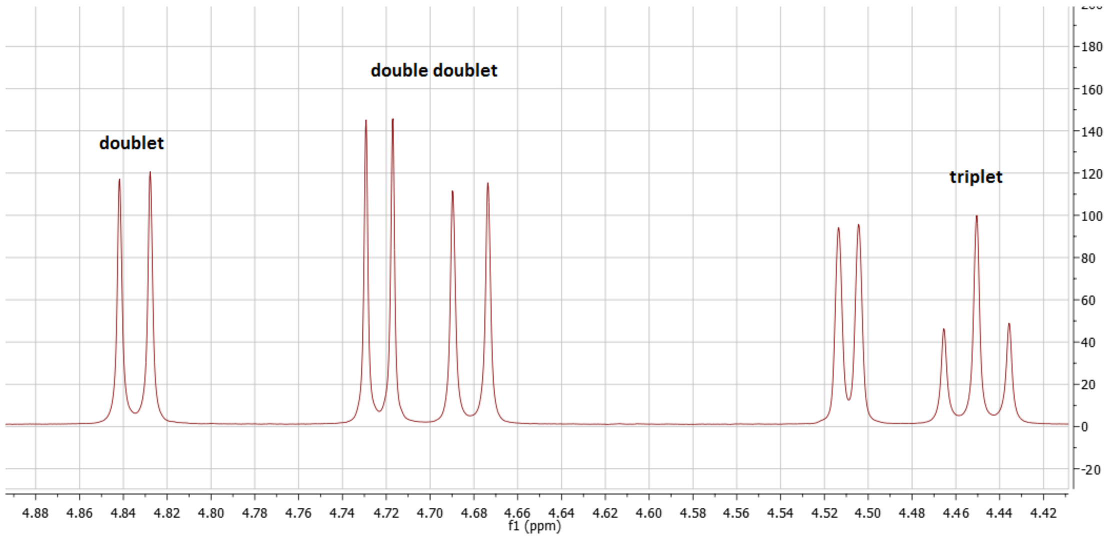

Figure 7: NMR spectra of peak splitting, showing example of doublet, double doublet and triplet.

Flash Chromatography

All since it was first introduced 1978[54], flash chromatography has been a popular tool for being easy to handle and providing a fast separation technique of organic molecules.[55]

For the setup of a flash column, silica powder with a fine and narrow particle size is used. Small sized particles have high surface area, meaning higher contact possibilities with the sample mixture. This reults in a better adsorption of organic molecules, which is key to effective separation. For an even faster separation, pressure is applied to drive the solvent through the column. A rack of tubes is normally used for collecting sample fractions. To identify if the fractions contain different molecules, thin layer chromatography-plates are used, followed by e.g. NMR for characterization of the fraction.[55]

Thin Layer Chromatography, TLC

Thin layer chromatography (TLC) is a prompt technique used to identify compounds based on their polarity. The principle is to use a plate of glass or plastic covered with silica or alumina, onto which a small amount of sample is added (about 0.5 cm from the bottom of the plate) before it is put into a liquid phase (reaching to about 0.3 cm of the plate) in a so called TLC tank. When the solvent has travelled almost to the top the plate is removed and the solvent line is marked and then detection can be achieved by some type of light source. For a non destructive technique a UV-lamp can be used to view the spots, if they are UV-active.

TLC is a must for flash chromatography, firstly to identify which solvent-system to be used (by identifying the R_f-value, being the distance travelled by a product (a) divided by the distance from the base line to the solvent line (b), as seen in Figure 8), and secondly to examine separated fractions.[55]

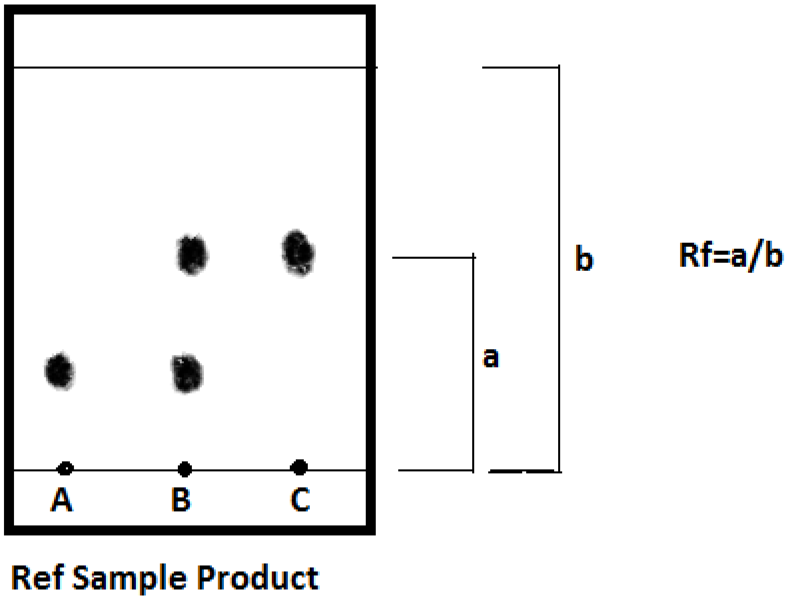

Figure 8: Picture of a TLC plate and how to calculate the R_f-value.

Infrared Spectroscopy, IR

Infrared spectroscopy, IR, is a commonly used technique in organic chemistry for detecting vibrations of molecular bonds. These vibrations, which are specific for different molecules and functional groups, are usually measured in the frequencies between 625 cm^{-1} and 4000 cm^{-1}. An infrared light source of the right frequency range, covering the vibrational wavelengths to be detected, is applied. The light is split into two beams of which one is passing through the sample. Energy from the beam passing through will then be absorbed by a molecule if vibrational frequency match a frequency of the light source. The resulting spectra is therefore a comparison between the beam passing through the sample and the unaffected beam and will show peaks of absorption plotted against wavelength or frequency.[52,53]

Fourier Transformed IR (FT-IR) is the more commonly used IR-technique today. The light source is split into two beams and one or both pass through the sample but the travelling distance for one beam is longer and the path difference is systematically changed to produce a signal varying with length. The two beams recombine and an interference pattern for each wavelength of the beam produces an interferogram.

The interferogfram is computationally converted by fourier transformation to produce a plot of absorption to wavenumber. The spectra produced look very similar to the standard IR spectra but requires less time. In this thesis FT-IR has been applied to examine if a carboxyl peak is formed, which should be present at 1732 cm^{-1} in the spectra.[52]

X-ray Photoelectron Spectroscopy, XPS

XPS is a surface sensitive technique that quantitatively measure the elemental composition and functionality of a surface. By using an x-ray source and ultrahigh vacuum, electrons are excited from a filament and travels towards a metal with which it interacts. The interaction creates x-rays that reach the sample subject to analysis. When the sample is hit by incoming x-rays it will emit photoelectrons that are detected. The stage onto which the sample is mounted can be manouvered to adjust the X, Y and Z positions. This function makes it possible to decide the relative angle of the sample to incoming x-rays, which in turn decides the depth from which the photoelectrons are emitted, in the range of 1-20 nm, from the sample. Electrons generated from inner orbitals result in stronger lines in a spectrum than those from valence orbitals and are displayed at some hundred eV of binding energy compared to below 30 eV for the latter. The C1s peak for example is used as reference of 285 eV.[56]

Emitted electrons can originate either from different orbitals but also from the same orbital when having different spin states. The vacancies generated by emission of inner orbital electrons can be reoccupied by the relaxation of an outer electron. The energy released may give rise to the emission of a secondary electron, which provides additional information and is referred to as an Auger electron. The Auger effect is named after the male physicist Pierre Auger who discovered it concurrenty as the female physicist Lisa Meitner, who unsurprisingly did not get the same credit for it.[56]

The following information can be provided by an XPS spectrum:[56]

- Information on oxidation state, bonding energy and neighboring atoms by displayed shifts, which enables quantification by measuring their (relative) intensities by peaks from core electrons.
- Peak splitting, which is due to electrons from the same orbital (except the s-orbital) that can have different spins.
- Valence band electron lines, which provide information from the valence electrons and makes it possible to distinguish between different forms of the same molecule, such as isomers. The region for these lines are found below 30 eV, which is much lower than for core electron peaks.
- Chemical composition and quantitative information provided by Auger electrons.

Experimental

Materials

The electrochemical experiments were performed using Ag/AgCl as the reference electrode. The working electrode was glossy carbon and the counter electrode was either Pt or glossy carbon. The separation vessels were bought from Metrohm and the Nafion 424 membrane was bought from Sigma Aldrich. The electrochemical setup can be seen in Figure 9, and the electrodes can be seen in Figure 10, Figure 11 and Figure 12. For electrochemical experiments, an electrochemical workstation (Chi650 from CH Instruments, Inc.) was used.

Figure 9: Tempo mediated electrochemical oxidation setup.

Figure 10: Glossy Carbon as working electrode.

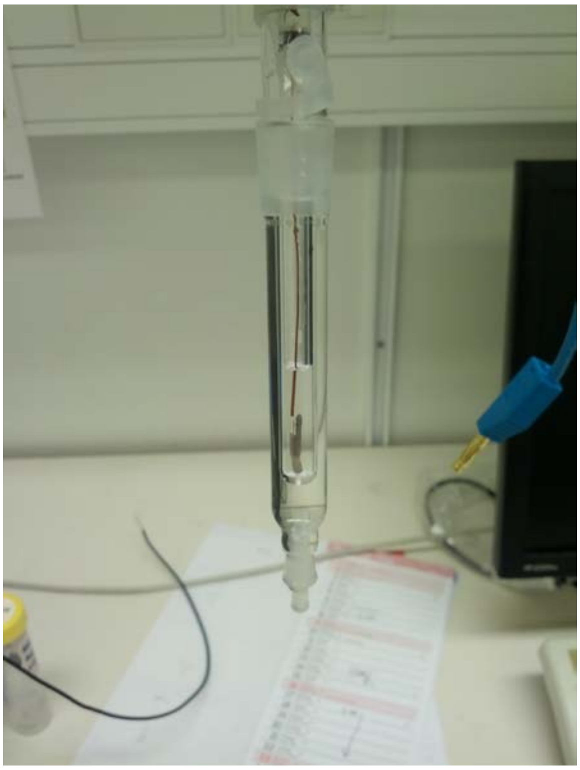

Figure 11: Ag/AgCl as reference electrode.

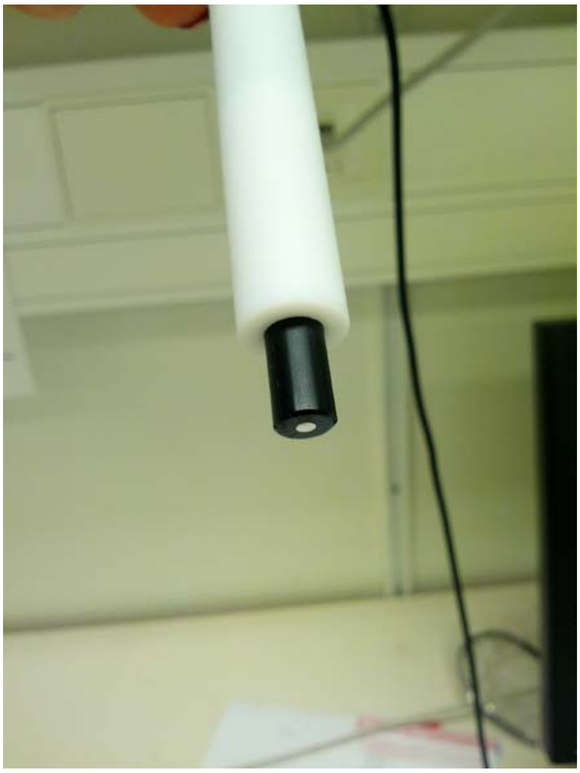

Figure 12: The Pt-counter electrode.

The cellulosic substrates were bed-linen *cotton* obtained from Textilia, commercial *dissolving pulp* from Brazil and a reactive bleached pre-hydrolyzed softwood kraft pulp (*Innventia pulp*) obtained from Innventia AB.

All chemicals were purchased from Sigma Aldrich and used with no further purification.

Experimental 1st part: TEMPO mediated electrochemical oxidation of cotton and MGP

TEMPO (2 mmol/g cellulose) was dissolved in a NaOH/$NaHCO_3$, pH 10 buffer solution at vigorous stirring and then added to a three-electrode electrolyte vessel, with Pt as counter electrode, connected to a potentiostat. Cyclic Voltammetry (-0.2 – 0.6V) was run for three sweeps under observation to make sure that the setup was working. MGP was then added (by monomeric units corresponding to 1 wt% cellulose) and stirring applied before i-t voltammetry (0.6 V) was started and run for 24 h under room temperature. The obtained solution was then extracted with DCM to remove

TEMPO, neutralized with Dowex (Spectra/por and finally the solvent was evaporated. The sample could then be prepared for further analysis.

Flash Chromatography

To prepare the flash-column, Silica gel (6 g) was mixed with EtOAc/MeOH as solvent to form a slurry. A flash column was then filled with slurry and let to pack with solvent added to keep the level some centimeters above the silica surface. The excess solvent was let to run through the column until the silica surface was just covered. Subsequently, the sample (E12, 0.3 g) dissolved in methanol (10ml) was sprinkled with a pasteur pipette around the walls of the column close to the surface of the silica and then a large amount of solvent was added on top. Finally the column was allowed to run until molecules had been detected in three different fractions (number 5, 11 and 12). A total of 20 fractions of about 5 ml each was collected.

Experimental 2nd part: Revised setup of TEMPO mediated electrochemical oxidation of four substrates

TEMPO (2 mmol/g cellulose) was dissolved in a NaOH/$NaHCO_3$ pH 10 buffer solution at vigorous stirring and then added to a three-electrode electrolyte vessel, with glossy carbon as counter electrode, connected to a potentiostat. Cyclic voltammetry was run for three sweeps under observation to ensure current was passing through the sample. The substrate (corresponding to 1 wt% cellulose) was then added and stirring applied before i-t voltammetry (0.7 V) was started and run for 4 h. The slurry obtained was extracted with dichloromethane to remove TEMPO. The cellulosic substrates were then dialyzed to remove all ions, washed with ethanol and collected by suction filtration. With MGP as substrate the work-up is as described in the previous section.

Experimental 3rd part: TEMPO-mediated oxidation

TEMPO (0.1 mmol/g cellulose) was dissolved in deionized water under vigorous stirring and subsequently added to a three necked round bottomed flask together with the substrate (6 mmol) and NaBr (1 mmol/g cellulose). Stirring was applied and NaOH (0.5M) was added dropwise until a pH of 10.5 was reached. NaOCl (4.2 mmol/g cellulose) was then added slowly and NaOH (0.5M) was continuously added to keep the pH at 10.5. When no more decrease in pH could be detected the reaction was quenched with ethanol. The work-up then followed the same procedure as in the previous sections.

Results

The model system with MGP showed oxidation peaks after 24 h oxidation reactions. For cellulose substrates, no oxidation peaks were seen, only an affected macromolecular structure for a 24 h sample analyzed by solid state NMR analysis. The atomic surface composition was analyzed by XPS and here was also a 24 h sample affected towards a more oxidized surface. Results in detail will be presented in this chapter for each characterization method.

Optimizing experimental setup

With the aim of achieving TEMPO-mediated electrochemical oxidation and developing the instrumental setup, the work was divided into three parts. In the first experimental part, Methyl α-D-glucopyranoside, referred to as MGP in this text, was the substrate subjected to electrochemical oxidation. Being an analogue to cellulose by resembling the monomeric units of the macromolecule, the oxidation of MGP was expected to be similar but faster compared to cellulose because of the smaller size and solubility in buffer, hence reaction times covering 1-24 h were tried. Cyclic voltammetry was run before each experiment to make sure that electricity went through the sample. A vessel for separation of the reducing counter electrode was used in some runs to prevent reduction of material; the first one used was a handcrafted vessel produced from a Nafion membrane. The second one, an electrolyte vessel with glass filter bottom, was bought from Metrohm. A small (5 mm in length) magnetic stirrer bar was used as not to be in contact with and possibly damage the electrodes.

For the second part of the experimental work the reaction time was set to 4 h. Results from the 1st part indicated that at least 24 h was needed but due to lack of time this was not possible. A complete oxidation was therefore not expected, but an indication of the reactivity in the system and further understanding of how the setup was functioning and what could be improved. Since a newly published article[57] had shown promising results after 4 h oxidation time and a potential at 0.7 V, the same reaction time and potential setup was also chosen for this work, instead of chosing a random (short) reaction time. Further, four different substrates (MGP, cotton and two more reactive cellulosic substrates; innventia pulp and dissolving pulp) were chosen for oxidation as to see if their reactivity differed. Other changes that were done in the second part was that the magnetic stirring bar was changed to a bigger one (15 mm), the counter electrode (Pt) was replaced by a glossy carbon electrode that had a slightly larger surface area, and finally a control to remove bubbles in the reference system was performed before each experiment. For all substrates, experiments were performed both with and without the Metrohm-vessel on the counter electrode.

For the third part, the same four substrates as in the previous section were oxidized using TEMPO-mediated oxidation with co-oxidants NaBr and NaOCl, to enable comparison with the electrochemical method, using various analysis methods.

The reaction conditions for the 1st, 2nd and 3rd part of the experimental work and an overview of the analysis can be seen in table 1, 2 and 3 respectively.

Table 1: Setup for the 1st experimental part.

Trial	Potential [V]	Time [h]	pH	Substrate	Cellulose [mmol]	TEMPO [mmol]	Separation vessel	Liquid NMR: ^{1}H and ^{13}C	FT-IR
E1	0.6	1	10.6	Cotton	0.926	0.305	No	-	-
E2	0.6	24	10.6	Cotton	0.930	0.301	No	-	-
E3	0.6	24	10.6	Cotton	0.926	0.301	No	-	-
E4	0.6	24	10.6	MGP	0,911	0.301	No	Yes	-
E5	0.6	24	10.6	MGP	0.899	0.301	Nafion	-	-
E6	0.6	24	10.6	MGP	0.918	0.310	Nafion	Yes	-
E7	0.5	24	10.3	MGP	0.912	0.308	No	-	-
E8	0.5	24	10.3	MGP	1.805	0.609	Nafion	Yes	-
E9	0.5	24	10.3	MGP	1.808	0.624	Metrohm	Yes	-
E10	0.5	24	10.3	Cotton	1.856	0.609	Metrohm	-	-
E11	0.5	24	10.3	Cotton	1.855	0.610	Metrohm	-	-
E12	0.5	24	10.3	MGP	0.905	0.317	No	Yes	-
E13	0.7	4	10.3	MGP	0.907	0.304	No	Yes	Yes
E14	0.7	4	10.3	Cotton	1.851	0.632	No	-	-

Table 2: Setup for the 2nd experimental part.

Trial	Potential [V]	Time [h]	pH	Substrate	Substrate [mmol]	TEMPO [mmol]	Separation vessel	Solid NMR ^{13}C	XPS	FT-IR
A3	0.7	4	10.3	Cotton	1.910	0.652	Metrohm	-	Yes	Yes
A4	0.7	4	10.3	Cotton	1.879	0.632	No	Yes	Yes	Yes
A5	0.7	24	10.3	Cotton	1.868	0.615	No	Yes	Yes	Yes
A6	0.7	24	10.3	Cotton	1.909	0.676	Metrohm	-	Yes	Yes
C3	0.7	4	10.3	Innventia	1.862	0.679	Metrohm	-	-	Yes
C4	0.7	4	10.3	Innventia	1.865	0.631	No	-	Yes	Yes
D3	0.7	4	10.3	Dissolving	1.850	0.637	Metrohm	-	-	Yes
D4	0.7	4	10.3	Dissolving	1.875	0.651	No	-	Yes	Yes

Table 3: Setup for the 3rd experimental part.

Trial	Substrate	Substrate [mmol]	TEMPO [mmol]	NaClO [mmol]	NaBr [mmol]	NaOH [M]	NMR	FT-IR
R1	MGP	6.037	0.109	4.2	1	0.5	Yes (liquid state: ^{1}H, ^{13}C)	Yes
R2	Cotton	6.204	0.124	4.3	1	0.5	Yes (solid state: ^{13}C)	Yes
R3	Dissolving	6.176	0.102	4.2	1	0.5	-	Yes
R4	Innevntia	6.227	0.116	4.2	1	0.5	-	Yes
R5	MGP	6.034	0.103	12	1	0.5	Yes (liquid state: ^{1}H, ^{13}C)	Yes

Results from i-t voltammetry

Below some graphs from the electrochemical experiments are shown. A reference sample with only TEMPO in buffer solution can be seen in Figure 13 for comparison. Graphs not displayed in this chapter can be found in Appendix I.

The slope in a graph show how much current is passing through the system for an applied voltage. An increase would mean that more material is available for oxidation, and a decrease that less material can be oxidized. In TEMPO-mediated electrochemical oxidation, the expectation is to see highest current from start and subsequently a decrease with time, given that mass transfer is working accurately.

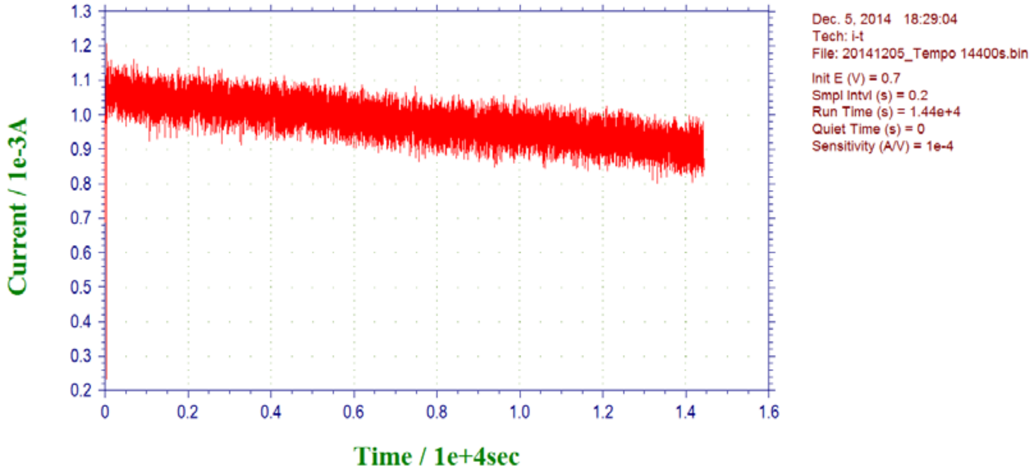

Figure 13: Reference (TEMPO run for 4h).

Electrochemical experiments: 1st part

How the graphs appear varies between different experiments. In Figure 14-15, 24 h oxidation is run with cotton and MGP respectively. Some graphs show gaps, especially when a separate compartment for the counter electrode is used, as in Figure 16. For shorter runs, Figure 17 shows a representative picture of MGP oxidation. All these graphs show a current decrease with time, indicating that less material is available for oxidation.

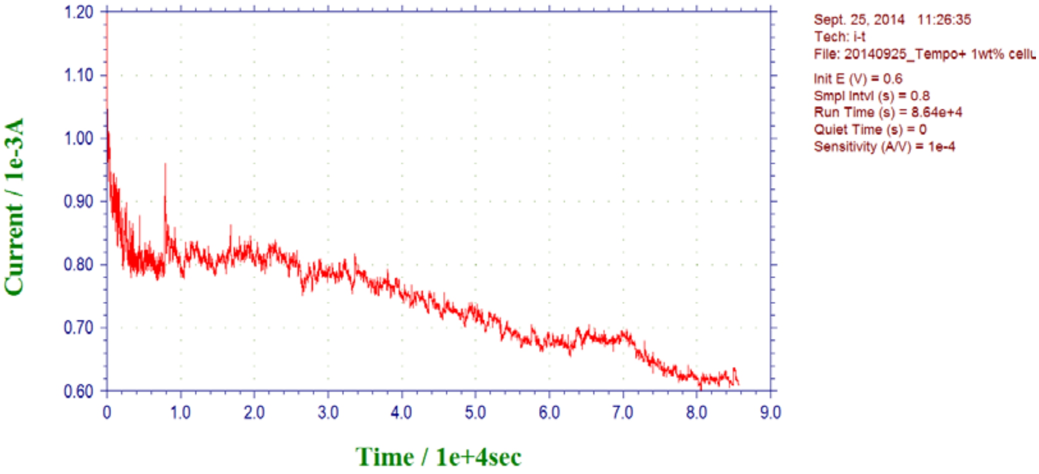

Figure 14: Electrochemical oxidation of sample E3 (Cotton run for 24 h).

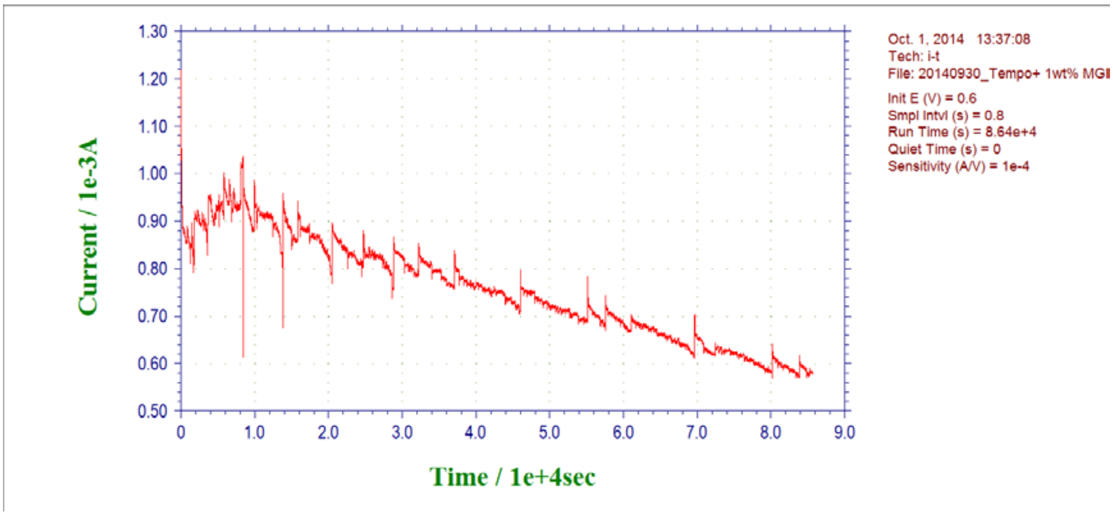

Figure 15: Electrochemical oxidation of sample E4 (MGP run for 24 h).

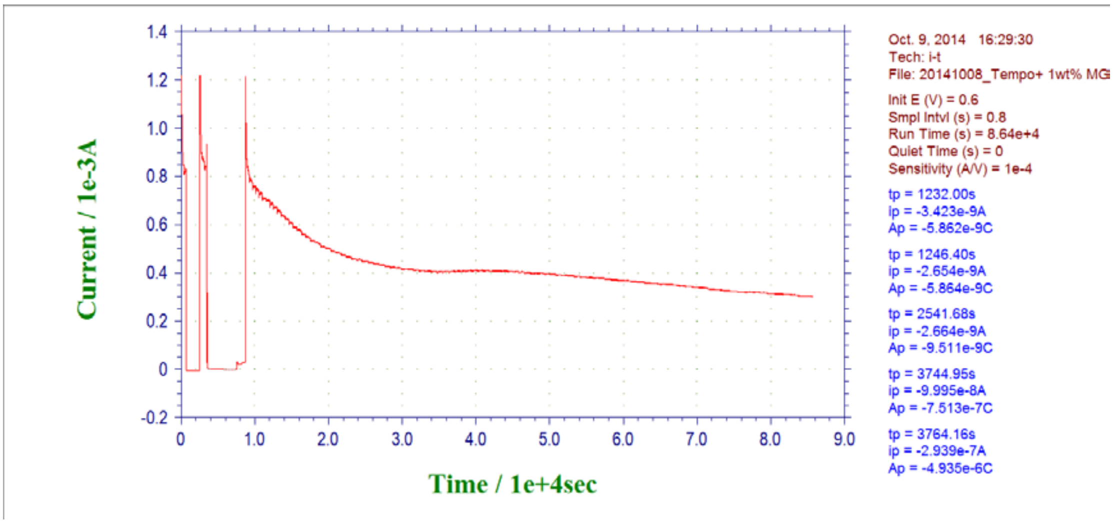

Figure 16: Electrochemical oxidation of sample E6 (MGP run for 24 h with a nafion membrane on the counter electrode).

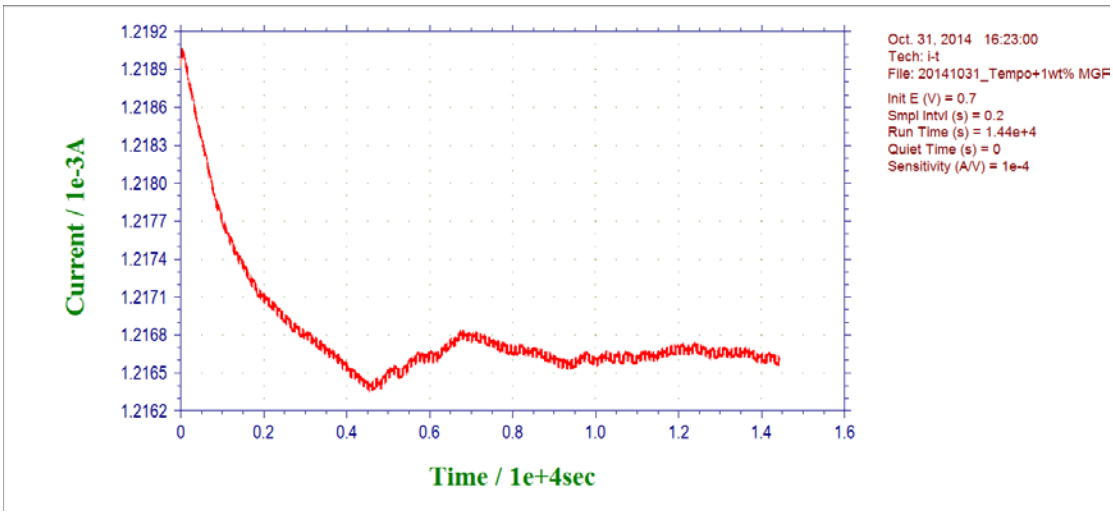

Figure 17: Electrochemical oxidation of sample E13 (MGP run for 4h).

Electrochemical oxidation of different substrates

In the 2nd part, all experiments except A5 and A6 were run for 4 h. Some graphs (A4 and A5, see appendix I) display a similar look to sample E13 in Figure 17. When a separate compartment on the counter electrode was applied, graphs instead tend to show an unexpected increasing slope, as in Figure 18 and 19. Yet other graphs show disturbances, as seen in Figure 20, displaying D4 run without separation of the counter electrode.

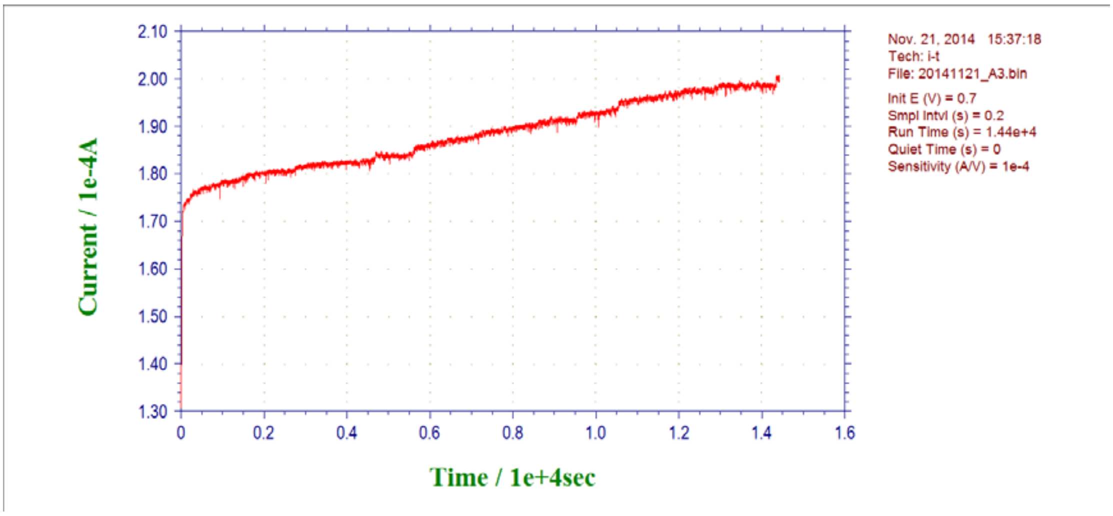

Nov. 21, 2014 15:37:18
Tech: i-t
File: 20141121_A3.bin
Init E (V) = 0.7
Smpl Intvl (s) = 0.2
Run Time (s) = 1.44e+4
Quiet Time (s) = 0
Sensitivity (A/V) = 1e-4

Figure 18: Electrochemical separated oxidation of cotton, sample A3.

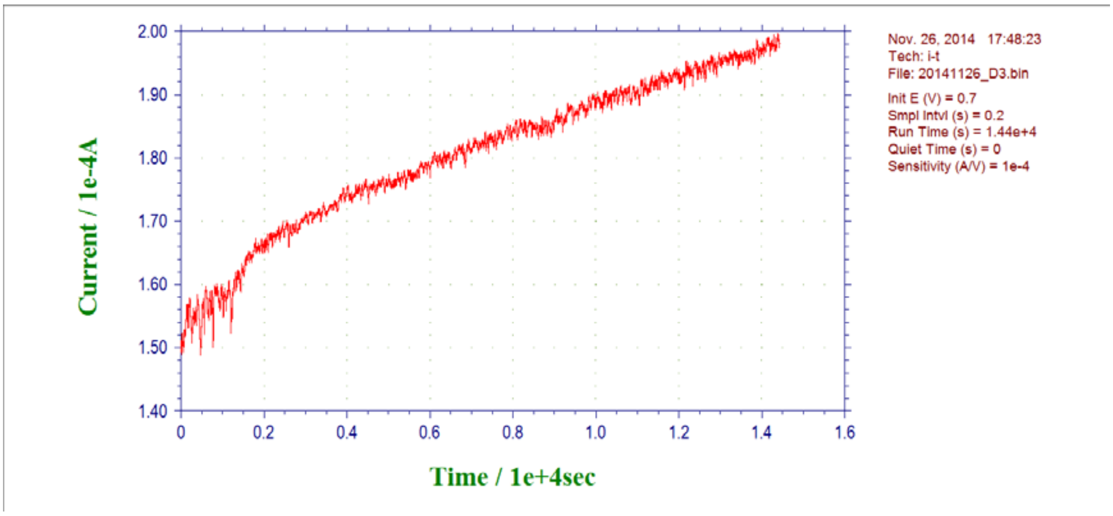

Nov. 26, 2014 17:48:23
Tech: i-t
File: 20141126_D3.bin
Init E (V) = 0.7
Smpl Intvl (s) = 0.2
Run Time (s) = 1.44e+4
Quiet Time (s) = 0
Sensitivity (A/V) = 1e-4

Figure 19: Electrochemical separated oxidation of dissolving pulp, sample D3.

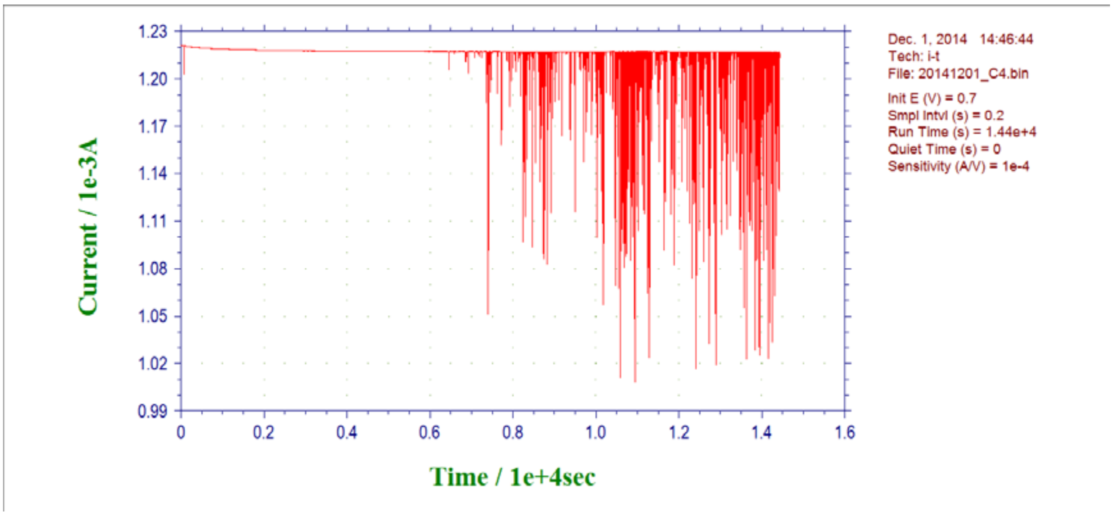

Figure 20: Electrochemical oxidation of innventia pulp, sample C4.

Short summary of electrolysis

What is seen from the electrochemical experiments is that an increase in current is obtained when separating the counter electrode from the oxidation products. When no separation is applied for the counter electrode the current is instead decreasing. This indicates that oxidation is increasing with time in the separated system and decreasing in the non-separated system.

Results from characterization methods

Characterization methods were chosen after availability and possibility to detect oxidation products from the electrochemically oxidized substrates. Due to lack of time and relevance for the project, not all samples were examined by NMR, XPS and/or FT-IR. Samples were chosen as to represent each type of setting and substrate.

After an experiment, analysis was performed by in first hand using liquid state NMR, applicable for all experiments with MGP as substrate. Analysis was performed with either D_2O and DMSO as solvent. FT-IR was performed on experiments in the 2nd and 3rd part and also on sample E13 from the 1st part.

For cellulosic solid substrates from the 2nd experimental part, XPS was performed on cotton samples A3-A6, Innventia sample C4, dissolving sample D4 and their corresponding references. Analysis was performed by SP in Stockholm.

Solid state NMR was performed on two cotton samples from the 2nd experimental part, A4 and A5, and cotton sample R2 from the 3rd part. Reference samples were analyzed for Innventia pulp, dissolving pulp and cotton. The analysis was performed by Innventia in Stockholm.

NMR

Liquid state NMR

Liquid state NMR was performed on a 400 MHz Varian Inc. NMR Systems, for some oxidized samples in the 1st experimental part. Both DMSO and D_2O were used as solvents. No quantitative measurements regarding concentrations etc. were done, since this was planned for later samples after the wanted oxidation had been proven. With this in mind, the peak height is not comparable between different samples but only internally in a sample spectra for relative comparison, hence the scale on the y-axis is not relevant in these results. Additional spectra can be seen in Appendix II.

References were made on pure MGP as well as on an evaporated sample of MGP in buffer solution. The carbons were assigned to their corresponding peak(s) as can be seen in Figure 22 and Figure 23. An MGP-molecule with numbered carbons is shown in Figure 21.

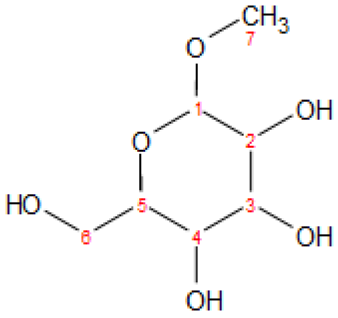

Figure 21: MGP with numbered carbons.

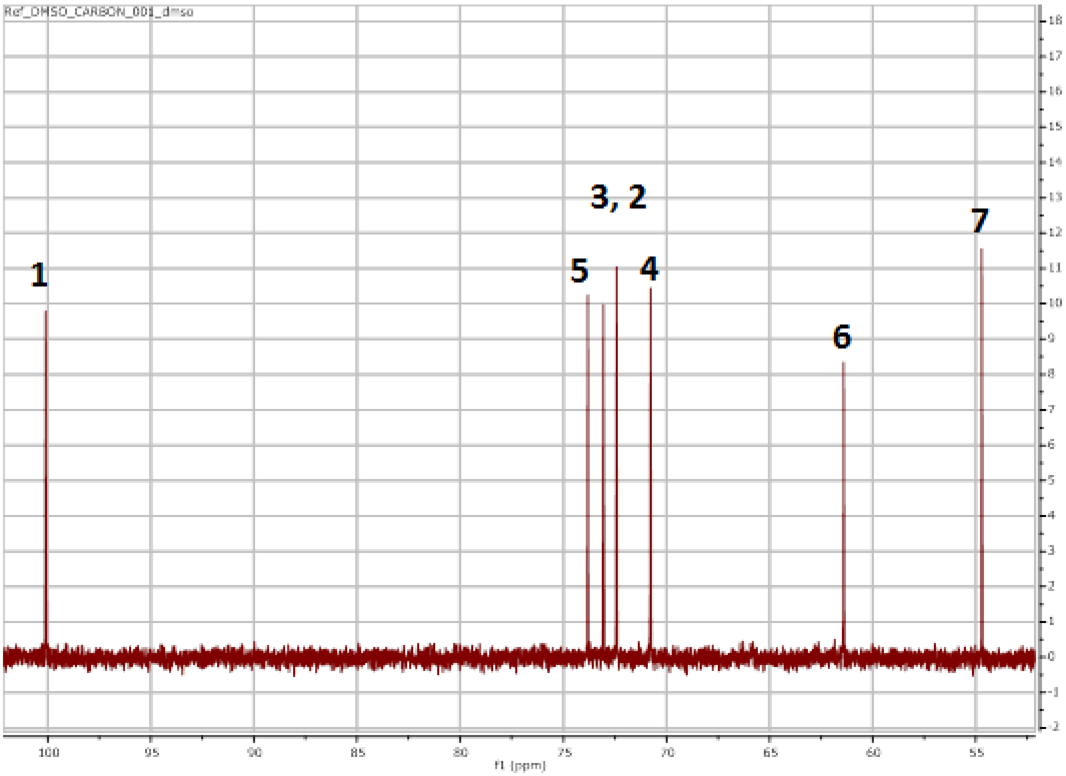

Figure 22: Reference ^{13}C NMR with assigned peaks for MGP.

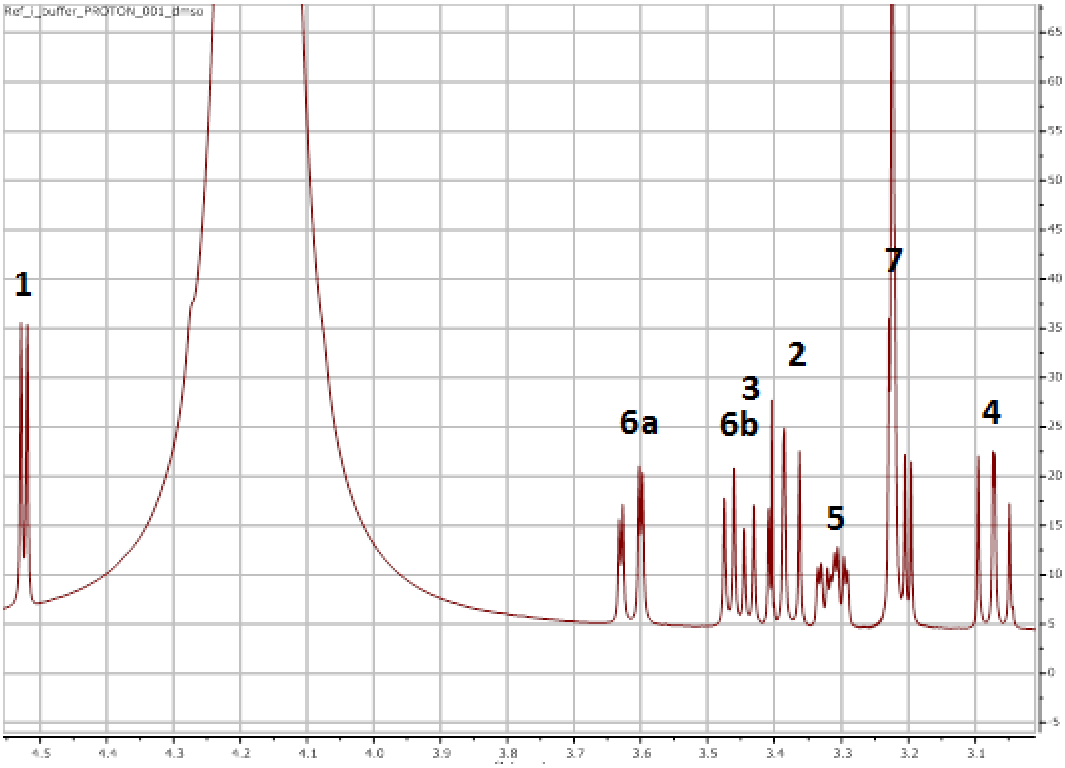

Figure 23: Reference 1H NMR with assigned peaks for MGP.

From comparison of these references with the oxidized samples, differences imply formation of new molecules during the experiment. In the ^{13}C-NMR spectra a shift of the C6-peak from around 62 ppm to around 173 ppm is proof of carboxylic group formation, based on chemdraw-projections. Additionally, the carbons on position C1-C5 are also estimated to shift sligthly. For ^{1}H NMR, estimated shifts of C4- and C5-protons would increase and the C6-protons would disappear, if formation of a carboxylic acid. If instead an aldehyde would form, the two protons on C6 would shift to around 9 ppm. The potentially formed carboxylic proton has an estimated peak around 12 ppm but this type of protons, like for other hydroxyl groups, are often difficult to detect and is not seen in obtained graphs. The large peak at around 4-5 ppm, visible in all ^{1}H NMR spectra, is water. This large peak can hide new peaks of C4 and C5 which additionally may also be quite small and are therefore hard to detect. But new small peaks in the area between 3.4 and 3.9 ppm are seen.

In the ^{13}C spectras, no removal of the 62 ppm peak can be seen. Instead a small new peak around 170 ppm is seen for some samples (E4, E12 and R5, seen in Figure 24, 26 and 27). Also many new peaks can be seen in the range between 60 and 110 ppm for some of the oxidized samples (see Figure 25). The same tendency is seen in the ^{1}H spectra with many new small peaks for the oxidized samples compared to a reference, exemplified in Figure 31. Additionally, the ^{1}H spectra of Figure 28-30 show oxidized samples E4, E12 and E13 displaying a new peak at around 9 ppm, which could be a carboxyl or carbonyl peak.

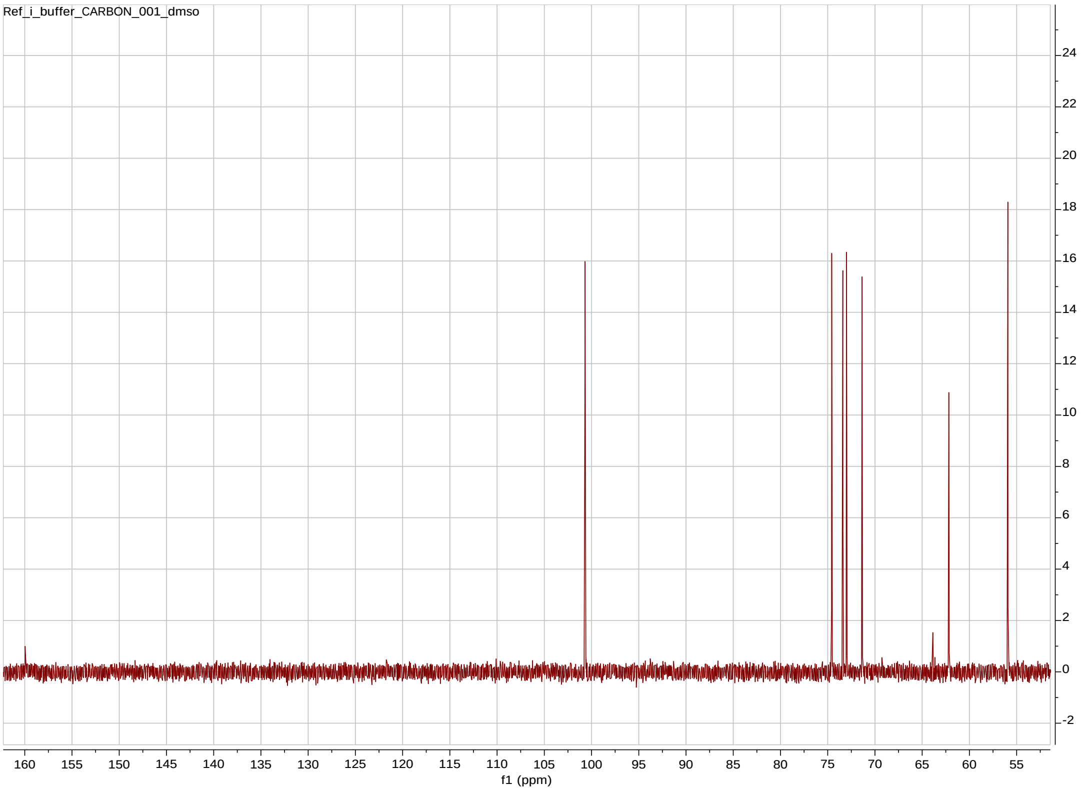

Figure 24: ^{13}C-NMR spectra on reference MGP, prepared in buffer.

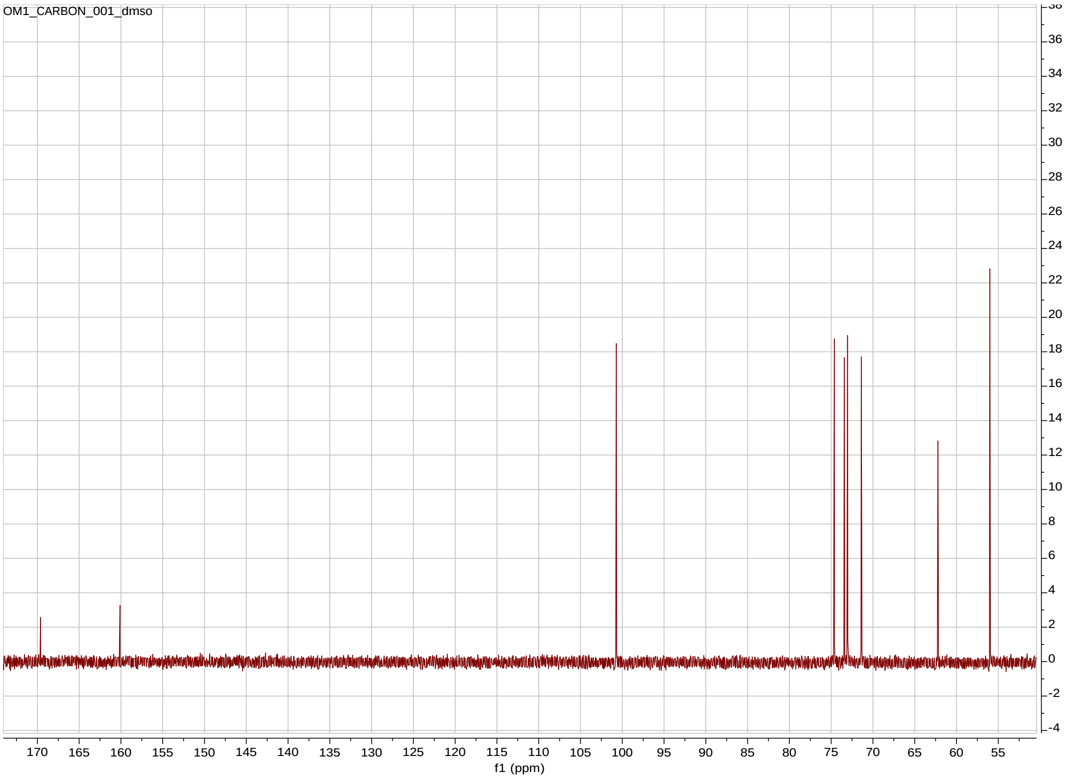

Figure 25: ^{13}C-NMR spectra of oxidized E12 showing a potential carboxyl peak at 170 ppm.

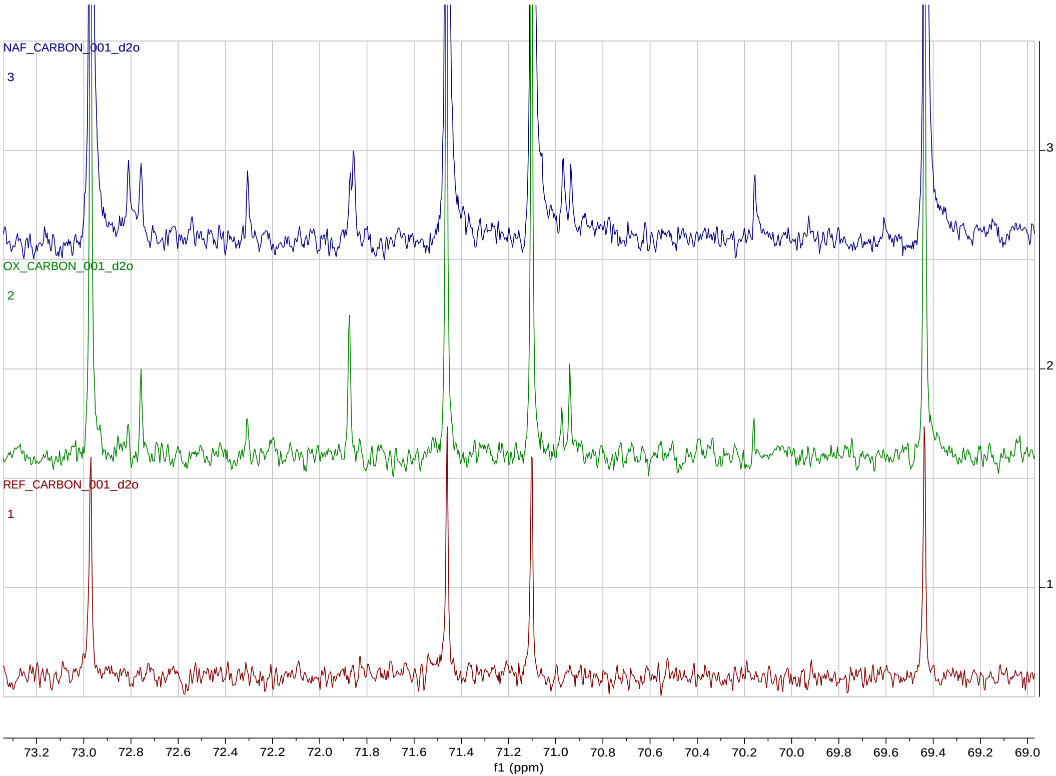

Figure 26: Comparison of ^{13}C-NMR for E6 (Naf), E4 (Ox) with a reference of MGP, in D2O.

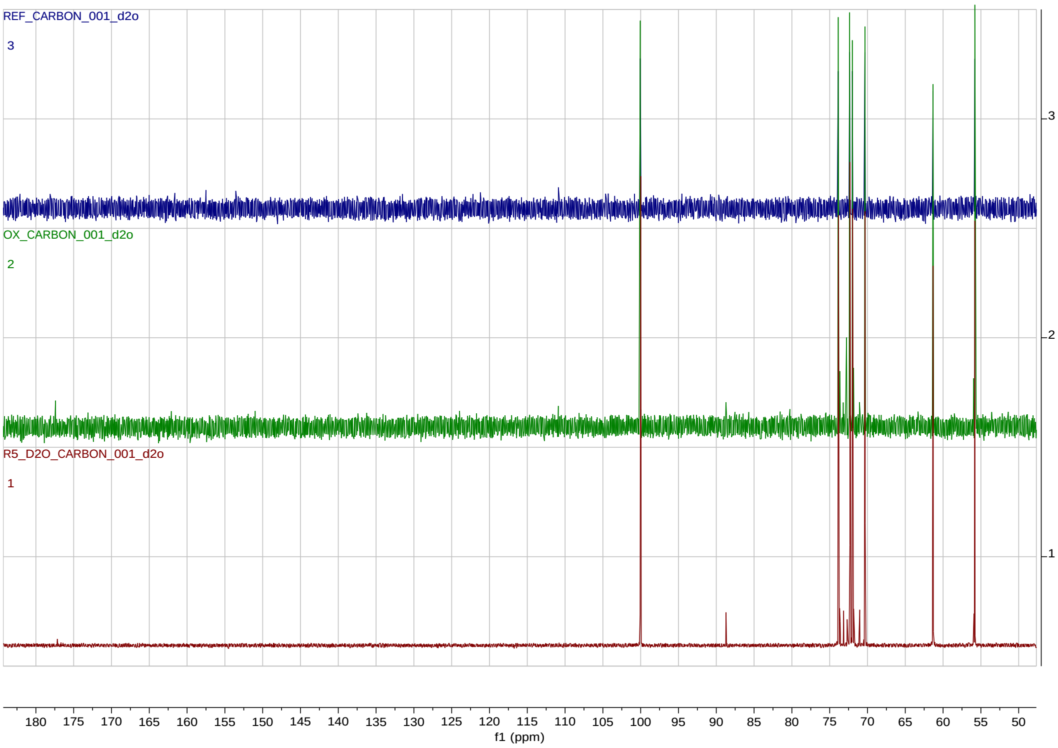

Figure 27: Comparison of ^{13}C-NMR for E4 (Ox) and R5 with reference sample of MGP, in D2O.

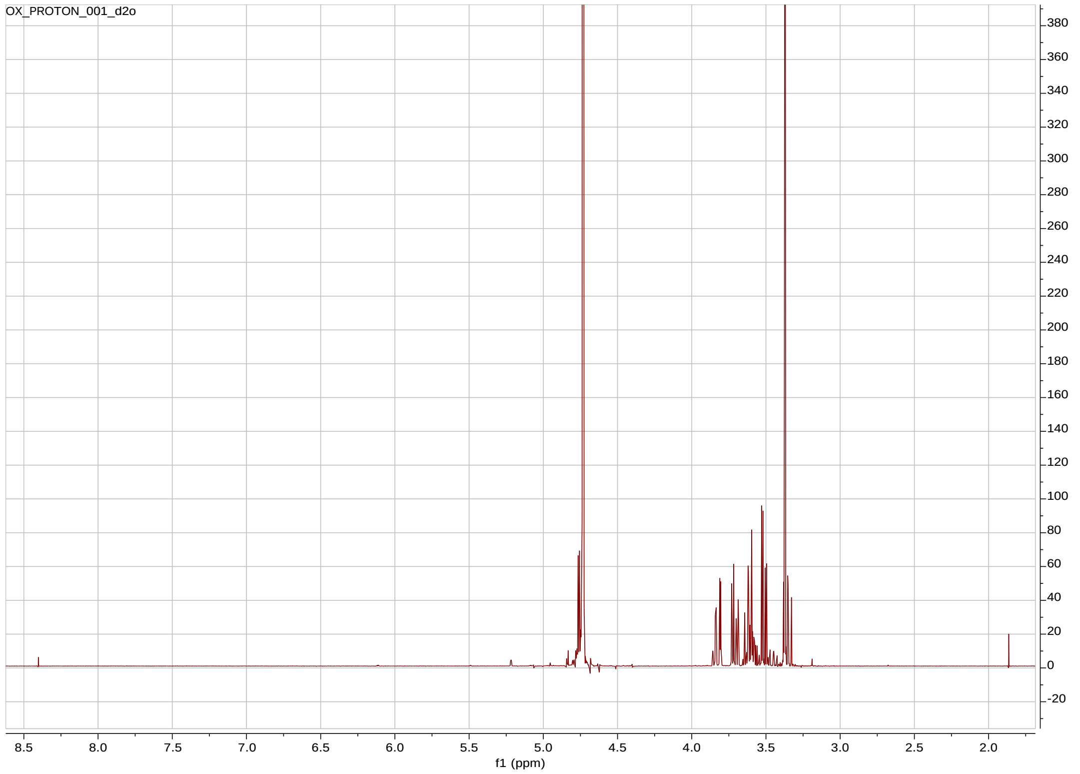

Figure 28: ^{1}H-NMR spectra of oxidized E4 showing a potential carboxyl peak at 8.5 ppm.

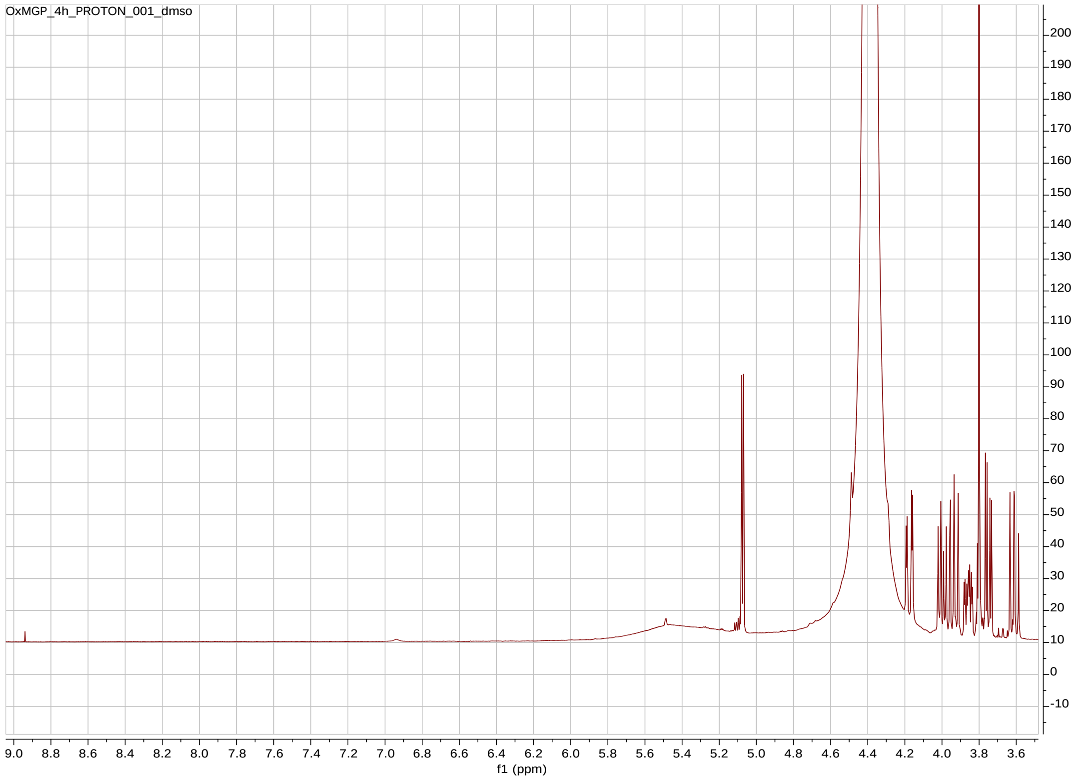

Figure 29: ^{1}H-NMR spectra of oxidized E13 showing a potential carboxyl peak close to 9 ppm.

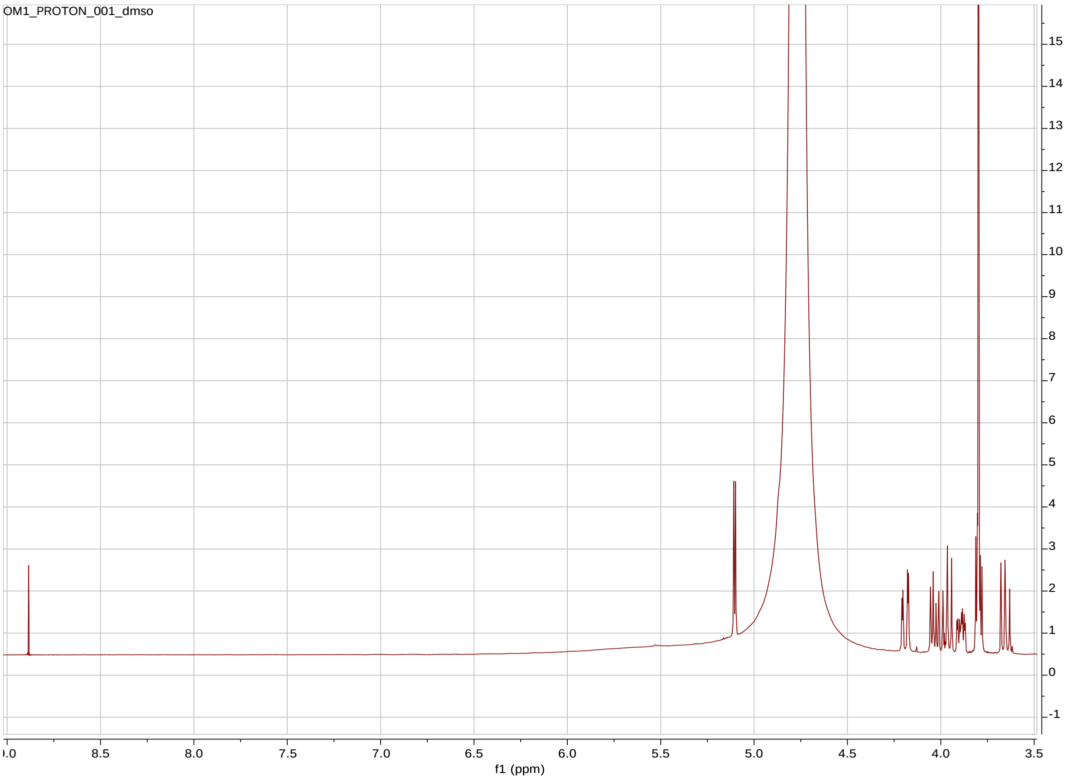

Figure 30: ^{1}H-NMR spectra of oxidized E12 showing a potential carboxyl peak close to 9 ppm.

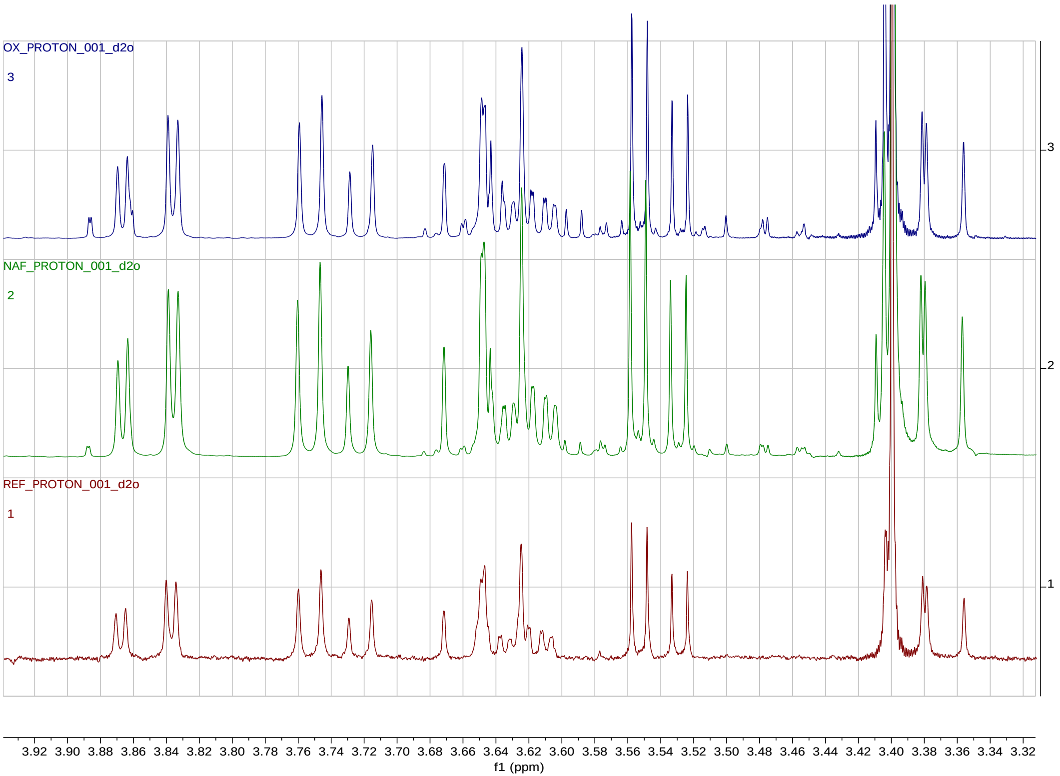

Figure 31: Comparison with ^{1}H-NMR for Ox (E4), Naf (E6) and Ref (pure MGP).

Flash chromatography, performed on sample E12

On sample E12, a flash chromatography was performed to purify the sample. From what was shown with the sample fractions dotted onto TLC plates, it was concluded that fraction 5 and combined fractions 11-12 contained a detected molecule each. Based on these implications, liquid state NMR, using DMSO as solvent, was performed on sample fraction 5 and sample fraction 11-12.

As seen in Figure 32-33, fraction 5 is likely to be the starting material. The result from fraction 11-12 (see Figure 34-35) on the other hand is not comparable with any other sample. A strong peak at around 170 ppm can be seen but not the other carbon peaks at 55-110 as would be expected.

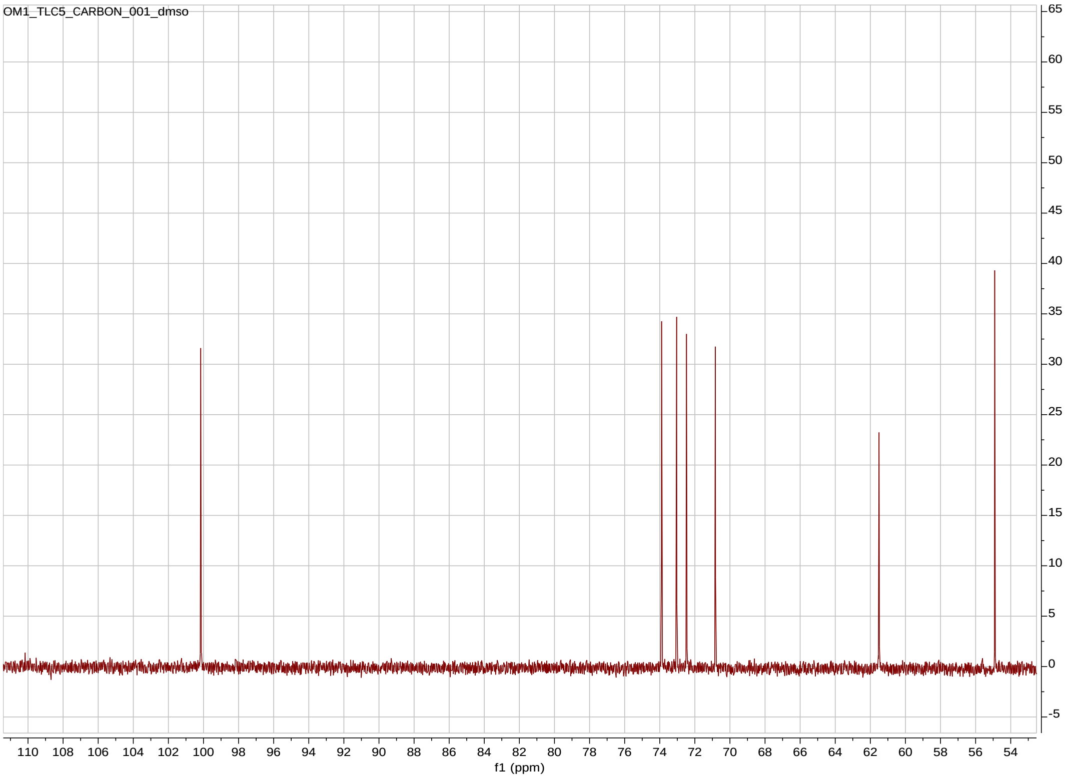

Figure 32: E12 fraction 5, analyzed with ^{13}C-NMR.

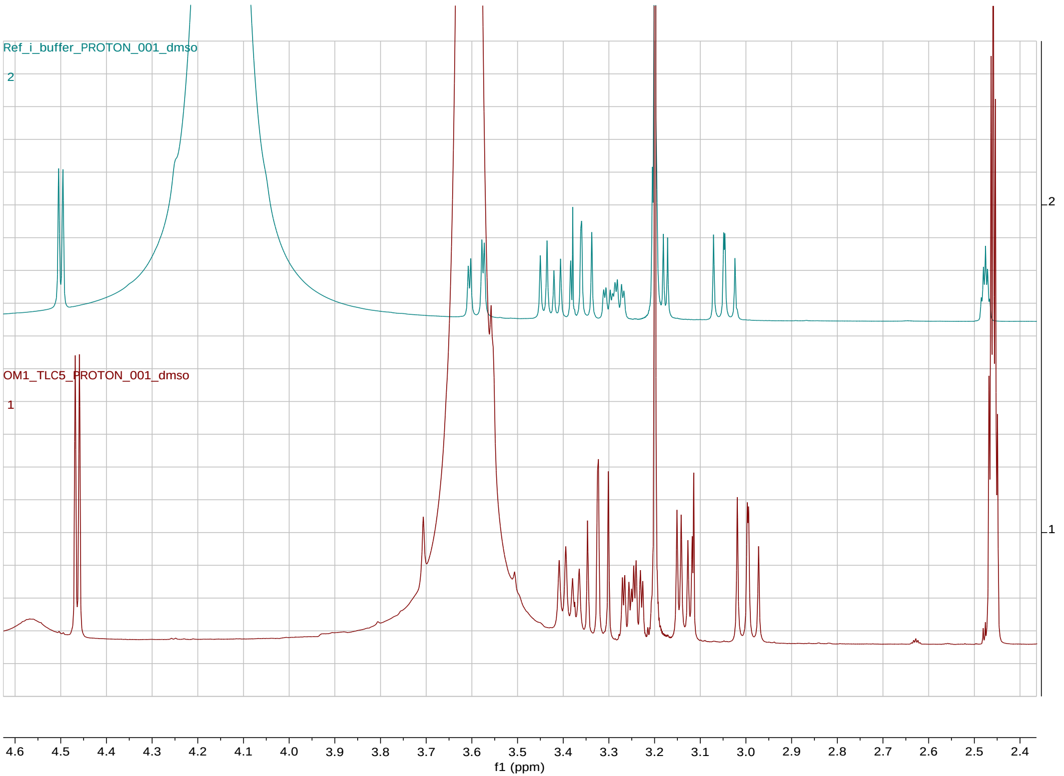

Figure 33: Comparison of ^{1}H NMR-spectra for E12 fraction 5 with reference.

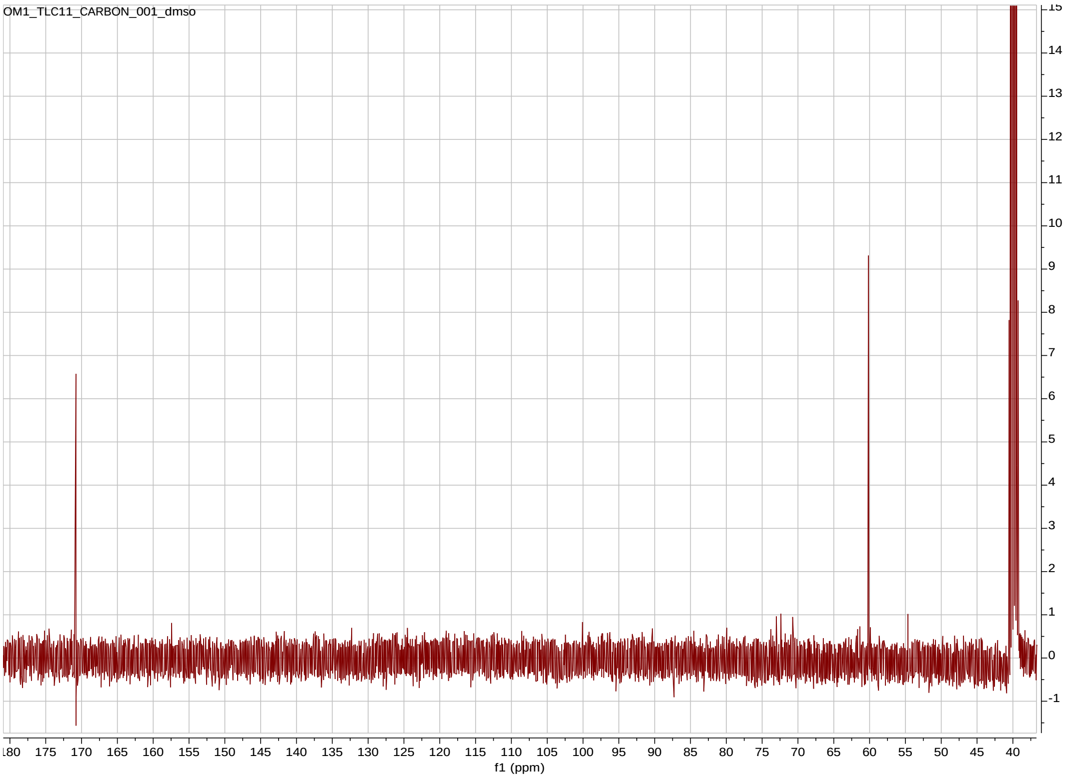

Figure 34: ^{13}C NMR-spectra of E12 fraction 11-12.

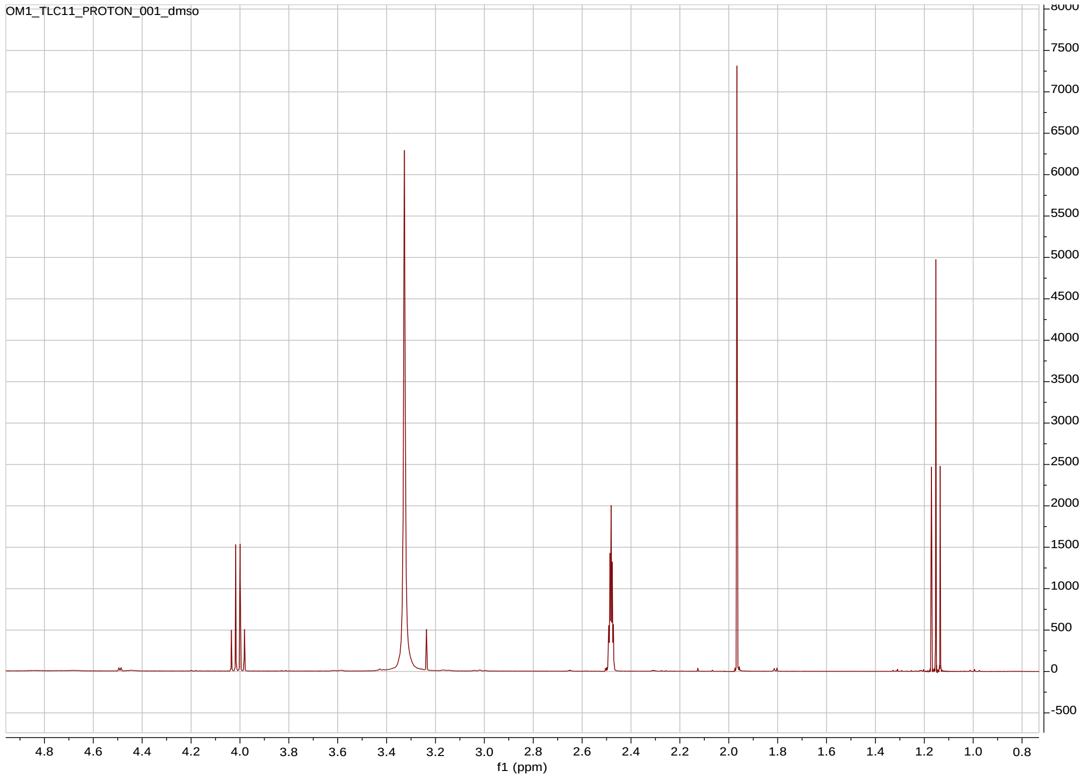

Figure 35: ^{1}H NMR-spectra of E12 fraction 11-12.

Solid state ^{13}C NMR on samples from 2nd and 3rd part

The specific surface area (SSA) of the three solid cellulose substrates were analyzed using solid-state NMR at Innventia and can be seen in Table 4. The results show that cotton has a lower SSA than the other substrates which in theory implies a lower yield from a comparable treatment. The Innventia pulp was shown to have the highest SSA, and is thus suggested to be the most reactive substrate.

Table 4: Specific surface area of the sample run in Solid state NMR.

Sample	LFAD SSA (m2/g)	SE (m2/g)
Cotton ref	71	5
Innventia ref *(Confidential)*	X	X
Dissolving ref	107	4
A4	66	5
A5	n/a	n/a
R2	78	8

A5's macromolecular structure seem to be affected by the longer oxidation it has been subjected to compared to other samples, which might be an effect from mechanical stirring and/or longer exposure to the mediator. It can be seen in Figure 36 that the C6-peak at around 62 ppm has decreased, which could be an indication of partial oxidation. The other peaks are also partly transformed. All spectra from the analyzed samples can be seen in Figure 37.

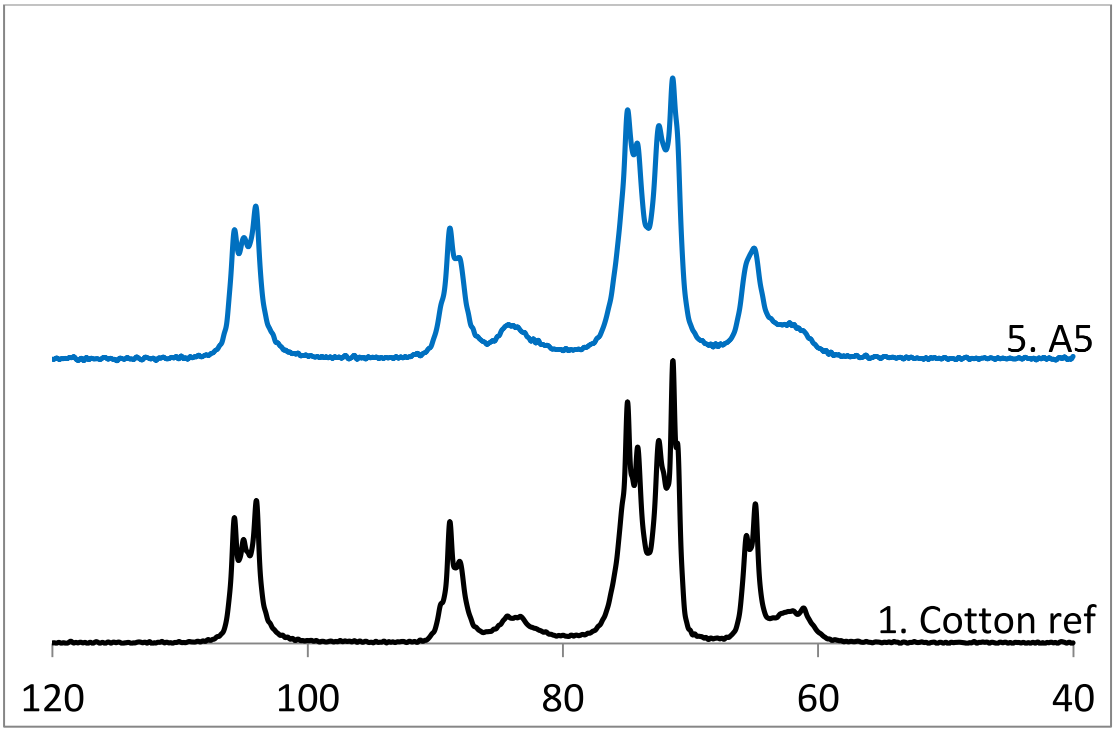

Figure 36: Solid state 13C NMR For cotton sample A5 and reference.

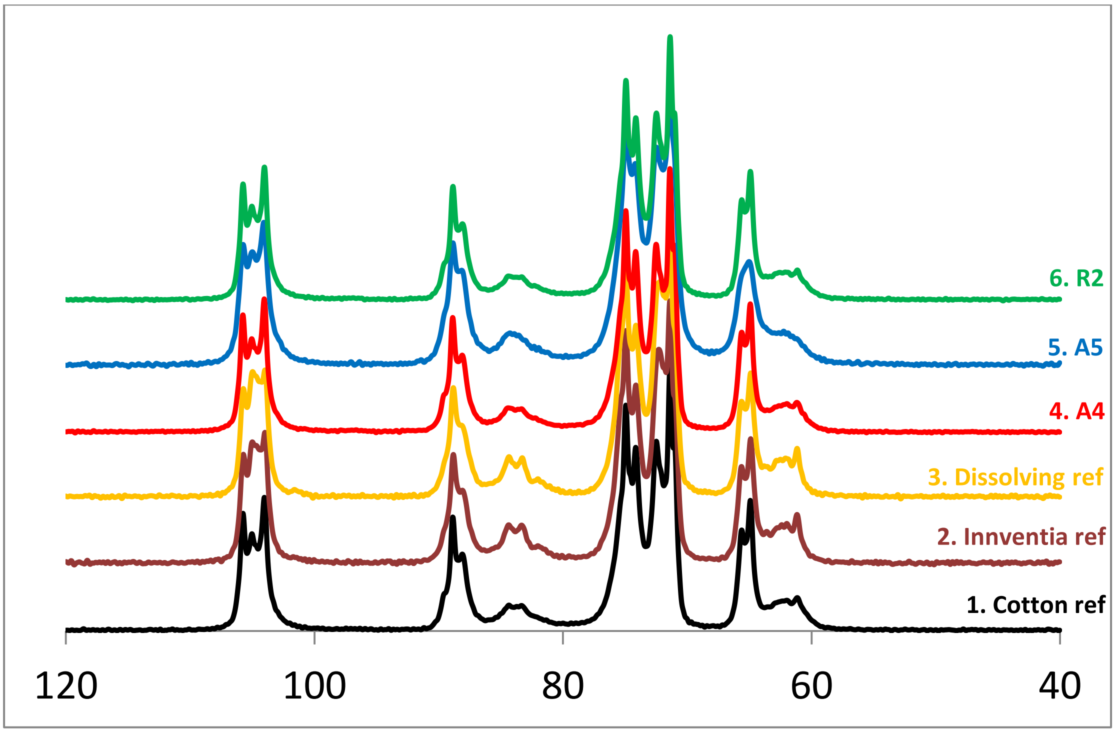

Figure 37: All solid state NMR spectra.

Short summary of NMR-characterization

From the spectra shown in this section, it can be concluded that new products are formed in the MGP-experiments, and that long run cotton-samples show a morphological change. However, new products might be degradation products from running MGP at too high potential. The flash chromatography resulted in NMR-spectra of Figure 34-35, which do not show all the peaks of an expected product.

FT-IR

Fourier Transformed Infrared Spectroscopy, FT-IR, was performed using a Perkin Elmer Frontier FT-IR. The IR-spectra are shown overlapping for an easy comparison between references with electrochemically oxidized samples (Figure 38-41), for the oxidized samples of part 3 (Figure 42) as well as for all references together (Figure 43).

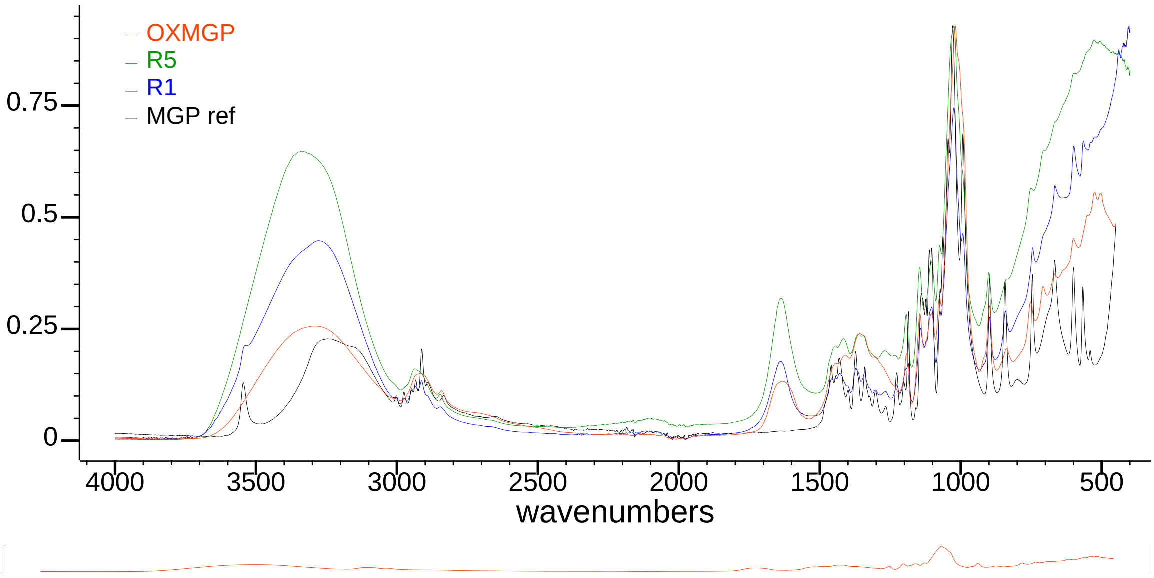

Figure 38: IR spectra for MGP-samples (E12, R1, R5 and reference).

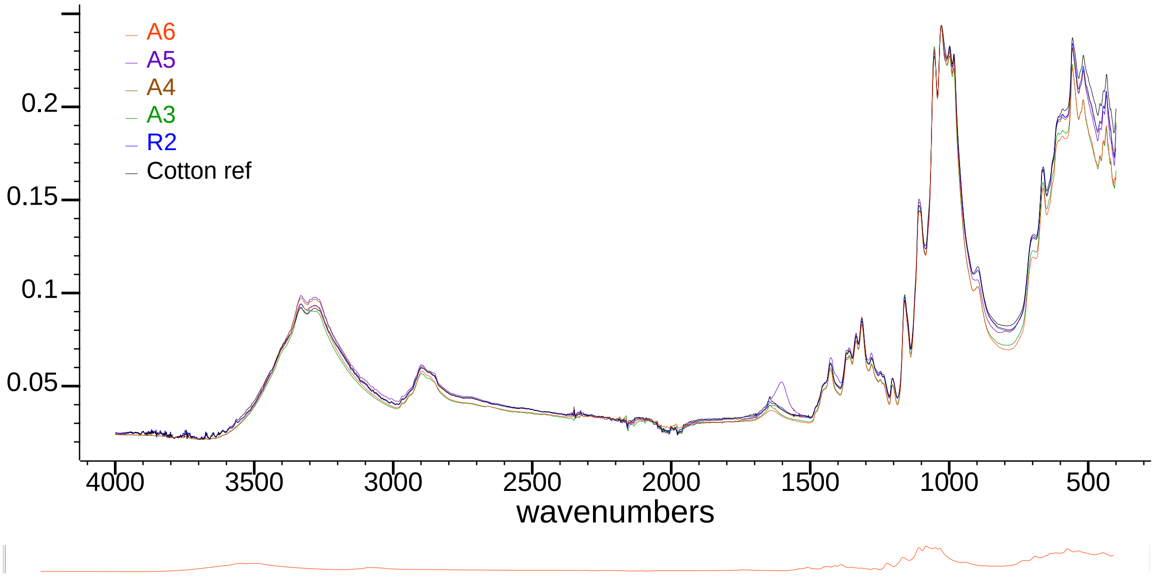

Figure 39: IR spectra for Cotton-samples (A3-A6, R2 and reference).

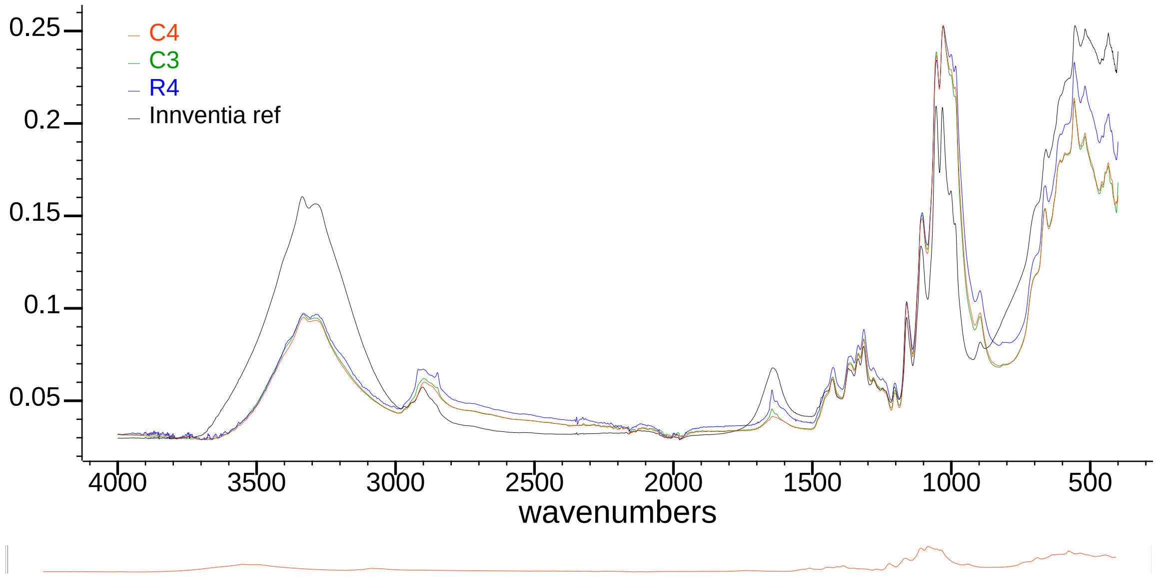

Figure 40: IR spectra for Innventia pulp samples (C3-C4, R4 and reference).

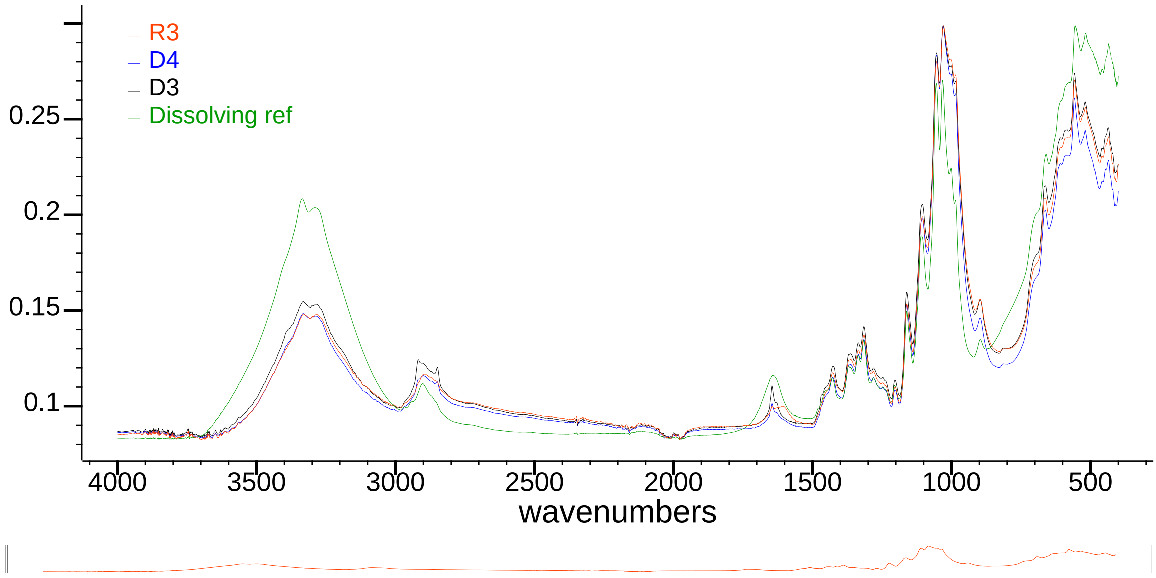

Figure 41: IR spectra for Dissolving pulp samples (D3-D4, R3 and reference).

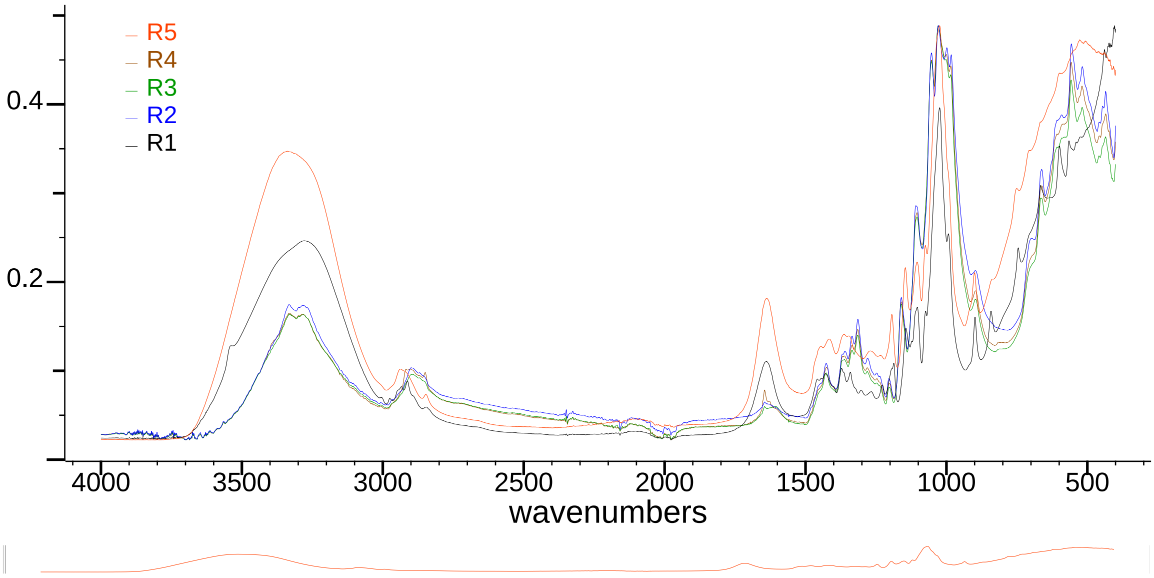

Figure 42: IR spectra for the oxidized samples (R1-R5) from experimental part 3.

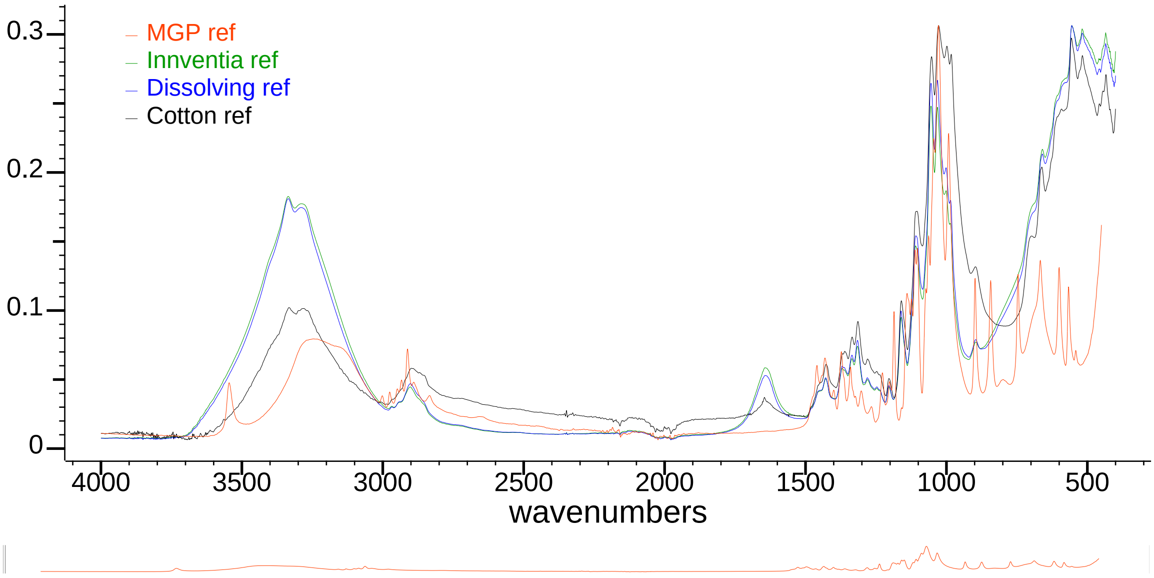

Figure 43: IR spectra for all reference samples for comparison.

Short summary of FT-IR characterization

The results shown in this section does not point out any proof of carboxylic group formation, allthough it shows differences at around 2900 cm^{-1} and 1650 cm^{-1} (at 3300 cm^{-1} the water peak is an obvious variation). It is hard to say if the peak-variation is due to differing amount of water bound in a substrate or if it results from new products formed.

XPS

Some samples (cotton samples A3-A6, Innventia sample C4, dissolving sample D4 and their corresponding references) from the 2nd part of experiments *electrochemical oxidation of different substrates,* were analyzed using a monochromatic Al x-ray source. Spectra were recorded with a Kratos AXIS Ultra^{DLD} XPS (Kratos Analytical, Manchester, UK). Reference chemical shifts were adapted from a database[58]. The results can be seen in Tables 5-7 below, where Table 5 is showing chemical composition in atomic % for all analyzed samples and Table 6 is showing relative composition specified for each type of (relevant) carbon functionality, for all samples except C4 and D4. In Table 7 the total amount of carbon in atomic % is shown for each carbon functionality of sample A6, since this seems to be the most oxidized hence most interesting sample.

A6 displays a higher atomic ratio O/C (0.86) compared to the reference (0.79), which implies an increase in oxidation. The Innventia pulp also shows a slight increase in atomic ratio when comparing the reference (0.81) to C4 (0.84). When looking at Table 6, a relative increase in the carbons C3 and C4 simultaneously as a decrease in C2 implies oxidation. A decrease in C2 is seen for all samples compared to their references, but a relative increase in C3 is only seen for the 24 h oxidized cotton with a separation vessel on the counter electrode (A6). When looking at carbon C4 a very small increase can be seen for samples A5 and C4, whereas it is unaffected for samples A6 and D4.

The samples A5 and D4 (also A6 and C4 are slightly affected) show traces of contamination, seen in Table 6 where carbon C1 has increased for both samples from around 5 relative % to above 20 relative %.

Samples C4 and D4 have not been curve-fitted, but their curves were of similar shape to cotton reference and sample A6.

Table 5: Relative surface composition in atomic % and the atomic ratios O/C.

Sample	**Atomic %**								**Atomic ratio**
	C	**O**	**Na**	**F**	**N**	**Ca**	**Cl**	**Si**	**O / C**
Cotton ref.	56.0	44.0	-	-	*	-	-	*	0.79
A3	55.9	44.1	-	-	-	-	-	-	0.79
A4	55.8	44.2	*	-	*	*	-	-	0.79
A5	58.3	40.0	1.0	0.1	0.4	-	-	0.2	0.69
A6	53.5	46.2	0.1	-	0.2	-	-	0.1	0.86
Innventia ref.	55.2	44.8	-	-	-	-	-	-	0.81
C4	54.1	45.5	0.3	-	-	-	-	0.1	0.84
Dissolving ref.	56.3	43.7	-	-	-	-	-	-	0.78
D4	62.3	37.4	0.1	-	-	0.1	0.1	0.1	0.60

- = signal at noise level in detail spectra (below about 0.05-0.1 atomic%)

* = weak peaks detected in detail spectra, low amounts estimated to << 0.5 atomic%

Table 6: Chemical shifts in high-resolution carbon spectra, with the binding energy positions for each carbon peak after adjusting C1-carbon to 285.0 eV as reference value. The chemical shifts are due to carbons in different functional groups with mainly oxygen.

Sample	C 1s tot = 100%			
	C1 285.0 eV	C2 286.7-8 eV	C3 288.1-3 eV	C4 289.3-6 eV
Cotton ref.	7.2	70.7	20.1	2.1
A5	21.6	57.3	18.8	2.2
A6	5.5	69.9	22.5	2.1
Innventia ref.	2.7	75.1	20.7	1.5
C4	4.9	73.5	19.9	1.7
Dissolving ref.	3.1	77.0	18.8	1.1
D4	23.4	59.8	15.7	1.1

Table 7: The total amount of carbon (in atomic%) is divided into different carbon peaks for sample A6 and compared to reference cotton.

Sample	Atomic %				
	C tot	C1	C2	C3	C4
Cotton ref.	56.0	4.0	39.6	11.2	1.2
A6	53.5	2.9	37.4	12.1	1.1

The high-resolution carbon spectra, with chemical shifts due to carbons in different functional groups, have been grouped into four types of carbon peaks. Here mainly bonds between C and O have been taken into account.

C1-carbon: unoxidised carbon C-C, C-H, C=C

C2-carbon: carbon with one bond to oxygen C-O, C-O-C

C3-carbon: carbon with two bonds to oxygen C=O, O-C-O

C4-carbon: carbon with three bonds to oxygen O-C=O, C(=O)OH

Short summary of XPS-characterization

Small changes indicating oxidation are seen, especially for the longer oxidized sample A6. It is obvious that a longer reaction time is needed.

Discussion

As can be seen from studying the electrochemical graphs from the first experimental part, they display many interruptions. To make the electrochemical setup work was the most troublesome task. In a theoretical point of view, a separation vessel on the counter electrode is a must for an oxidized sample not to be affected by reduction. In reality the separation vessel seem to affect the current, resulting in gaps that were seen for many of the samples when this was applied (E5-E6, E8-E11, A3, A6, C3 and D3 had all a vessel on the counter electrode). One possible explanation is that the surface area of the counter electrode, which was relatively small compared to the working electrode, was in fact too small to get an effective current working in the system. Another problem was formation of salt crystals in the separation vessel membrane for the reference electrode, even though it was constantly kept in a buffer solution.

When the setup was modified for the second experimental part (more vigorant stirring with a larger bar, a higher voltage applied and a sligthly larger surface area of the counter electrode) the graphs were not as much affected by disturbances. This was also a fact when the counter electrode was separated from the oxidized species, concluding that the separation vessel was not the only reason for the interruptions in the first part. Instead the experiments from the second part showed, when separation of the counter electrode was applied, that the graphs were not as disrupted as in the previous setup and had a positive slope, indicating that oxidation increased with time. Connecting these thoughts to the characterization might suggest that degradation products were formed from MGP, since new peaks can be seen but not the wanted carboxyl-peak. A suggestion is to examine the reaction over time to see when the reaction is finished and what products are formed at different intervals.

Regarding the setup when running electrochemical oxidation of MGP, pH might have been too high since the conditions were designed for cellulose. Possibly MGP is not suited for a reaction designed for cellulose, hence a deeper understanding of how these substrates are affected by different settings, such as pH, reaction time and temperature are crucial for further development. In [21] it is stated that degradation of the substrate occurs with pH above 9 accompanied by side-reactions of TEMPOH, with a low yield as result. In this article it is also stated that β-alkoxy elimination occurs when oxidized glucopyranosides are subjected to alkaline conditions. From these statements follows that MGP might not be suitable to use under same conditions as cellulose but it will need further investigations.

Regarding the characterization analysis, changes are seen with liquid state NMR spectra when comparing samples of MGP oxidized for 24 h with reference. The formation of many small new peaks is an indication that some new structure has formed, and this is especially interesting for samples showing a new peak at 170 ppm, which is significant for carboxylic groups. On the other hand there is no removal of the C6 unoxidized peak, suggesting that oxidation was performed to mild for the C6 hydroxyl group to be fully oxidized. It is also a possibility that degradation products have formed and this needs further investigation and characterization studies.

Results from the first part indicated that a longer reaction time was needed for full oxidation, but due to lack of time this was not possible to do in the second part, hence a total oxidation was therefore not expected. Instead an indication of the reactivity and further understanding of how to improve the system was sought. A more stable setup was achieved in the second experimental part, but poorer signs of oxidation products was obtained. When comparing experiments from TEMPO-mediated electrochemical oxidation with regular TEMPO-mediated oxidation, no distinct difference can be seen in the spectra from either NMR or FT-IR. This indicate that both methods used in this project performed inadequate oxidation. In this study, a stop in pH-decrease was used as a reference for when to quench the regular TEMPO-mediated oxidation. Another approach, used in many studies, is to let the reaction run for 1 h, which suggests a higher yield if the substrate is not available for oxidation from the start.

For further optimization regarding oxidation of cellulose, a counter electrode with a larger surface area kept in a separation vessel is suggested for electrochemical experiments, along with extended reaction time, pH-control and temperature control to minimize degradation products.

NMR

From the NMR studies, new peaks can be seen indicating a chemical reaction, but it can not be fully proven that a carboxyl group is formed. From the fractionated sample E12 (oxidized MGP for 24 h at 0.5 V) which was thought to have been oxidized due to the peak formed around 170 ppm, it can be stated that the starting material was in fraction 5. In fraction 11-12 on the other hand, it can not be concluded what is shown in the spectrum. But the fact that these molecules could be separated by a flash column and further showing different peaks in NMR spectra is proof of that new products, but possibly degradation products, were formed in the reaction.

Different types of cellulose have been shown previously[59] to be oxidized with varying success. In this study it was expected from the potentially more reactive substrates (Innventia pulp and dissolving pulp) to be more oxidized, which was not proven. A reason for the vague results are probably too short reaction times suggesting that a longer time is required for oxidation changes to be fully observed.

FT-IR

In the FTIR-spectra, a distinct carboxyl peak at 1732 should be seen on the oxidized samples and to be proof of a carboxylic group. On the other hand, if the carboxyl is not protonated and still in a sodium form it will show a peak at around 1600[51], as shown in Figure 44.

As can be seen in Figure 38-42, a peak around 1630 cm^{-1} is present for all oxidized samples of MGP, but it is also seen for some of the reference samples in Figure 43, though in different shapes. The peak at 1630 cm^{-1} may possibly be a carboxylate bound to a sodium ion if not all have been removed from dialysis. But for the other substrates, which contain some water, the peak is visible also in the references. So most probably the peak is connected to water bending. Another speculative possibility is that TEMPO has reacted with MGP in some way and formed an amide bond, which would give an N-H bending around 1600 cm^{-1}.

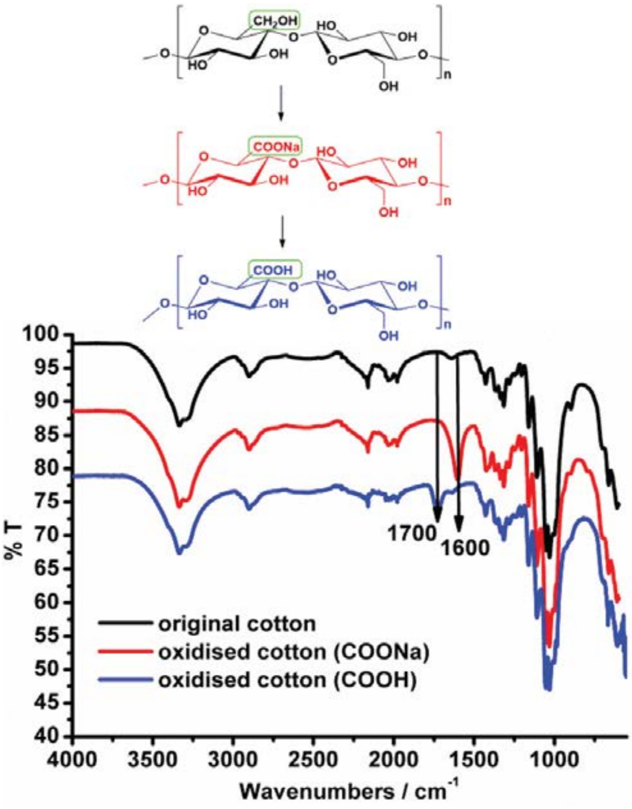

Figure 44: IR-spectra on cotton. Reproduced from Ref. 45 with permission from The Royal Society of Chemistry.

XPS

The small increase in atomic ratio for oxygen content in sample A5, which was exposed to oxidative conditions for 24 h compared to 4 h for the other samples, shows that a longer time is needed for a complete oxidation with the existing setup. The expected higher original oxidation of Innventia pulp and dissolving pulp was not observed. They also did not react faster in the electrochemical experiments compared to cotton with same reaction time.

Conclusions

The main goal was to develop a setup to achieve environmentally friendly electrochemical oxidation of cellulose, with a future goal of producing high quality recycled fibres.

This has been performed by characterization studies aiming to determine the oxidized products functionality. For this reason, structural changes have not been thoroughly investigated. These changes will obviously occur simultaneously as the functionality changes when bonds are broken, hence the methods chosen could have been expanded to include some type of method for structural observations, such as XRD or SEM.

The setup used was not functioning optimal for the type of electrochemical experiment that was conducted in this work. A larger counter electrode would be needed and in that case it would also be applicable with a separate vessel for it, as to protect oxidized products from reduction. pH-control is also needed as well as specific pH adjustment, depending on which substrate is used. Still, some new product(s) was formed, indicated by new peaks shown in the liquid state NMR spectra, change of atomic ratio in XPS and the possibility to fractionate sample E12 by chromatography. It is possible (but not proven) that a small content of MGP/cellulose with fully oxidized C6 hydroxyl group was converted into a carboxylic group. If an aldehyde group was formed it is difficult to see this due to its diol/hemiacetal equilibrium state.

Upscaling of the samples would provide larger fractions for chromatographic separation and further enable higher concentrations for NMR analysis. The results from solid state NMR, which showed that longer oxidation affected the macromolecular structure, is important to take into consideration. Since this might imply depolymerization it is important to examine what is crucial for this unwanted effect. Perhaps a lower pH is better for longer oxidations, compared to the original TEMPO oxidation which is performed in a much shorter time. As Bragd et al.[21]

concluded, from seeing that many carbon peaks of an NMR-spectra were split into several smaller ones:

> *The pH optimum is lower in absence of NaBr (approximately 9.3 compared to 10.5 for a NaBr catalyzed oxidation)*

From what is presented above, a short summary of the major conclusions in this work is listed below:

- To develop the setup it must be concluded that C6 hydroxyl groups are truly oxidized into carboxyl groups
- Using methyl-α-D-glucopyranoside as a model system might not be the best way to develop an oxidation method for cellulose
- Longer time is needed and/or more efficient reaction conditions, e.g. larger electrodes (surface area) and better mass transfer (more stirring/lower substrate concentration) to develop optimal oxidation
- A better understanding of the electrochemistry equipment and how it should be designed to work properly
- A pH control by titration as to maintain wanted pH when carboxylic groups are formed
- Protonation of carboxylic groups by an acidic step, before characterizing the sample

Outlook

From the results presented in this master thesis, a lot of new questions have been raised. As a continuation of this project some specific suggestions are proposed.

- Further development and optimisation of the reaction:
    - By using larger electrodes, bigger volumes and more effective stirring
    - By studying the effect of pH and temperature
    - And subsequently design experiments for optimal reaction conditions by for example running 48 h reactions with removal of fractions every hour to study the reaction over time
- Making sure that C6 hydroxyl groups are truly oxidized into carboxyl groups:
    - Adding a protonization step
    - Characterization with mass spectrometry

Additionally I had a lot of ideas in the beginning of the project that did not fit into the short time provided. A short overview of what I think would be interesting to investigate connected to the scope of my project is presented below.

- *Preparation of nano cellulosic fibres:*
    - Examine the possibility of spinning oxidized fibres directly from the electrolyte media
    - Perform analysis in form of the application where the nanocellulosic fibres are to be used
- *Electrochemistry:*
    - Using ionic liquid / cold alkali as a combined solvent and electrolyte
    - Testing microwave (or another type of energy source, e.g. from the ones presented in the chapter: *activation of cellulose*) as a pre-treatment prior to electrochemical oxidation
    - Immobilize tempo on solid support (polymer / silica) to facilitate regeneration and to run a reaction for multiple cycles
- *Examine the effect of electrooxidation on fibre structure and quality:*
    - By e.g. XRD, SEM and the elastic modulus by tensile testing

References

---

[1] Palme, A., Idström, A., Nordstierna, L., and Brelid, H. (2014). Chemical and ultrastructural changes in cotton cellulose induced by laundering and textile use. *Cellulose*, 21(6), 4681-4691.

[2] Collinson, S. R., and Thielemans, W. (2010). The catalytic oxidation of biomass to new materials focusing on starch, cellulose and lignin. *Coordination Chemistry Reviews*, 254(15), 1854-1870.

[3] Coseri, S., Biliuta, G., Simionescu, B. C., Stana-Kleinschek, K., Ribitsch, V. and Harabagiu, V. (2013). Oxidized cellulose-survey of the most recent achievements. *Carbohydrate Polymers*, 93(1), 207-215.

[4] *World Cotton Production*. Cotton incorporated, monthly economic letter, November 2014.

[5] Lena Youhanan (2013) *Environmental assessment of Textile Material Recovery Techniques: Examining Textile Flows in Sweden (*Master of Science thesis, Industrial Ecology, Royal Institute of Technology)

[6] Gerland, P., Raftery, A. E., Ševčíková, H., Li, N., Gu, D., Spoorenberg, T., Alkema, L., Fosdick, B. K., Chunn, J., Lalic, N., Bay, G., Buettner, T., Heilig, G. K., and Wilmoth, J. (2014). World population stabilization unlikely this century. *Science*, 346(6206), 234-237.

[7] Boyer, R. F. (2005). *Concepts in Biochemistry*. 3rd edition. United States of America: John Wiley & Sons, Inc.

[8] Krässig, H. A. (1993) *Cellulose: structure, accessibility, and reactivity*. Amsterdam: Gordon and Breach Science Publishers.

[9] Isogai, A., Saito, T., and Fukuzumi, H. (2011). TEMPO-oxidized cellulose nanofibres. *Nanoscale*, 3(1), 71-85.

[10] Anastas, P. T., and Warner, J. S. (1998). *Green chemistry: Theory and practice.* Oxford: Oxford Univ. Press.

[11] Katsuki, T. (1995). Catalytic asymmetric oxidations using optically active (salen)manganese(III) complexes as catalysts. *Coordination Chemistry Reviews*, 140, 189-214.

[12] Sheldon, R. A. (2012). Fundamentals of green chemistry: efficiency in reaction design. *Chemical Society Reviews,* 41, 1437–1451.

---

[13] Noyori, R., Aoki, M., and Sato, K. (2003). Green oxidation with aqueous hydrogen peroxide. *Chemical Communications*, 9(16), 1977-1986.

[14] Bragd, P. L., van Bekkum, H., and Besemer, A. C. (2004). TEMPO-mediated oxidation of polysaccharides: Survey of methods and applications. *Topics in Catalysis,* 27(1), 49-66.

[15] Zouni, A., Witt, H., Kern, J., Fromme, P., Krauss, N., Saenger, W., and Orth, P. (2001). Crystal structure of photosystem II from synechococcus elongatus at 3.8 angstrom resolution. *Nature*, 409(6821), 739-743.

[16] Bäckvall, J-E. (2004). *Modern Oxidation Methods.* Wiley-VCH Verlag GmbH & Co.

[17] Song, X., and Law, K-N. (2010). Kraft pulp oxidation and its influence on recycling characteristics of fibres. *Cellulose Chemistry and Technology,* 44 (7-8), 265-270.

[18] Sun, B., Gu, C., Ma, J., and Liang, B. (2005). Kinetic study on TEMPO-mediated selective oxidation of regenerated cellulose. *Cellulose*, 12(1), 59-66.

[19] de Nooy, A. E. J., Besemer, A. C., and van Bekkum, H. (1995). Selective oxidation of primary alcohols mediated by nitroxyl radical in aqueous solution. Kinetics and mechanism. *Tetrahedron,* 51(29), 8023-8032.

[20] Arends, I. W. C. E., Li, Y., Ausan, R., and Sheldon, R. A. (2006). Comparison of TEMPO and its derivatives as mediators in laccase catalysed oxidation of alcohols. *Tetrahedron,* 62(28), 6659-6665.

[21] Bragd, P. L., Besemer, A. C., and van Bekkum, H. (2000). Bromide-free TEMPO-mediated oxidation of primary alcohol groups in starch and methyl α- d-glucopyranoside. *Carbohydrate Research*, 328(3), 355-363.

[22] Ma, Y. (2010) *Nitroxides in Mechanistic Studies: Ageing of Gold Nanoparticles and Nitroxide Transformation in Acids*. Chapter 4. PhD thesis, University of York.

[23] Wells, A., Teria, M., and Eve, T. (2006). Green oxidations with laccase-mediator systems. *Biochemical Society Transactions,* 34(2), 304-308.

[24] Saito, T., Kimura, S., Nishiyama, Y., and Isogai, A. (2007). Cellulose nanofibres prepared by TEMPO-mediated oxidation of native cellulose. *Biomacromolecules*, 8(8), 2485-2491.

[25] Isogai, T., Saito, T., and Isogai, A. (2011). Wood cellulose nanofibrils prepared by TEMPO electro-mediated oxidation. *Cellulose*, 18(2), 421-431.

---

[26] Ciriminna, R., Pagliaro, M., Blum, J., and Avnir, D. (2000). Sol-gel entrapped TEMPO for the selective oxidation of methyl α d-glucopyranoside. *Chemical Communications*, (15), 1441-1442.

[27] Brunel, D., Fajula, F., Nagy, J. B., Deroide, B., Verhoef, M. J., Verum, L., … van Bekkum, H. (2001). Comparison of two MCM-41 grafted TEMPO catalysts in selective alcohol oxidation. *Applied Catalysis A, General*, 213(1), 73-82.

[28] Bolm, C., and Fey, T. (1999). TEMPO oxidations with a silica-supported catalyst. *Chemical Communications*, (18), 1795-1795

[29] Dijksman, A., Arends, I. W. C. E., and Sheldon, R. A. (2000). Polymer immobilised TEMPO (PIPO): An efficient catalyst for the chlorinated hydrocarbon solvent-free and bromide-free oxidation of alcohols with hypochlorite. *Chemical Communications,* (4), 271-272.

[30] Dijksman, A., Arends, I. W. C. E., and Sheldon, R. A. (2001). The Ruthenium/TEMPO-catalyzed aerobic oxidation of alcohols. *Platinum Metals Review*, 45(1), 15-19.

[31] Yu Y., Gao B., and Li, Y. (2013) Immobilized 2,2,6,6-tetramethyl-piperidinyl-1-oxy catalyst on polymer microspheres and its catalytic oxidation of benzyl alcohol with molecular oxygen. *Chinese Journal of Catalysis,* 34(9), 1776-1786.

[32] Shi, S., Pelton, R., Fu, Q., and Yang, S. (2014). Comparing polymer-supported TEMPO mediators for cellulose oxidation and subsequent polyvinylamine grafting. *Industrial & Engineering Chemistry Research*, 53(12), 4748-4754.

[33] Coseri, S., and Biliuta, G. (2012). Bromide-free oxidizing system for carboxylic moiety formation in cellulose chain. *Carbohydrate Polymers*, 90(4), 1415-1419.

[34] Ben-Daniel, R., Alsters, P., and Neumann, R. (2001). Selective aerobic oxidation of alcohols with a combination of a polyoxometalate and nitroxyl radical as catalysts. *The Journal of Organic Chemistry*, 66(25), 8650-8653.

[35] Cecchetto, A., Fontana, F., Minisci, F., and Recupero, F. (2001). Efficient Mn–Cu and Mn–Co–TEMPO-catalysed oxidation of alcohols into aldehydes and ketones by oxygen under mild conditions. *Tetrahedron Letters*, 42(38), 6651-6653.

[36] Fabbrini, M., Galli, C., and Gentili, P. (2002). Comparing the catalytic efficiency of some mediators of laccase. *Journal of Molecular Catalysis.B, Enzymatic*, 16(5), 231-240.

---

[37] Jaušovec, D., Vogrinčič, R., and Kokol, V. (2015; 2014). Introduction of aldehyde vs. carboxylic groups to cellulose nanofibers using laccase/TEMPO mediated oxidation. *Carbohydrate Polymers*, 116, 74.

[38] Dijksman, A., Marino-González, A., Mairata I Payeras, A., Arends, I. W. C. E., and Sheldon, R. A. (2001). Efficient and selective aerobic oxidation of alcohols into aldehydes and ketones using ruthenium/TEMPO as the catalytic system. *Journal of the American Chemical Society*, 123(28), 6826-6833.

[39] Sheldon, R. A., and Arends, I. W. C. E. (2006). Catalytic oxidations mediated by metal ions and nitroxyl radicals. *Journal of Molecular Catalysis. A, Chemical*, 251(1), 200-214.

[40] Ha, S. H., Mai, N. L., An, G., and Koo, Y. (2011). Microwave-assisted pretreatment of cellulose in ionic liquid for accelerated enzymatic hydrolysis. *Bioresource Technology,* 102(2), 1214-1219.

[41] Brochette-Lemoine, S., Joannard, D., Descotes, G., Bouchu, A., and Queneau, Y. (1999). Sonocatalysis of the TEMPO-mediated oxidation of glucosides. *Journal of Molecular Catalysis. A, Chemical,* 150(1), 31-36.

[42] Loranger, E., Jradi, K., and Daneault, C. (2012). Nanocellulose production by ultrasound-assisted TEMPO oxidation of kraft pulp on laboratory and pilot scales. *Paper presented at the IEEE International Ultrasonics symposium*, 953-956.

[43] Rattaz, A., Mishra, S. P., Chabot, B., and Daneault, C. (2011). Cellulose nanofibres by sonocatalysed-TEMPO-oxidation. *Cellulose*, 18(3), 585-593.

[44] Henniges, U., Hasani, M., Potthast, A., Westman, G., and Rosenau, T. (2013). Electron beam irradiation of cellulosic materials-opportunities and limitations. *Materials*, 6(5), 1584-1598.

[45] Henniges, U., Okubayashi, S., Rosenau, T., and Potthast, A. (2012). Irradiation of cellulosic pulps: Understanding its impact on cellulose oxidation. *Biomacromolecules*, 13(12), 4171-4178.

[46] Bard, A. J., and Faulkner, L. R. (2001). *Electrochemical methods: fundamentals and applications*. 2nd edition. United States of America: John Wiley and sons, Inc.

[47] Isogai, T., Saito, T., and Isogai, A. (2010). TEMPO electromediated oxidation of some polysaccharides including regenerated cellulose fibre. *Biomacromolecules*, 11(6), 1593-1599.

---

[48] Belgsir, E. M., and Schäfer, H. J. (2001). Selective oxidation of carbohydrates on nafion®–TEMPO-modified graphite felt electrodes. *Electrochemistry Communications,* 3(1), 32-35.

[49] Parpot, P., Servat, K., Bettencourt, A.P., Huser, H., and Kokoh, K.B. (2010). TEMPO mediated oxidation of carbohydrates using electrochemical methods. *Cellulose,* 17(4), 815-824.

[50] Hill-Cousins, J. T., Kuleshova, J., Green, R. A., Birkin, P. R., Pletcher, D., Underwood, T. J., and Brown, R. C. D. (2012). TEMPO-mediated electrooxidation of primary and secondary alcohols in a microfluidic electrolytic cell. *ChemSusChem,* 5(2), 326.

[51] Jin, Y., Edler, K. J., Marken, F., and Scott, J. L. (2014). Voltammetric optimisation of TEMPO-mediated oxidations at cellulose fabric. *Green Chemistry,* 16(6), 3322-3327.

[52] Williams, D. H., and Fleming, I. (1995). *Spectroscopic methods in organic chemistry*. 5th edition. Berkshire: McGraw-Hill Publishing Company.

[53] McMurry, J., and Simanek, E. (2007). *Fundamentals of Organic Chemistry.* 6th edition. Belmont: Thomson Brooks/Cole.

[54] Still, W. C., Kahn, M., and Mitra, A. (1978). Rapid chromatographic technique for preparative separations with moderate resolution. *The Journal of Organic Chemistry*, 43(14), 2923-2925.

[55] Leonard, J., Lygo, B., and Procter, G. (1998). *Advanced practical organic chemistry*. 2nd edition. Boca Raton: Taylor & Francis Group.

[56] Istone, W. K. (1995). X-ray Photoelectron Spectroskopy. Conners, T. E., and Banerjee, S. (eds.), *Surface Analysis of Paper*. Boca Raton: CRC press.

[57] Carlsson, D. O., Lindh, J., Nyholm, L., Strømme, M., and Mihranyan, A. (2014). Cooxidant-free TEMPO-mediated oxidation of highly crystalline nanocellulose in water. *RSC Advances*, 4(94), 52289-52298.

[58] Beamson, G., and Briggs, D. (1992) *High Resolution XPS of Organic Polymers: The Scienta ESCA300 Database.* United states of America: John Wiley & Sons Ltd.

[59] Isogai, A., and Kato, Y. (1998). Preparation of polyuronic acid from cellulose by TEMPO-mediated oxidation. *Cellulose,* 5(3), 153-164

Appendix I: Electrochemical experiments

TEMPO

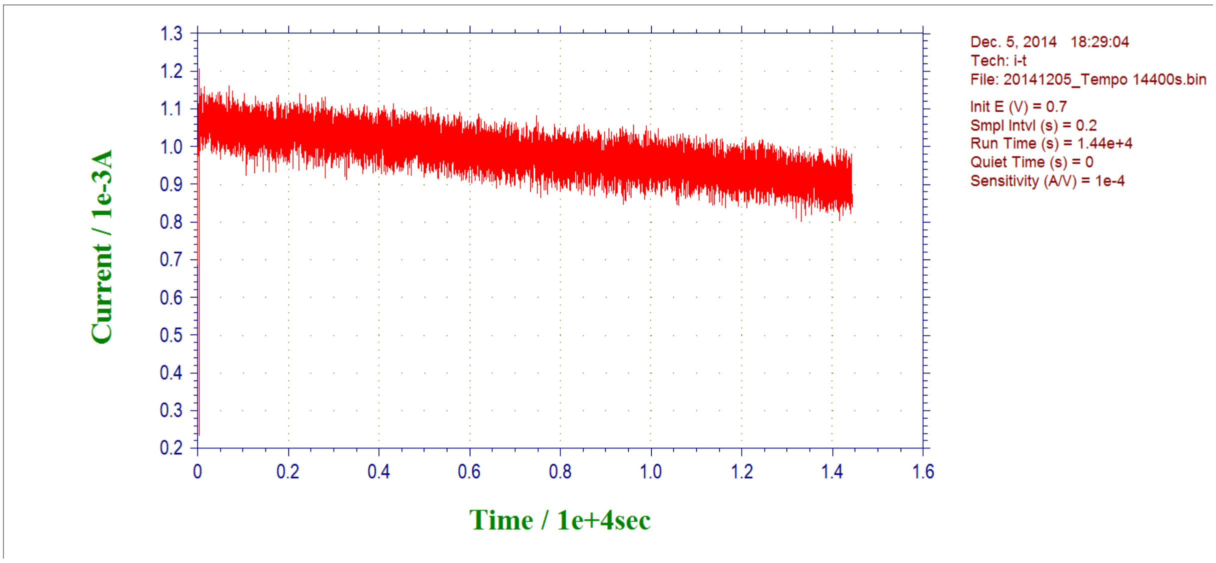

Dec. 5, 2014 18:29:04
Tech: i-t
File: 20141205_Tempo 14400s.bin
Init E (V) = 0.7
Smpl Intvl (s) = 0.2
Run Time (s) = 1.44e+4
Quiet Time (s) = 0
Sensitivity (A/V) = 1e-4

E1

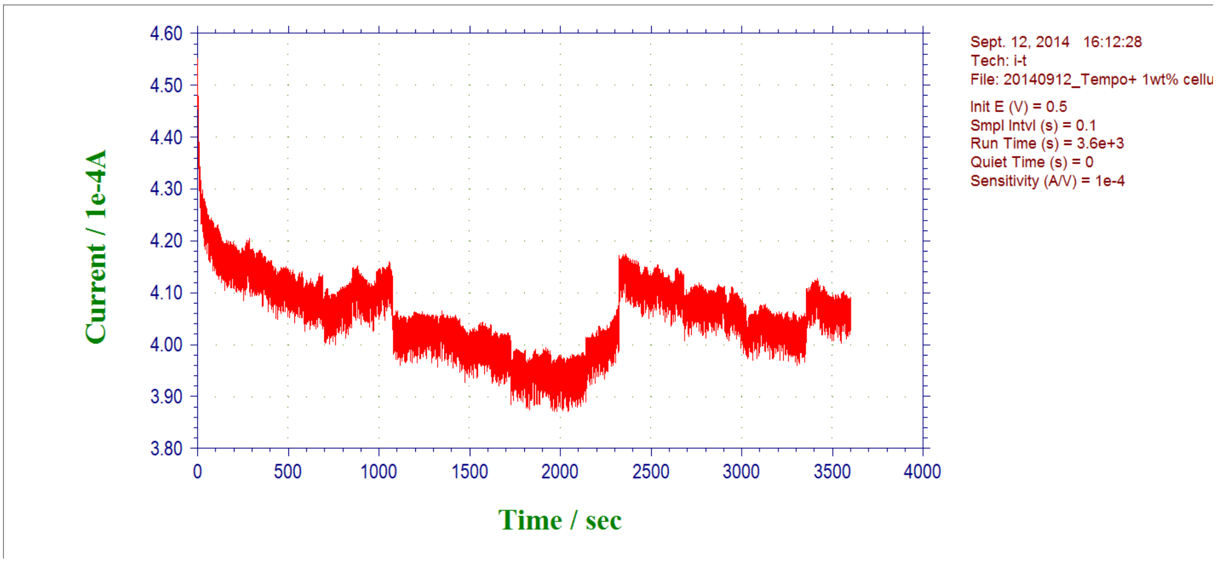

Sept. 12, 2014 16:12:28
Tech: i-t
File: 20140912_Tempo+ 1wt% cellu
Init E (V) = 0.5
Smpl Intvl (s) = 0.1
Run Time (s) = 3.6e+3
Quiet Time (s) = 0
Sensitivity (A/V) = 1e-4

E2

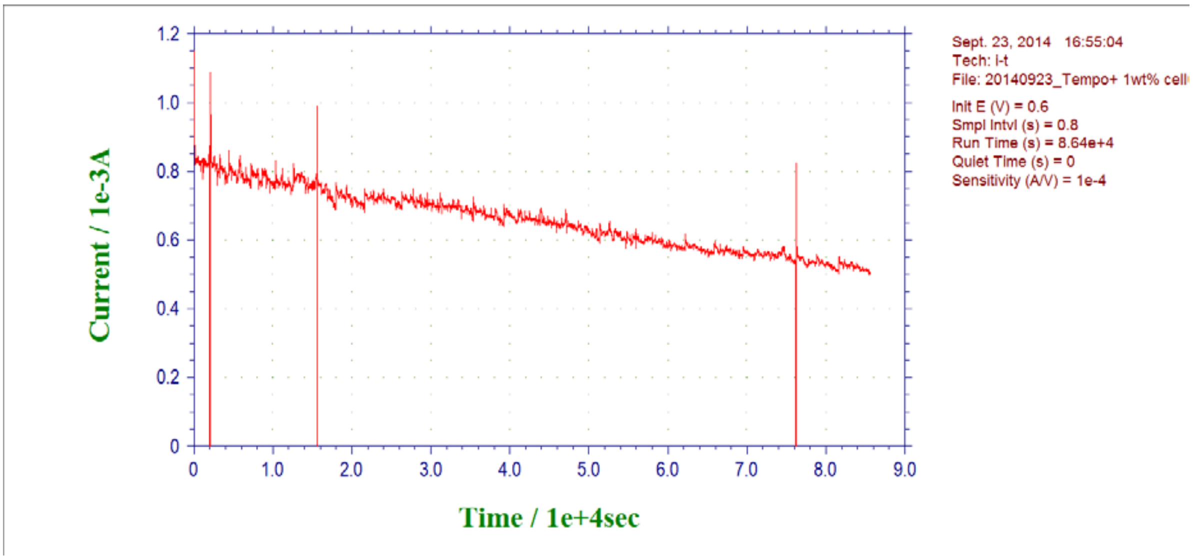

Sept. 23, 2014 16:55:04
Tech: i-t
File: 20140923_Tempo+ 1wt% cell

Init E (V) = 0.6
Smpl Intvl (s) = 0.8
Run Time (s) = 8.64e+4
Quiet Time (s) = 0
Sensitivity (A/V) = 1e-4

E3

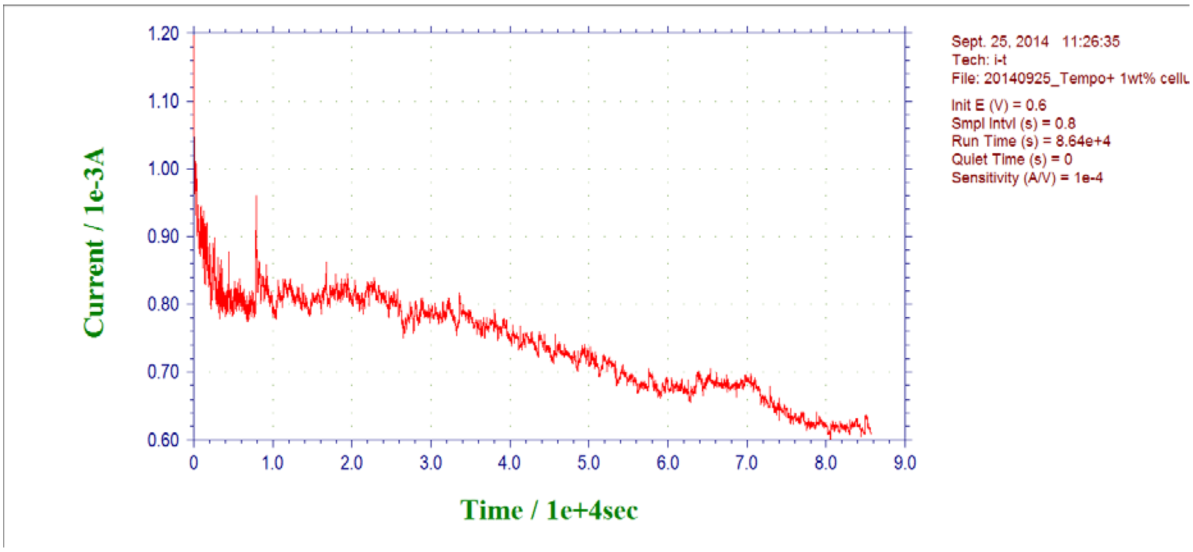

Sept. 25, 2014 11:26:35
Tech: i-t
File: 20140925_Tempo+ 1wt% cellu

Init E (V) = 0.6
Smpl Intvl (s) = 0.8
Run Time (s) = 8.64e+4
Quiet Time (s) = 0
Sensitivity (A/V) = 1e-4

E4 (Ox)

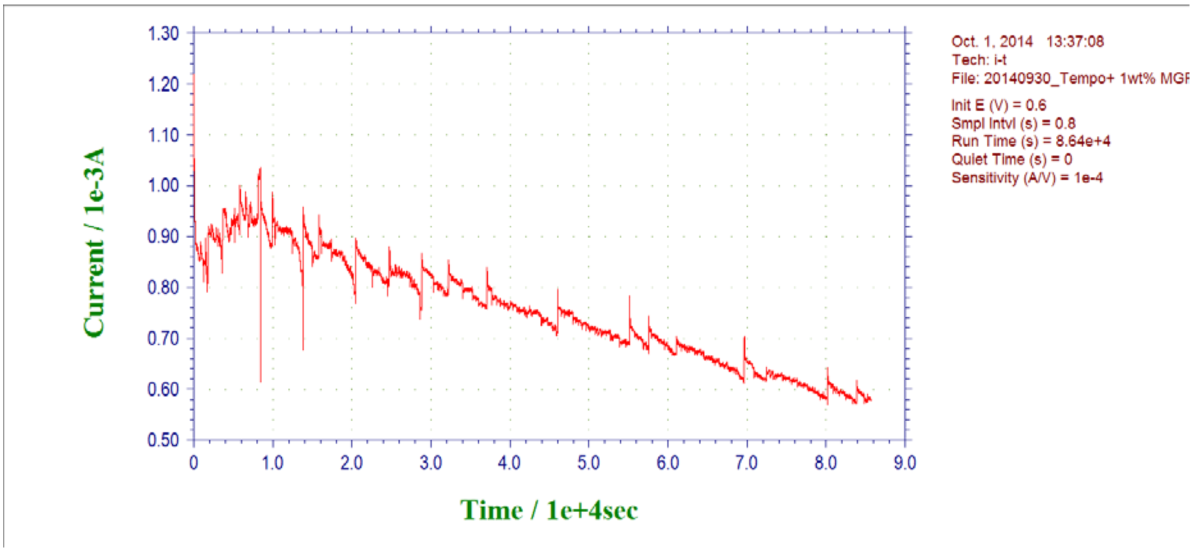

Oct. 1, 2014 13:37:08
Tech: i-t
File: 20140930_Tempo+ 1wt% MG

Init E (V) = 0.6
Smpl Intvl (s) = 0.8
Run Time (s) = 8.64e+4
Quiet Time (s) = 0
Sensitivity (A/V) = 1e-4

E5

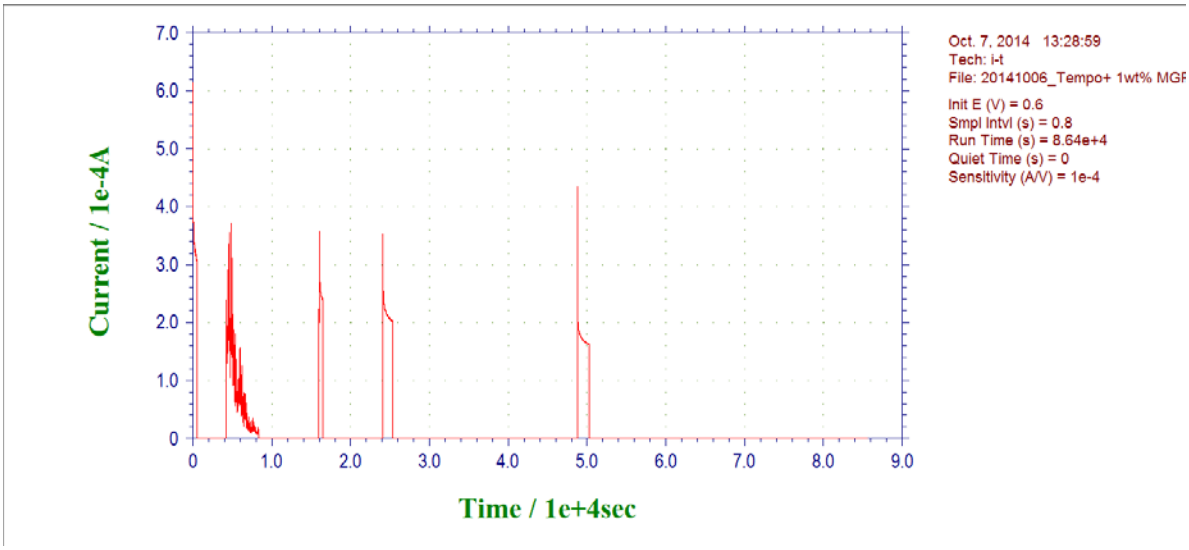

```
Oct. 7, 2014   13:28:59
Tech: i-t
File: 20141006_Tempo+ 1wt% MG
Init E (V) = 0.6
Smpl Intvl (s) = 0.8
Run Time (s) = 8.64e+4
Quiet Time (s) = 0
Sensitivity (A/V) = 1e-4
```

E6 (Naf), MGP 24 h with Nafion

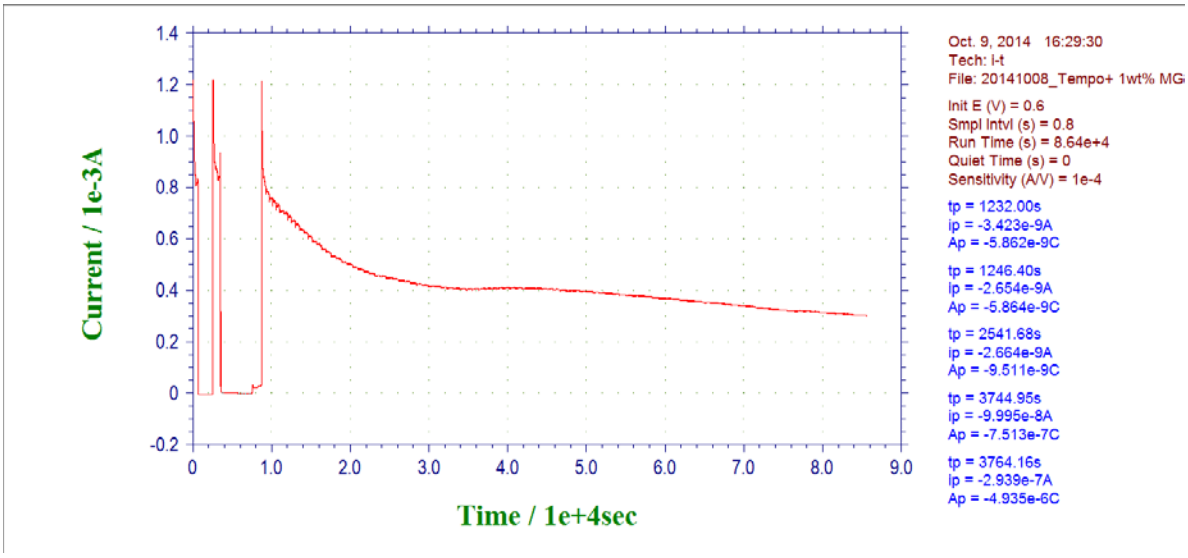

```
Oct. 9, 2014   16:29:30
Tech: i-t
File: 20141008_Tempo+ 1wt% MG
Init E (V) = 0.6
Smpl Intvl (s) = 0.8
Run Time (s) = 8.64e+4
Quiet Time (s) = 0
Sensitivity (A/V) = 1e-4
tp = 1232.00s
ip = -3.423e-9A
Ap = -5.862e-9C
tp = 1246.40s
ip = -2.654e-9A
Ap = -5.864e-9C
tp = 2541.68s
ip = -2.664e-9A
Ap = -9.511e-9C
tp = 3744.95s
ip = -9.995e-8A
Ap = -7.513e-7C
tp = 3764.16s
ip = -2.939e-7A
Ap = -4.935e-6C
```

E7

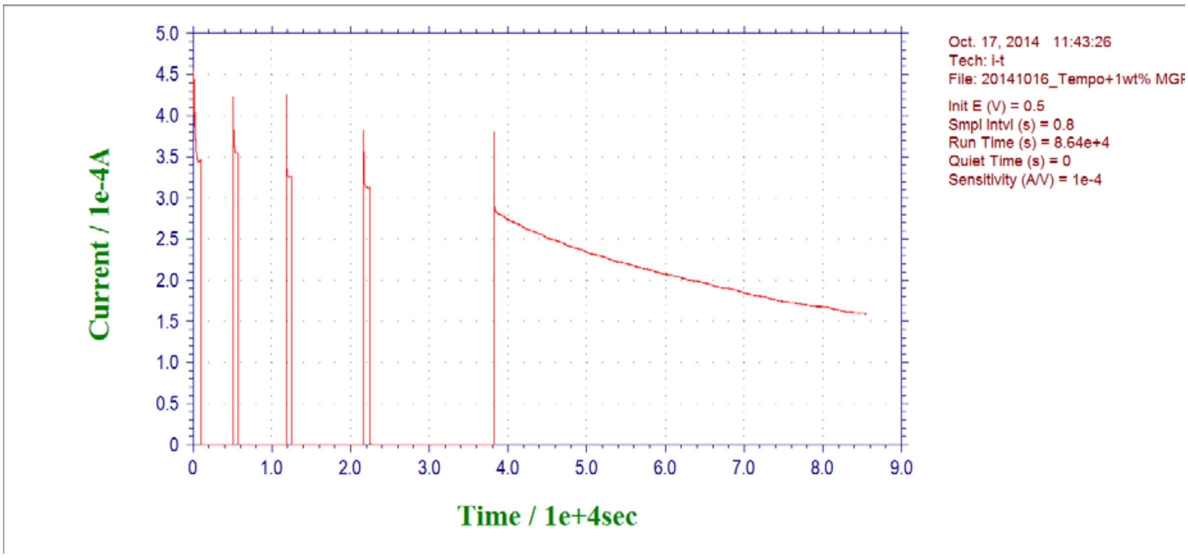

```
Oct. 17, 2014   11:43:26
Tech: i-t
File: 20141016_Tempo+1wt% MG
Init E (V) = 0.5
Smpl Intvl (s) = 0.8
Run Time (s) = 8.64e+4
Quiet Time (s) = 0
Sensitivity (A/V) = 1e-4
```

E8 (L1)

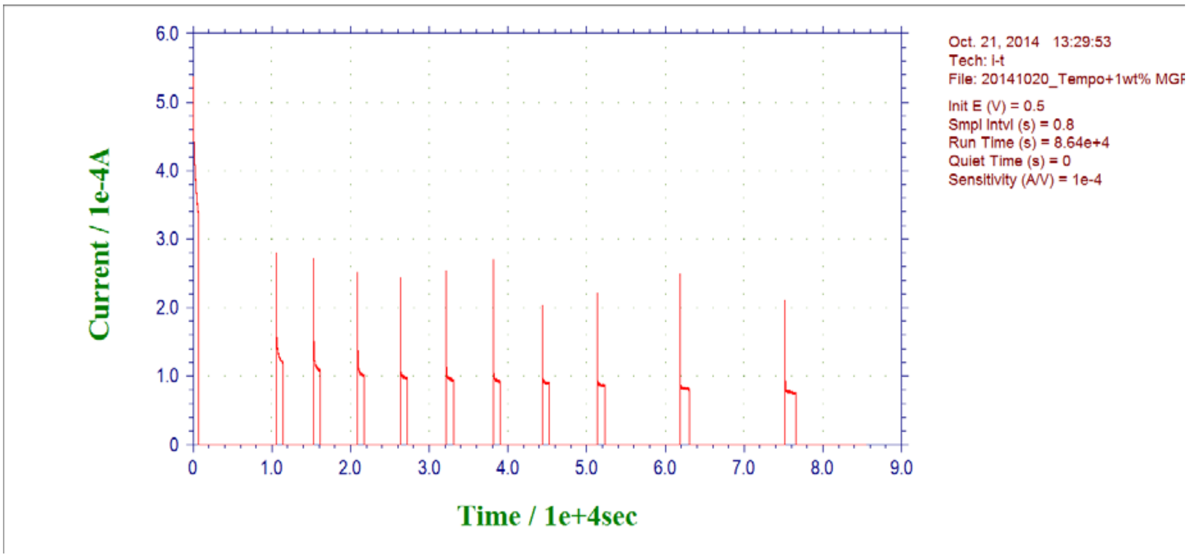

Oct. 21, 2014 13:29:53
Tech: i-t
File: 20141020_Tempo+1wt% MG
Init E (V) = 0.5
Smpl Intvl (s) = 0.8
Run Time (s) = 8.64e+4
Quiet Time (s) = 0
Sensitivity (A/V) = 1e-4

E9 (MMI), MGP 24 h with Metrohm

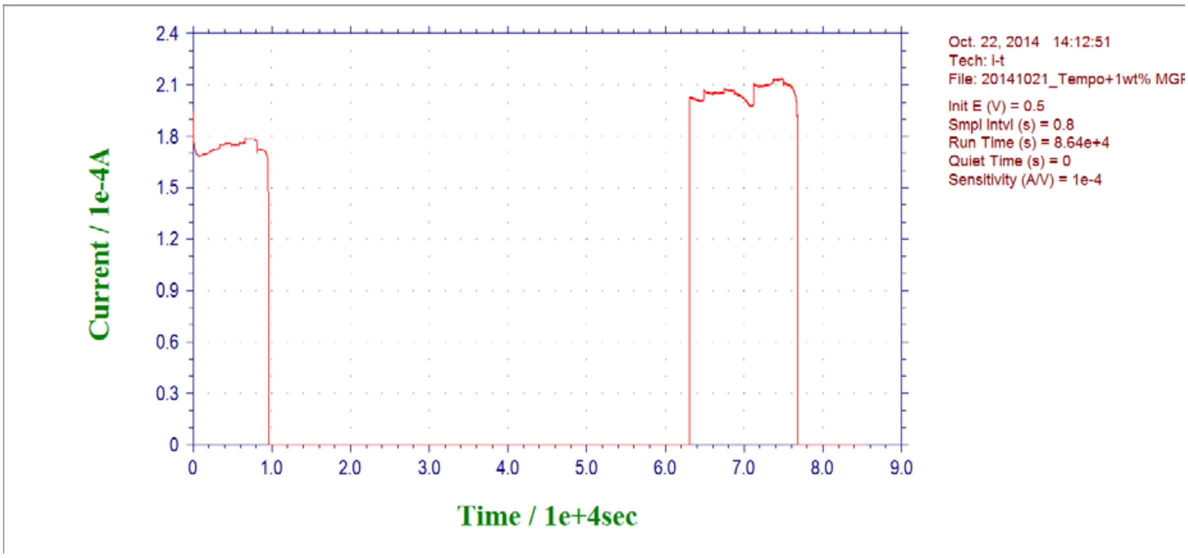

Oct. 22, 2014 14:12:51
Tech: i-t
File: 20141021_Tempo+1wt% MG
Init E (V) = 0.5
Smpl Intvl (s) = 0.8
Run Time (s) = 8.64e+4
Quiet Time (s) = 0
Sensitivity (A/V) = 1e-4

E10, Cotton 24h metrohm

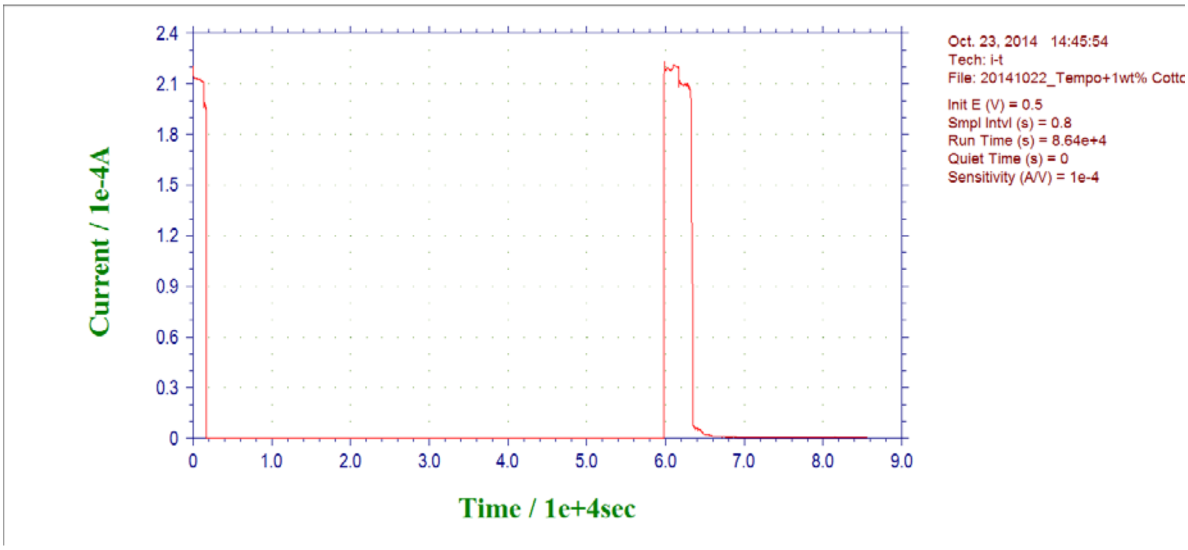

Oct. 23, 2014 14:45:54
Tech: i-t
File: 20141022_Tempo+1wt% Cott
Init E (V) = 0.5
Smpl Intvl (s) = 0.8
Run Time (s) = 8.64e+4
Quiet Time (s) = 0
Sensitivity (A/V) = 1e-4

E11, w NaCl

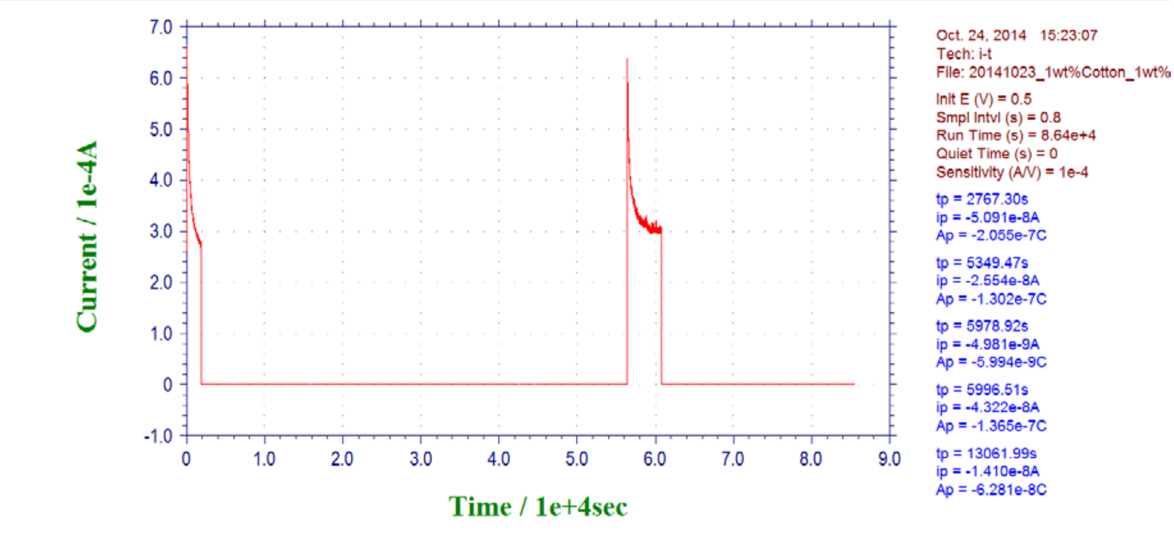

```
Oct. 24, 2014   15:23:07
Tech: i-t
File: 20141023_1wt%Cotton_1wt%
Init E (V) = 0.5
Smpl Intvl (s) = 0.8
Run Time (s) = 8.64e+4
Quiet Time (s) = 0
Sensitivity (A/V) = 1e-4
tp = 2767.30s
ip = -5.091e-8A
Ap = -2.055e-7C
tp = 5349.47s
ip = -2.554e-8A
Ap = -1.302e-7C
tp = 5978.92s
ip = -4.981e-9A
Ap = -5.994e-9C
tp = 5996.51s
ip = -4.322e-8A
Ap = -1.365e-7C
tp = 13061.99s
ip = -1.410e-8A
Ap = -6.281e-8C
```

E12 (OM1)MGP 24h

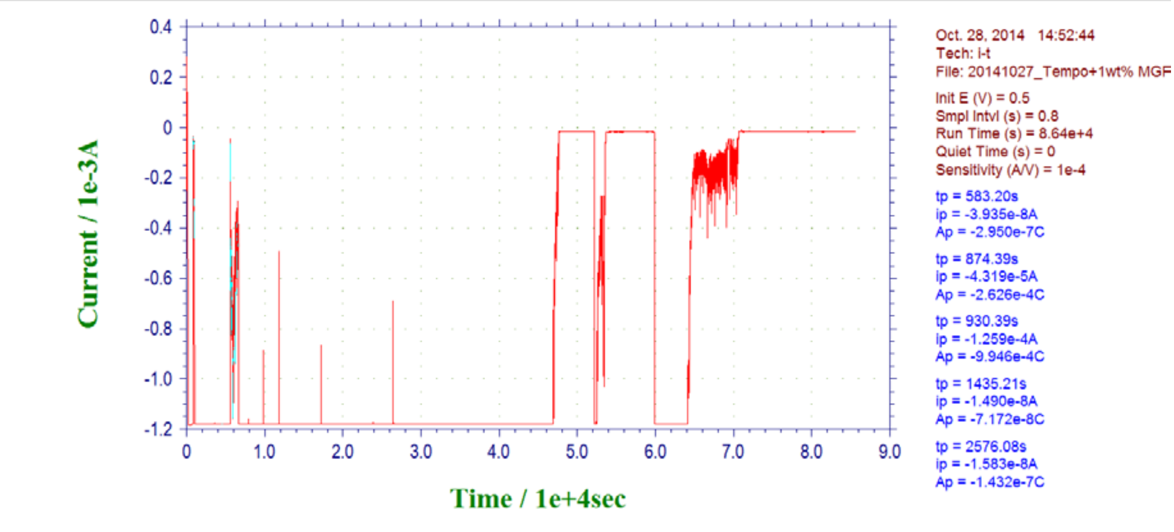

```
Oct. 28, 2014   14:52:44
Tech: i-t
File: 20141027_Tempo+1wt% MGF
Init E (V) = 0.5
Smpl Intvl (s) = 0.8
Run Time (s) = 8.64e+4
Quiet Time (s) = 0
Sensitivity (A/V) = 1e-4
tp = 583.20s
ip = -3.935e-8A
Ap = -2.950e-7C
tp = 874.39s
ip = -4.319e-5A
Ap = -2.626e-4C
tp = 930.39s
ip = -1.259e-4A
Ap = -9.946e-4C
tp = 1435.21s
ip = -1.490e-8A
Ap = -7.172e-8C
tp = 2576.08s
ip = -1.583e-8A
Ap = -1.432e-7C
```

E13 (OxMGP)

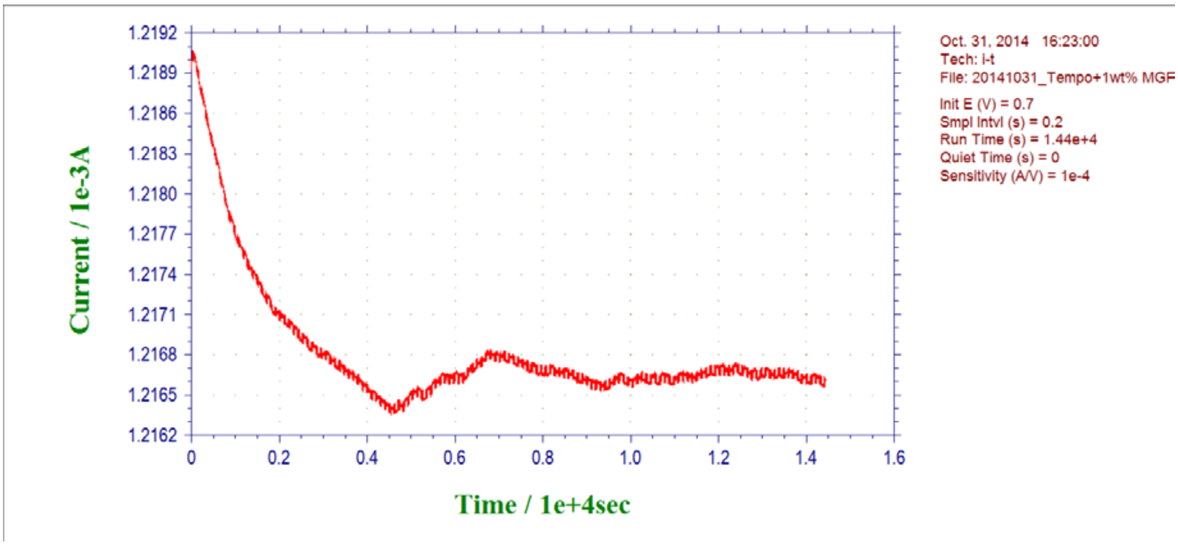

```
Oct. 31, 2014   16:23:00
Tech: i-t
File: 20141031_Tempo+1wt% MGF
Init E (V) = 0.7
Smpl Intvl (s) = 0.2
Run Time (s) = 1.44e+4
Quiet Time (s) = 0
Sensitivity (A/V) = 1e-4
```

E1

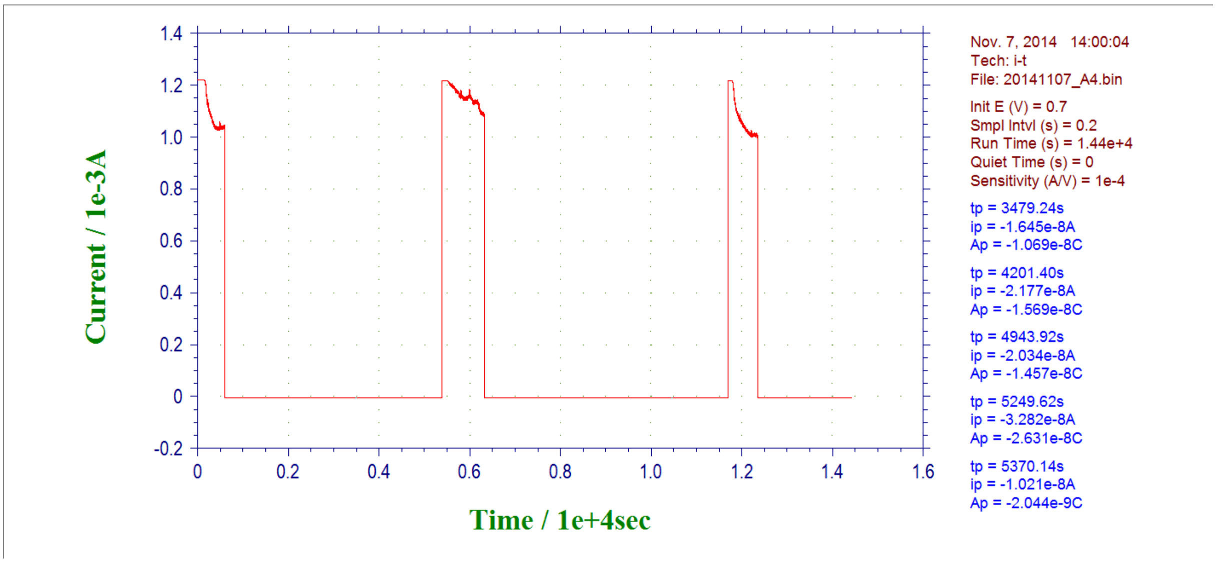

Nov. 7, 2014 14:00:04
Tech: i-t
File: 20141107_A4.bin

Init E (V) = 0.7
Smpl Intvl (s) = 0.2
Run Time (s) = 1.44e+4
Quiet Time (s) = 0
Sensitivity (A/V) = 1e-4

tp = 3479.24s
ip = -1.645e-8A
Ap = -1.069e-8C

tp = 4201.40s
ip = -2.177e-8A
Ap = -1.569e-8C

tp = 4943.92s
ip = -2.034e-8A
Ap = -1.457e-8C

tp = 5249.62s
ip = -3.282e-8A
Ap = -2.631e-8C

tp = 5370.14s
ip = -1.021e-8A
Ap = -2.044e-9C

A3

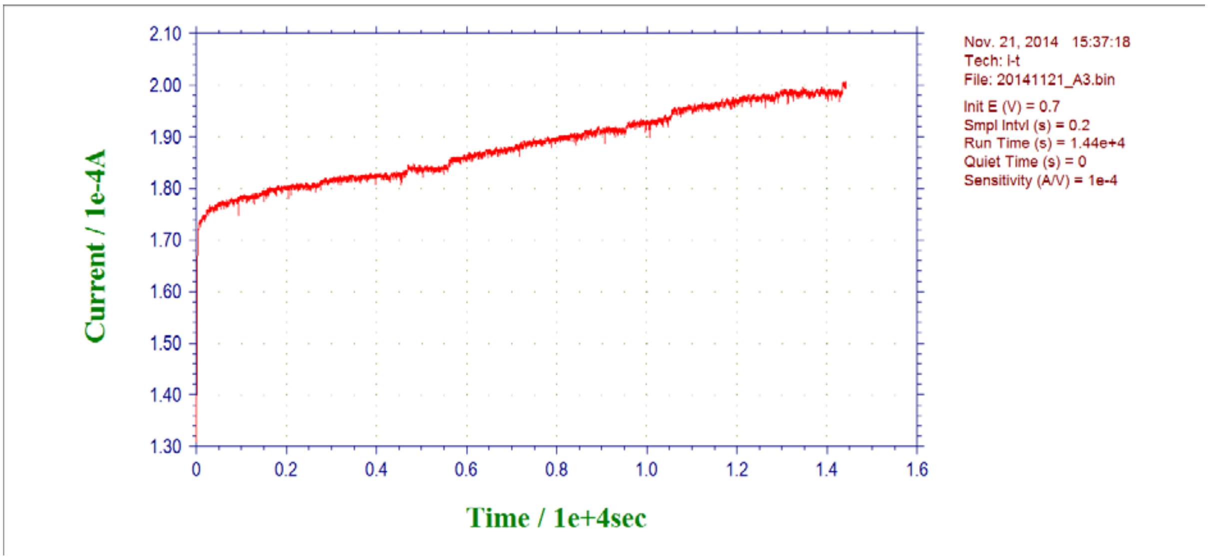

Nov. 21, 2014 15:37:18
Tech: I-t
File: 20141121_A3.bin

Init E (V) = 0.7
Smpl Intvl (s) = 0.2
Run Time (s) = 1.44e+4
Quiet Time (s) = 0
Sensitivity (A/V) = 1e-4

A4

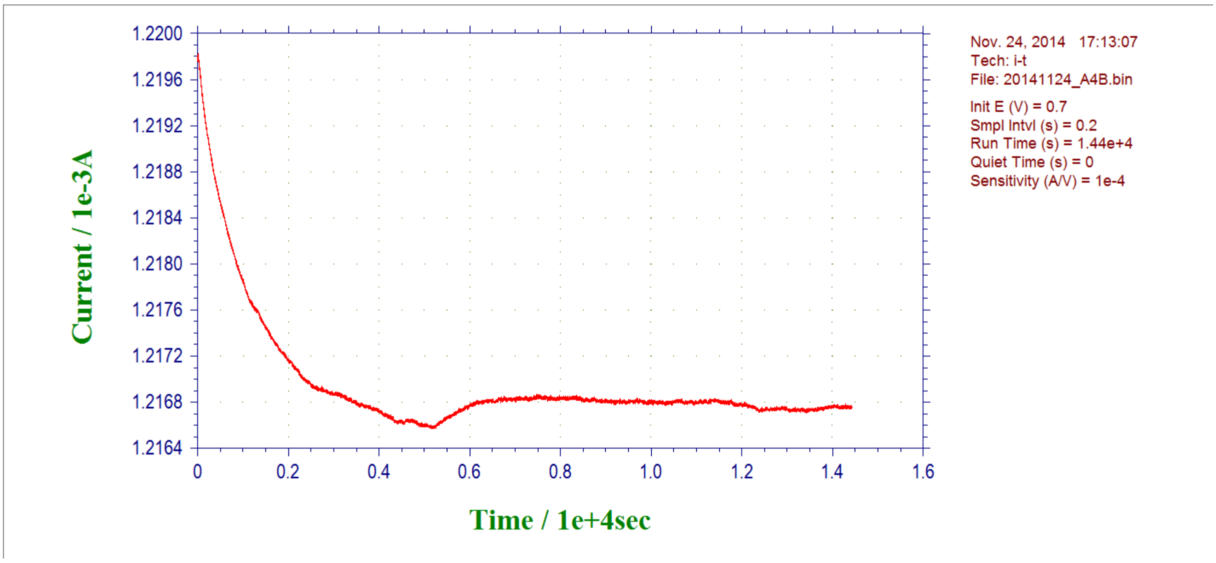

Nov. 24, 2014 17:13:07
Tech: i-t
File: 20141124_A4B.bin

Init E (V) = 0.7
Smpl Intvl (s) = 0.2
Run Time (s) = 1.44e+4
Quiet Time (s) = 0
Sensitivity (A/V) = 1e-4

A5

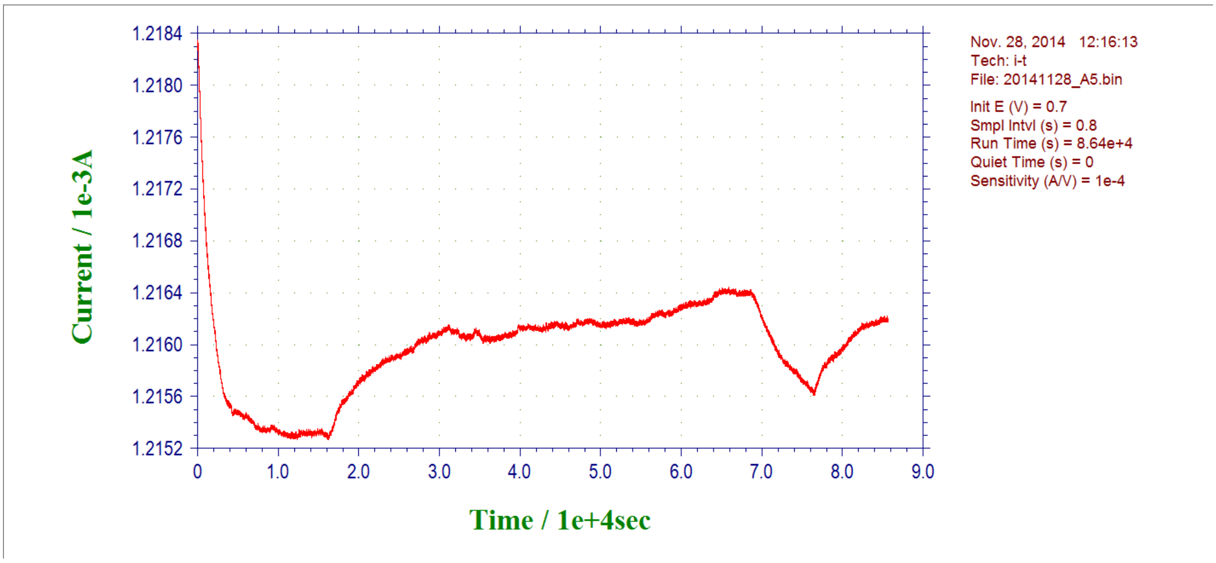

Nov. 28, 2014 12:16:13
Tech: i-t
File: 20141128_A5.bin

Init E (V) = 0.7
Smpl Intvl (s) = 0.8
Run Time (s) = 8.64e+4
Quiet Time (s) = 0
Sensitivity (A/V) = 1e-4

A6

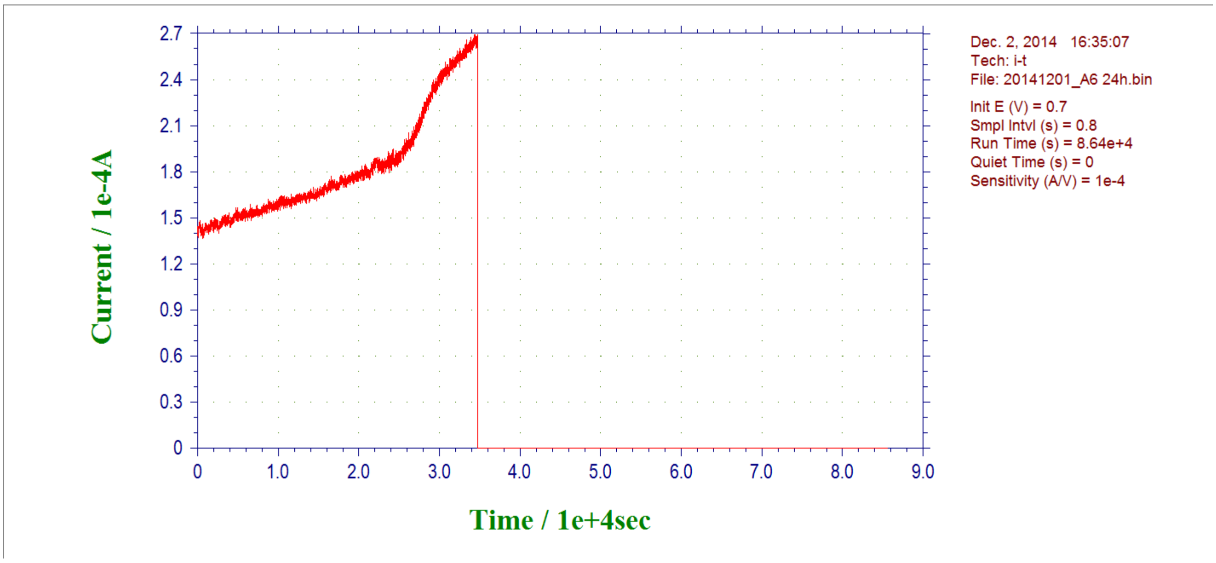

Dec. 2, 2014 16:35:07
Tech: i-t
File: 20141201_A6 24h.bin

Init E (V) = 0.7
Smpl Intvl (s) = 0.8
Run Time (s) = 8.64e+4
Quiet Time (s) = 0
Sensitivity (A/V) = 1e-4

C3

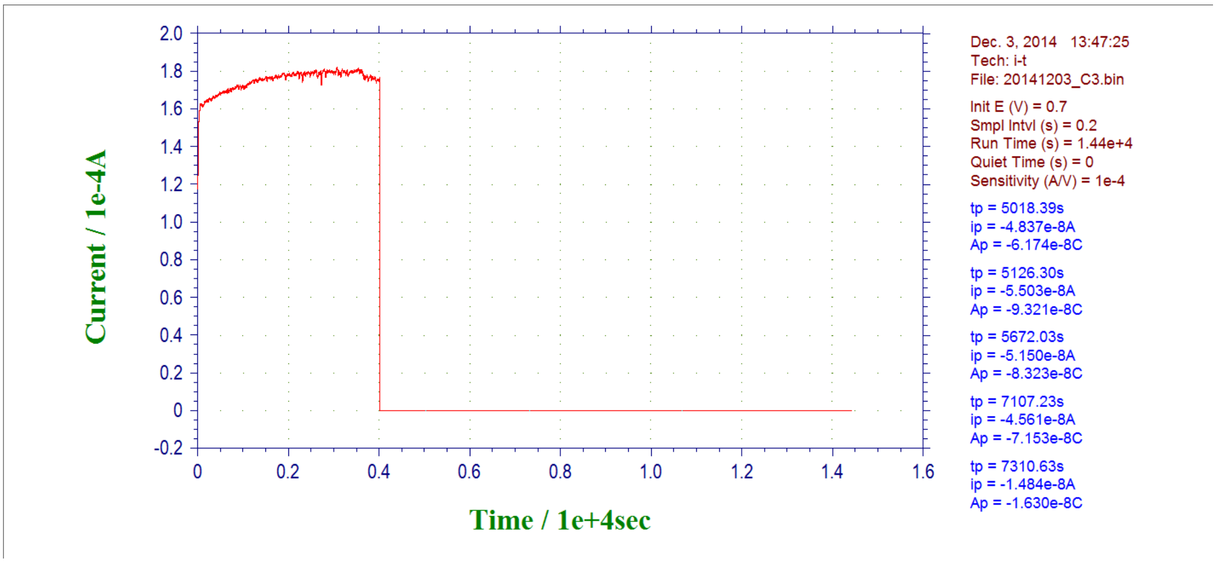

Dec. 3, 2014 13:47:25
Tech: i-t
File: 20141203_C3.bin

Init E (V) = 0.7
Smpl Intvl (s) = 0.2
Run Time (s) = 1.44e+4
Quiet Time (s) = 0
Sensitivity (A/V) = 1e-4

tp = 5018.39s
ip = -4.837e-8A
Ap = -6.174e-8C

tp = 5126.30s
ip = -5.503e-8A
Ap = -9.321e-8C

tp = 5672.03s
ip = -5.150e-8A
Ap = -8.323e-8C

tp = 7107.23s
ip = -4.561e-8A
Ap = -7.153e-8C

tp = 7310.63s
ip = -1.484e-8A
Ap = -1.630e-8C

C4

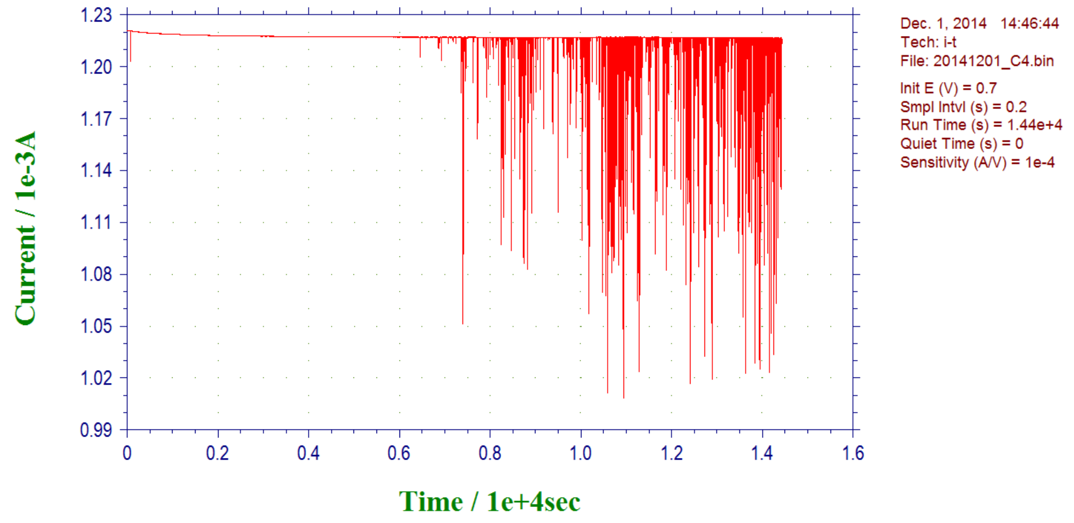

Dec. 1, 2014 14:46:44
Tech: i-t
File: 20141201_C4.bin

Init E (V) = 0.7
Smpl Intvl (s) = 0.2
Run Time (s) = 1.44e+4
Quiet Time (s) = 0
Sensitivity (A/V) = 1e-4

D3

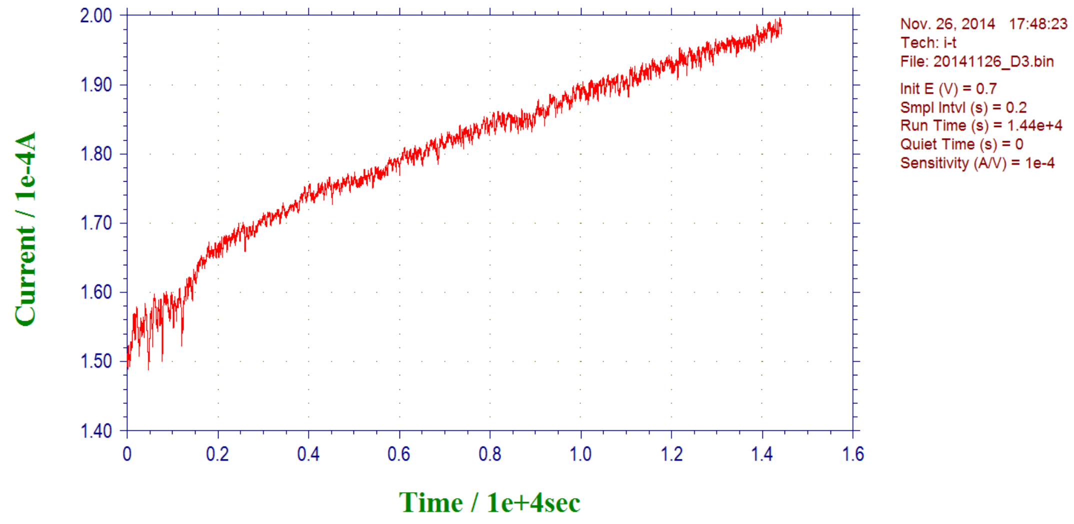

Nov. 26, 2014 17:48:23
Tech: i-t
File: 20141126_D3.bin

Init E (V) = 0.7
Smpl Intvl (s) = 0.2
Run Time (s) = 1.44e+4
Quiet Time (s) = 0
Sensitivity (A/V) = 1e-4

D4

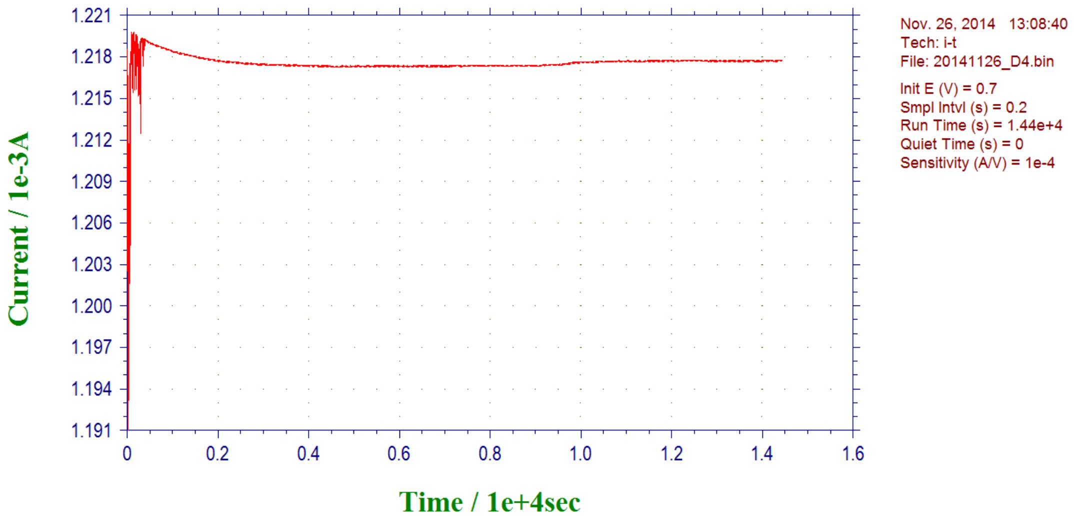

Nov. 26, 2014 13:08:40
Tech: i-t
File: 20141126_D4.bin

Init E (V) = 0.7
Smpl Intvl (s) = 0.2
Run Time (s) = 1.44e+4
Quiet Time (s) = 0
Sensitivity (A/V) = 1e-4

Appendix II: Liquid state NMR

The samples on which liquid state-NMR has been performed are depicted in Table 1. Graphs for each sample, including reference sample, are shown below.

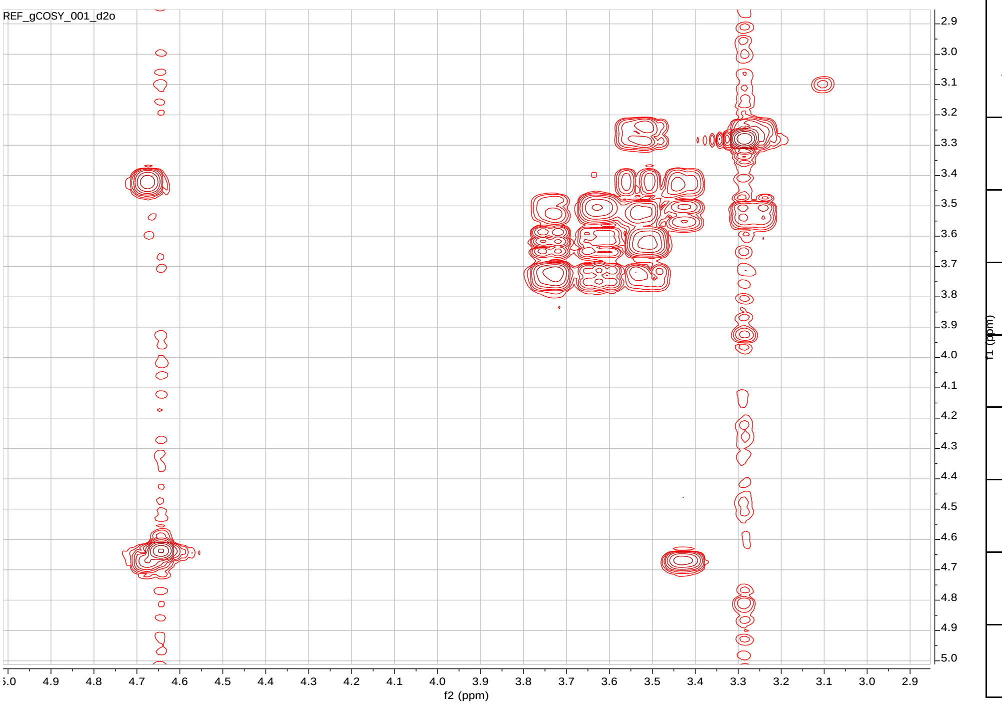

Figure 1: Cosy of reference sample in D_2O.

Table 1: NMR-samples

Liquid state-NMR have been performed on MGP-samples: *(old name in brackets)*
E4 (Ox)
E6 (Naf)
E8 (L1)
E9 (MM1)
E12 (OM1)
E13 (OxMGP)
R1
R5

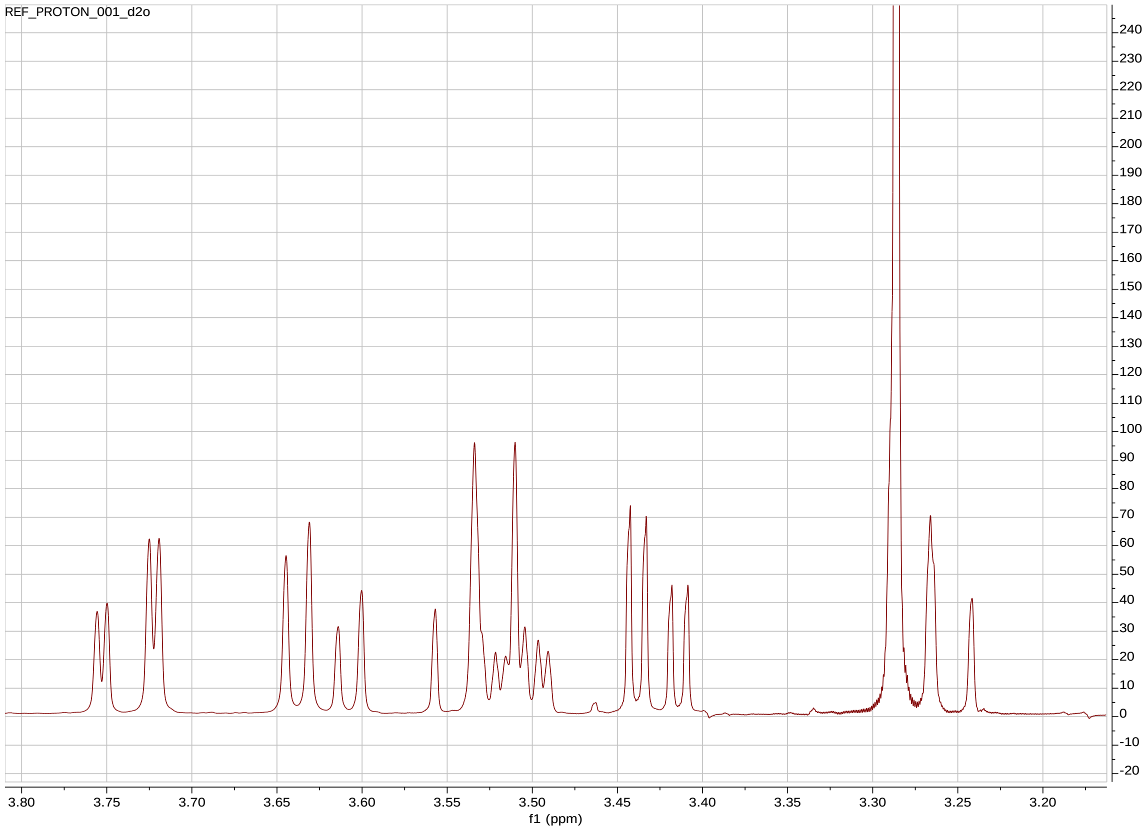

Figure 2: ^{1}H-NMR of reference in D2O.

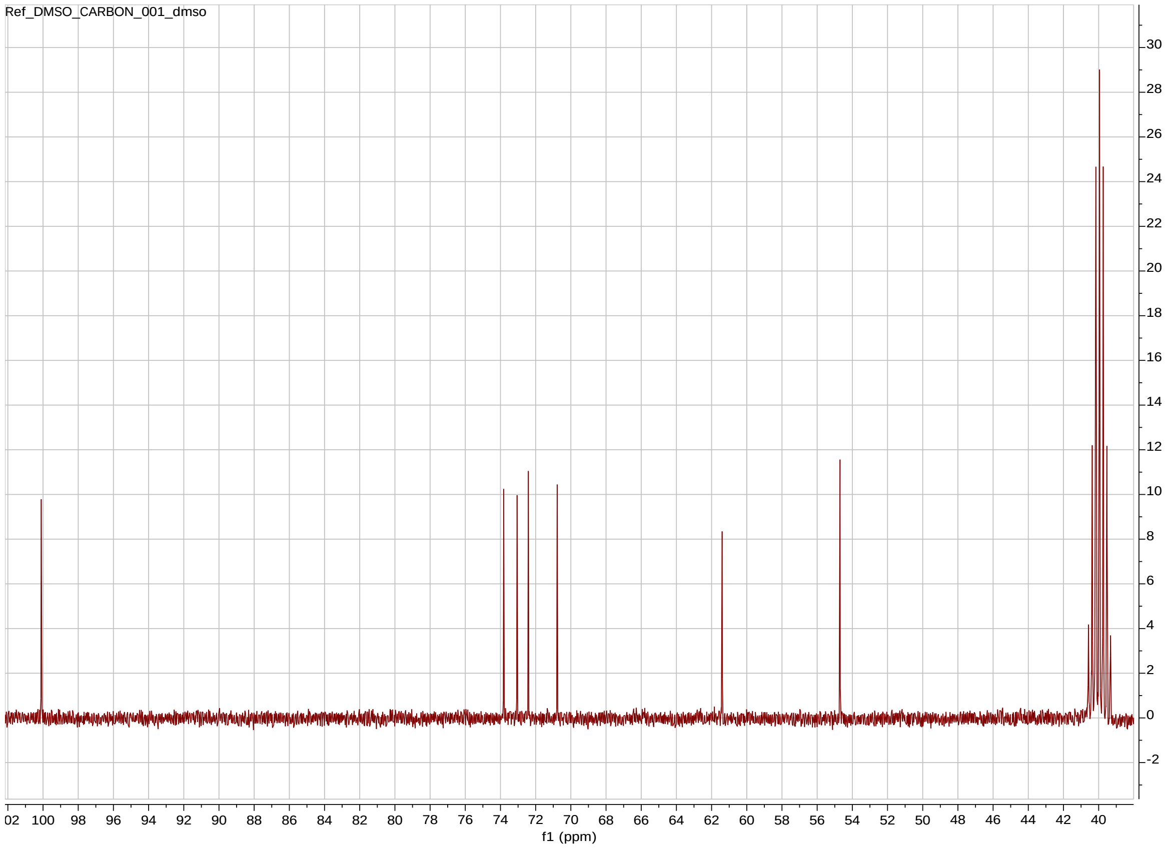

Figure 3: ^{13}C-NMR on reference in DMSO.

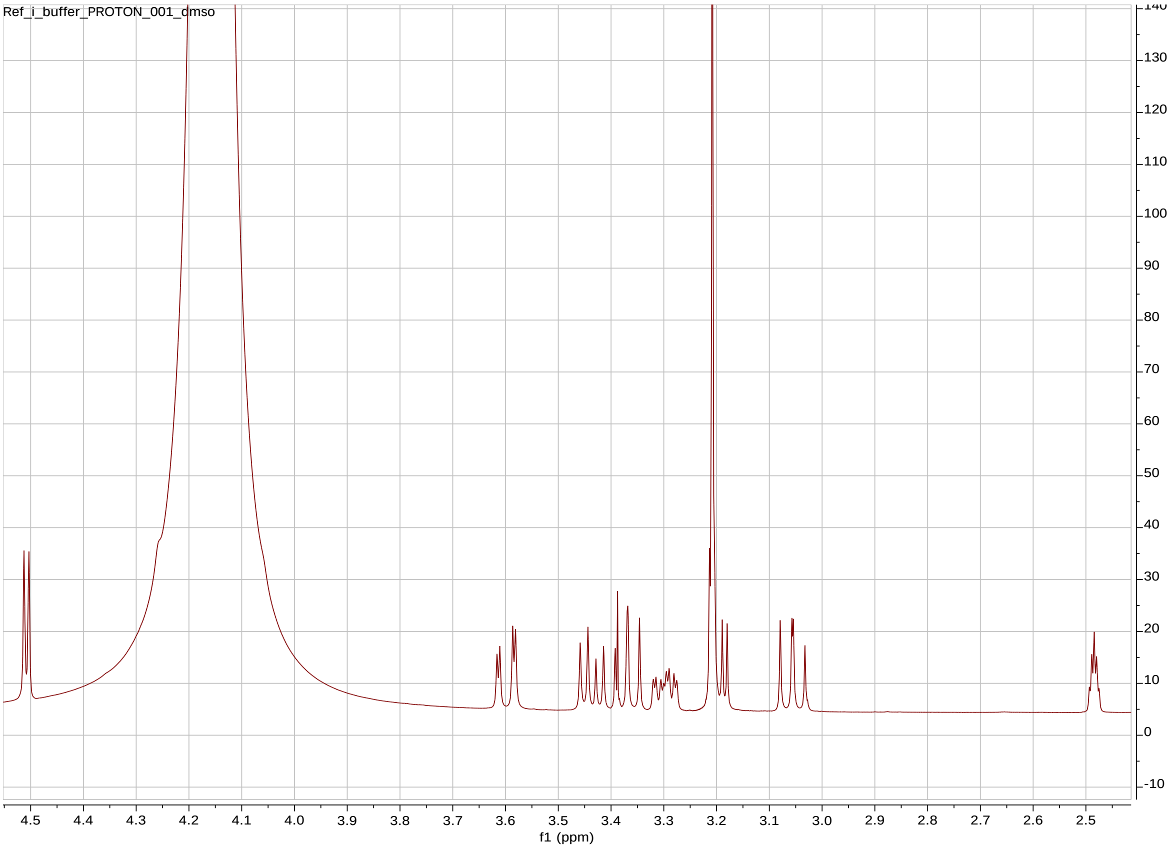

Figure 4: Reference in buffer, ^{1}H-NMR in DMSO.

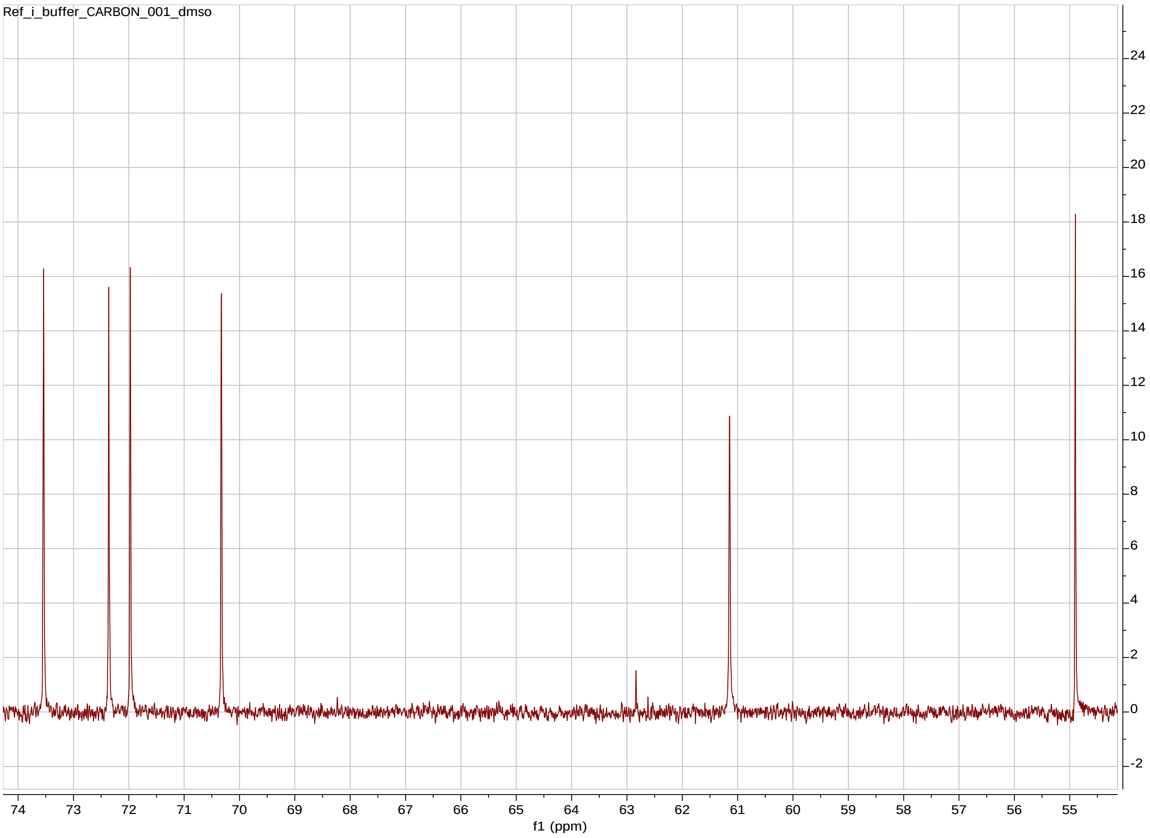

Figure 5: Reference in buffer, ^{13}C-NMR in DMSO.

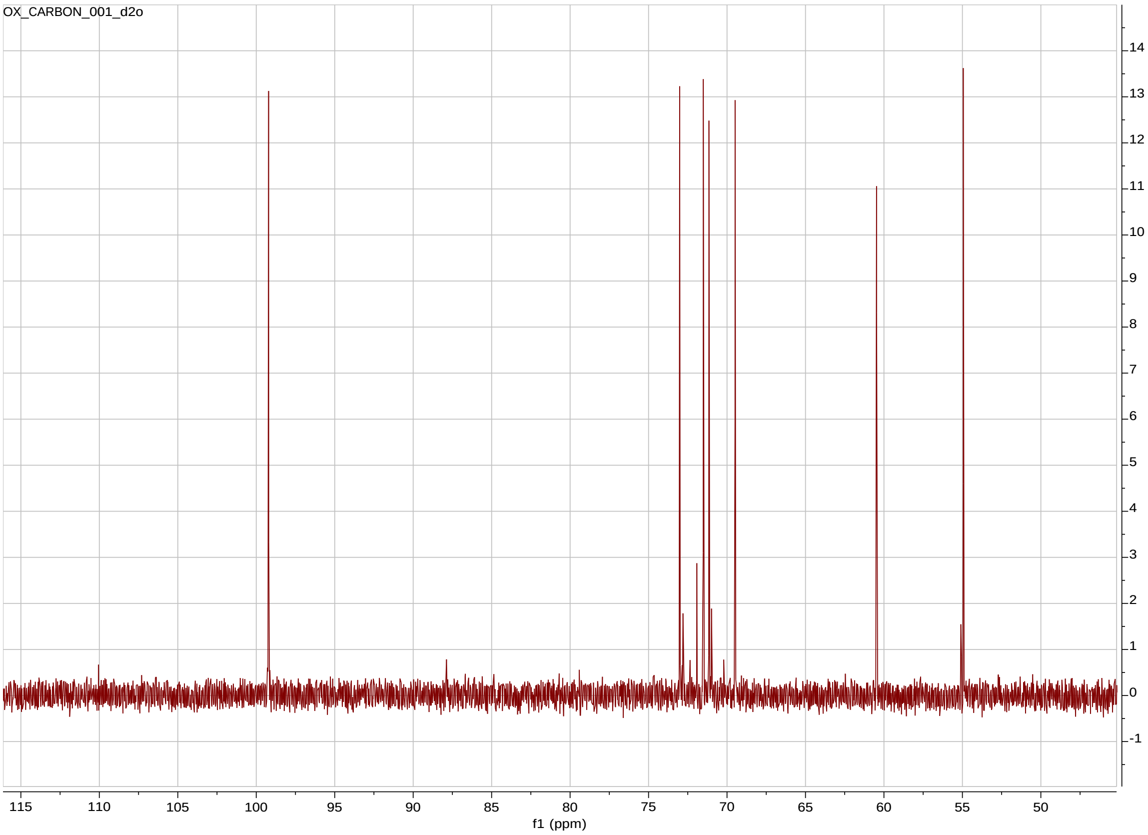

Figure 6: Zoomed in ^{13}C -NMR on E4 in D2O.

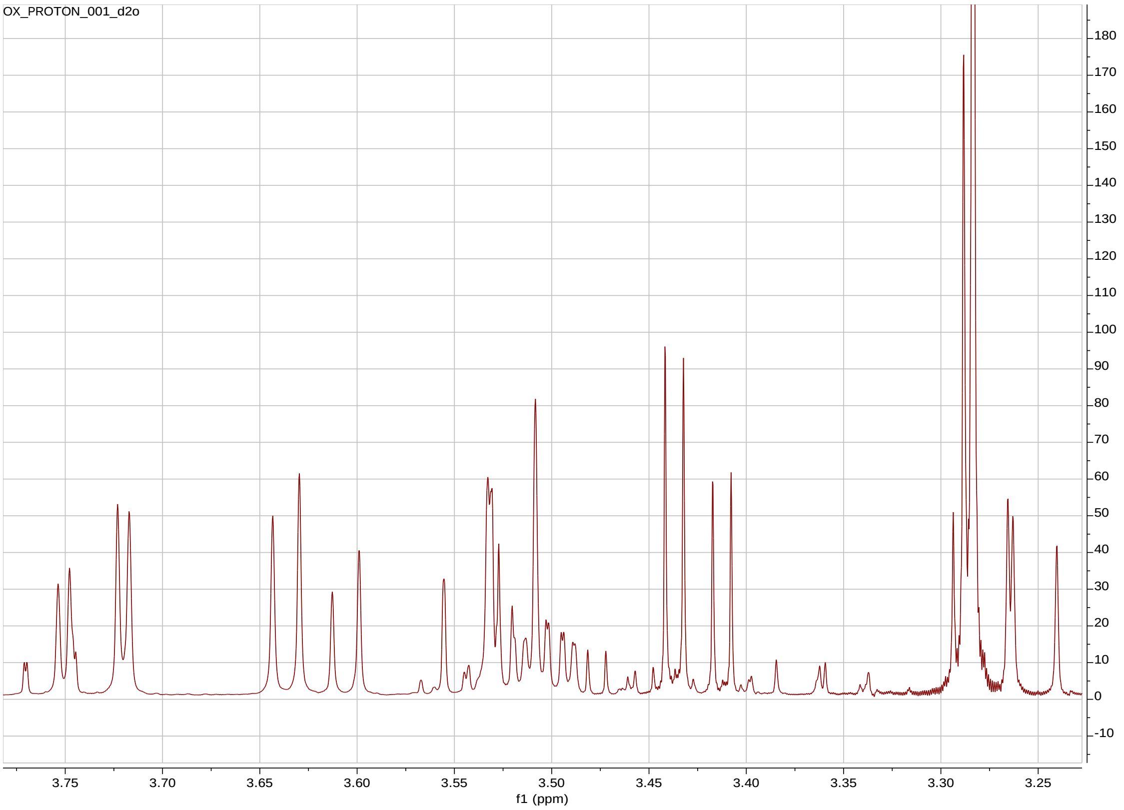

Figure 7: Zoomed in ^{1}H-NMR on E4 in D2O.

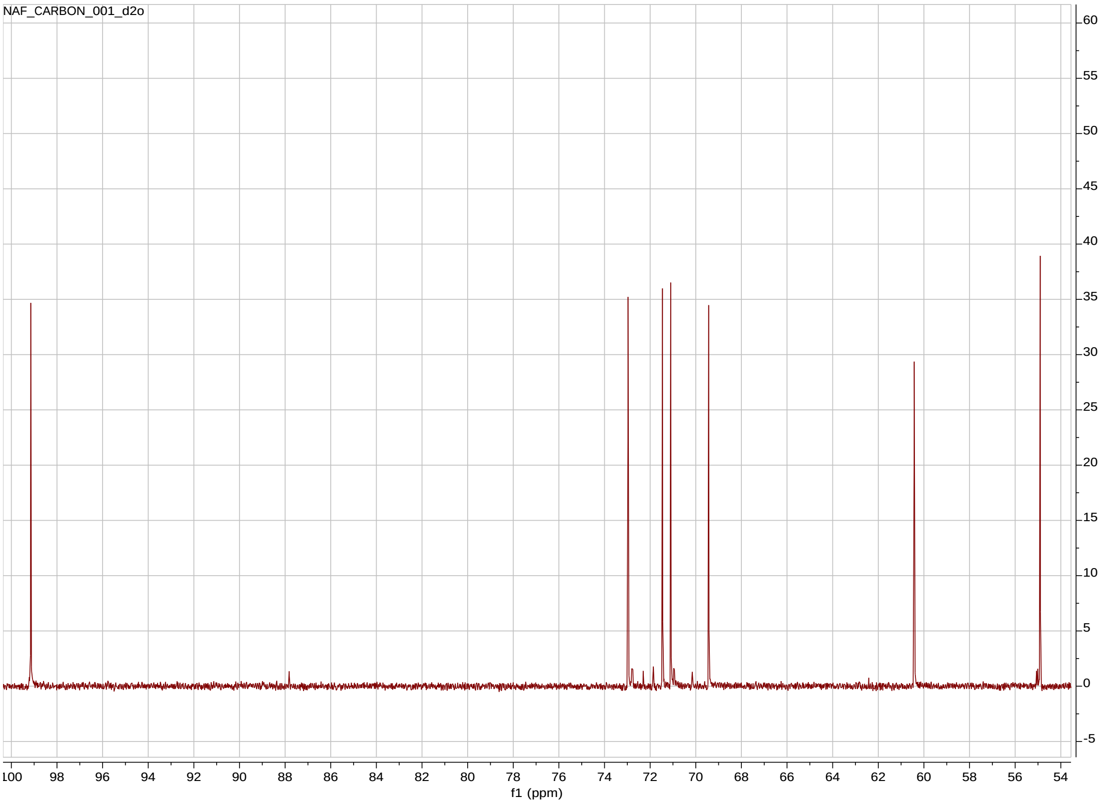

Figure 8: Zoomed in ^{13}C-NMR on E6 in D2O.

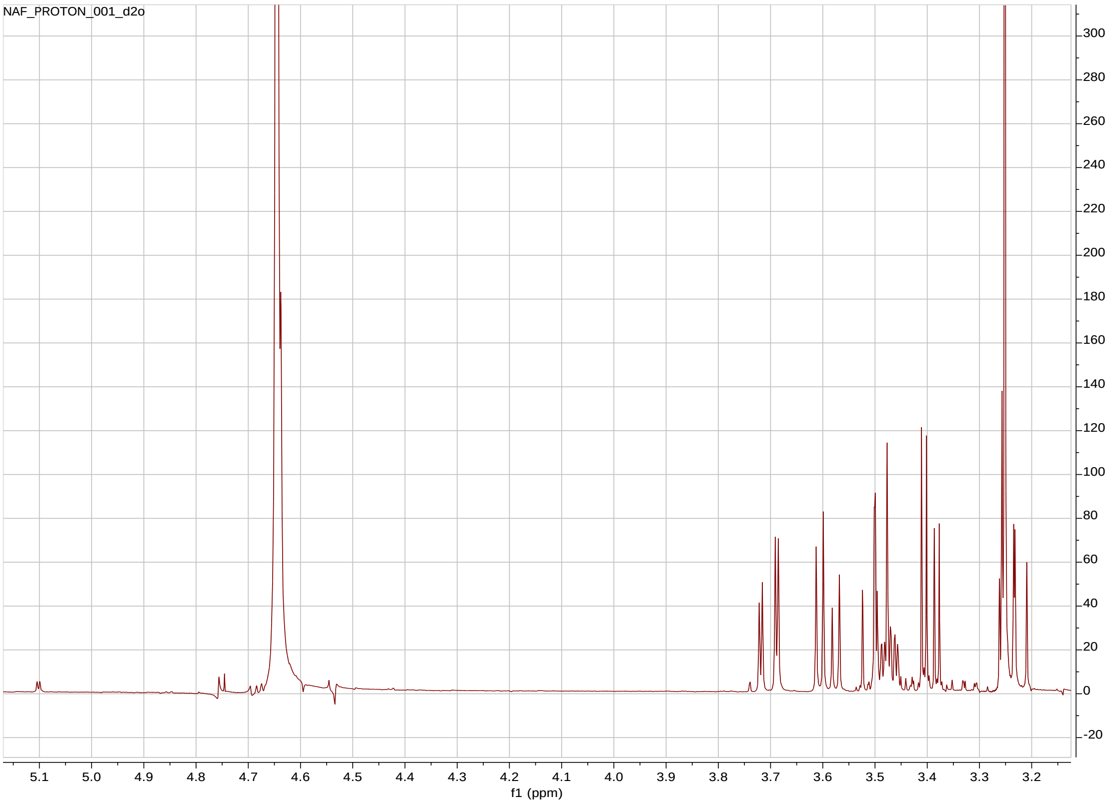

Figure 9: ^{1}H-NMR on E6 in D2O.

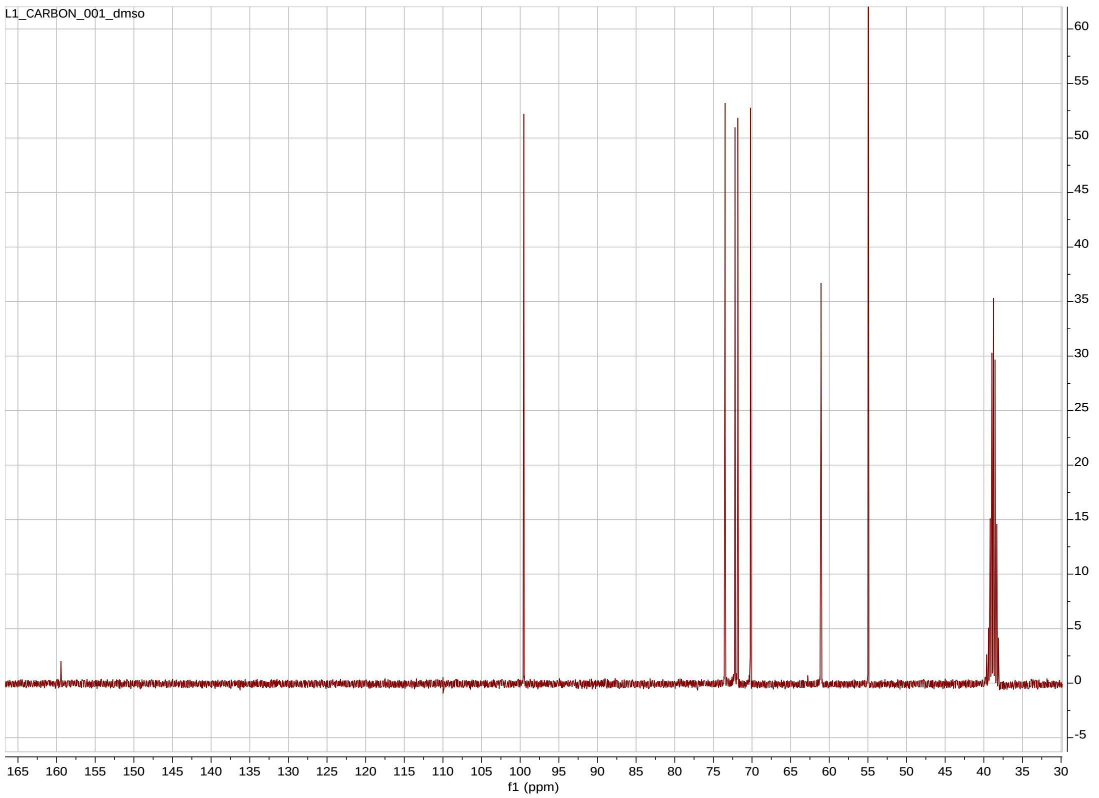

Figure 10: ^{13}C-NMR on E8 in DMSO.

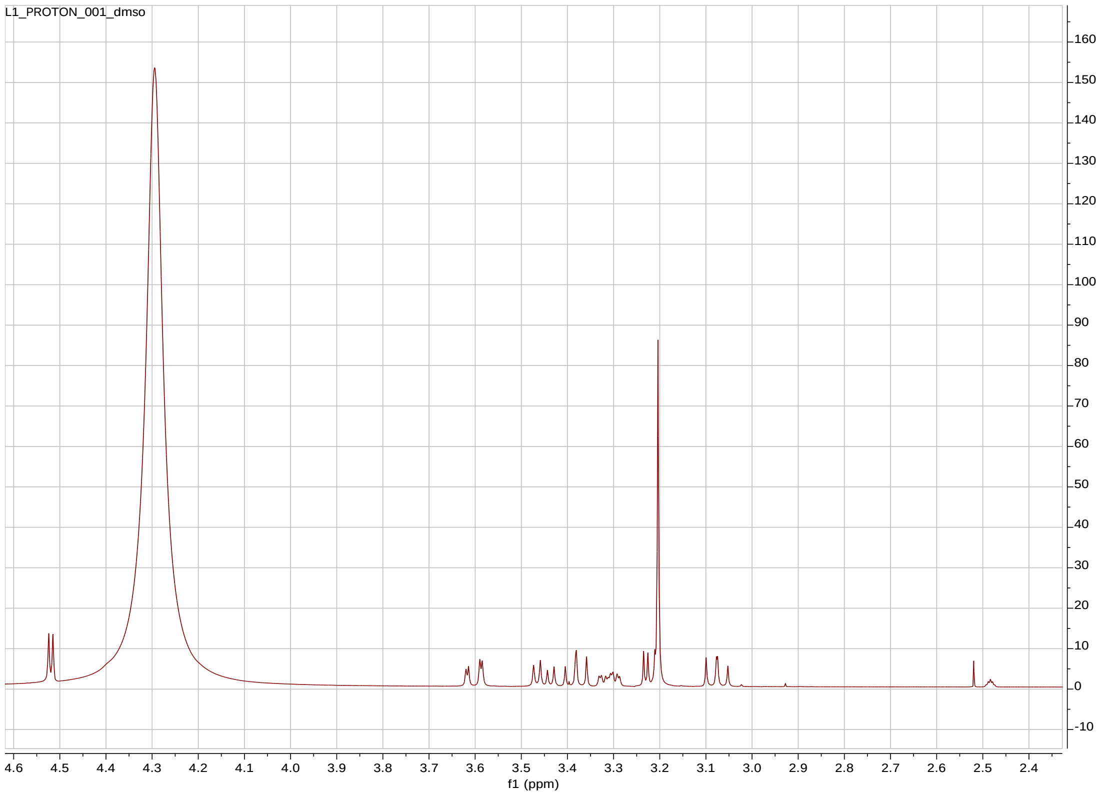

Figure 11: Zoomed in ^{1}H-NMR on E8 in DMSO.

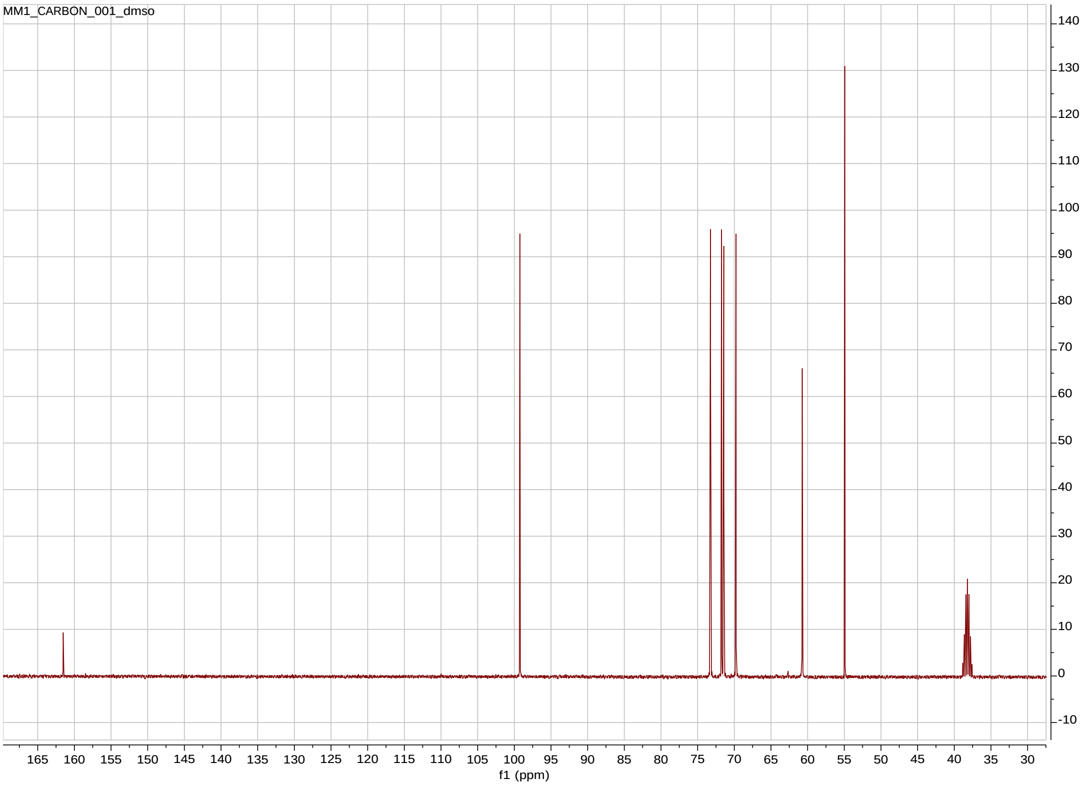

Figure 12: ^{13}C-NMR on E9 in DMSO.

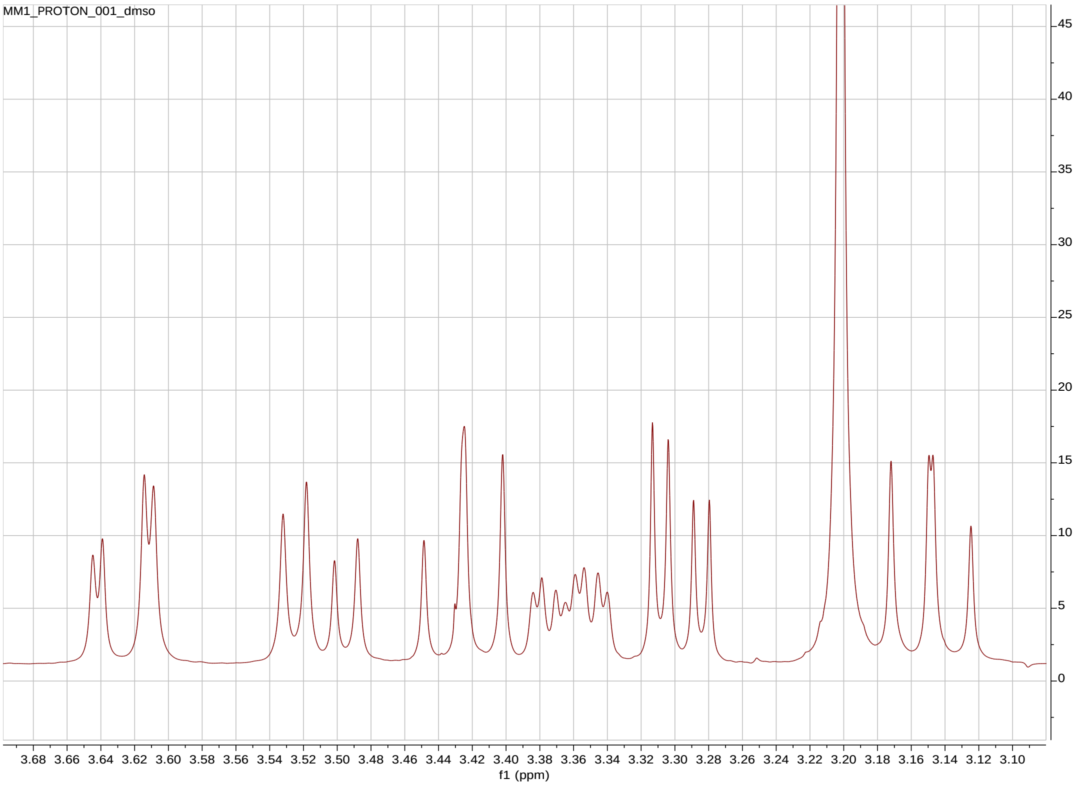

Figure 13: Zoomed in ^{1}H-NMR on E9 in DMSO.

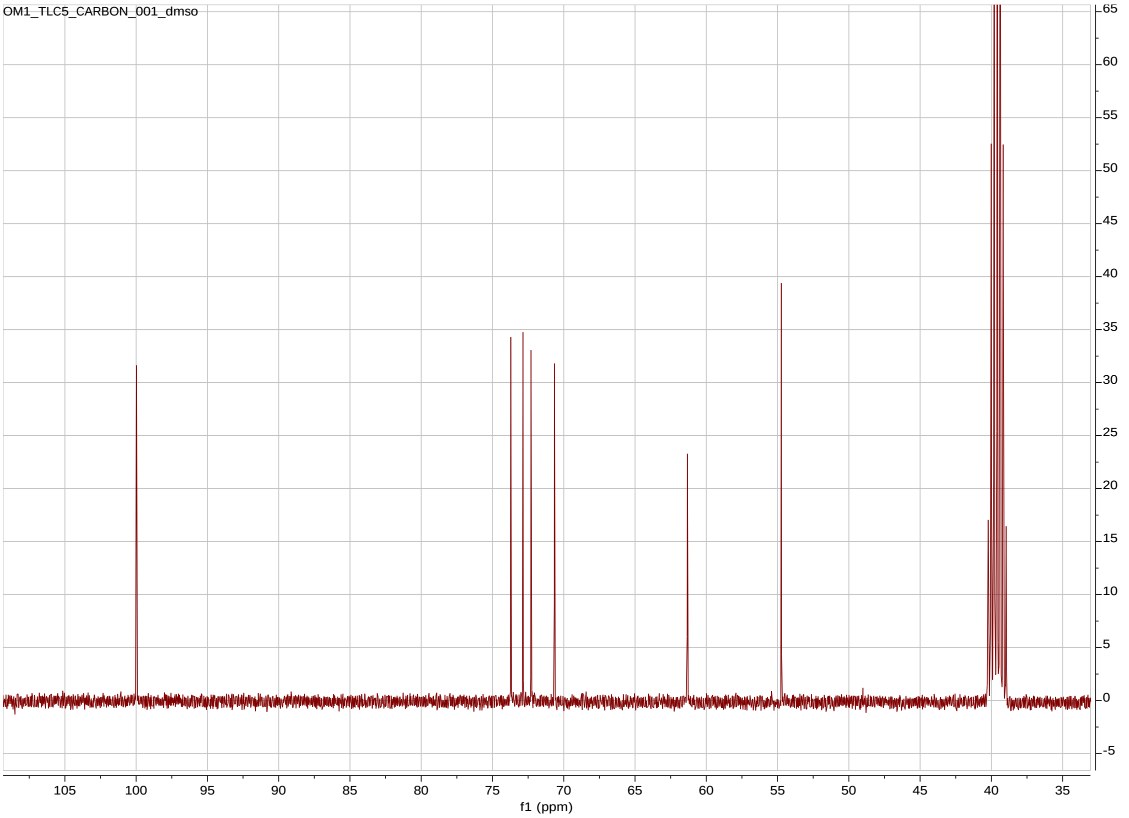

Figure 14: Zoomed in ^{13}C-NMR on E12 flash-fraction 5, in DMSO.

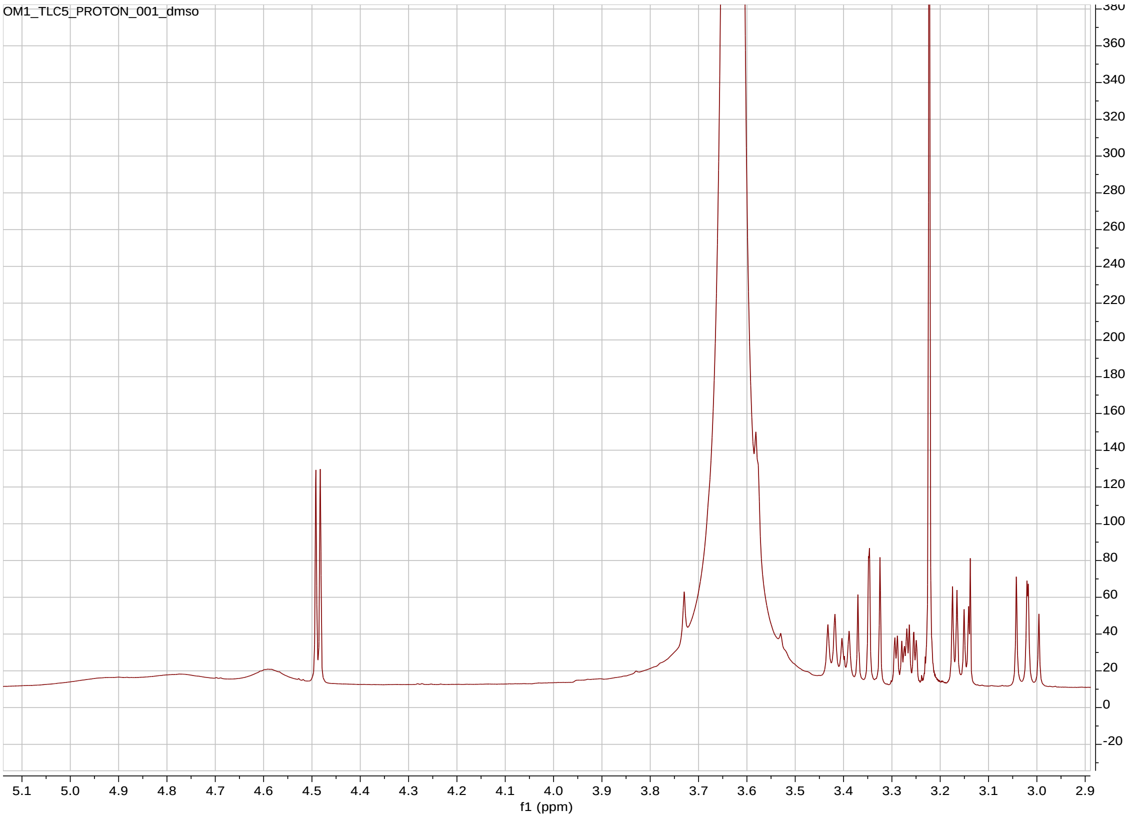

Figure 15: Zoomed in ^{1}H-NMR on E12 flash-fraction 5, in DMSO.

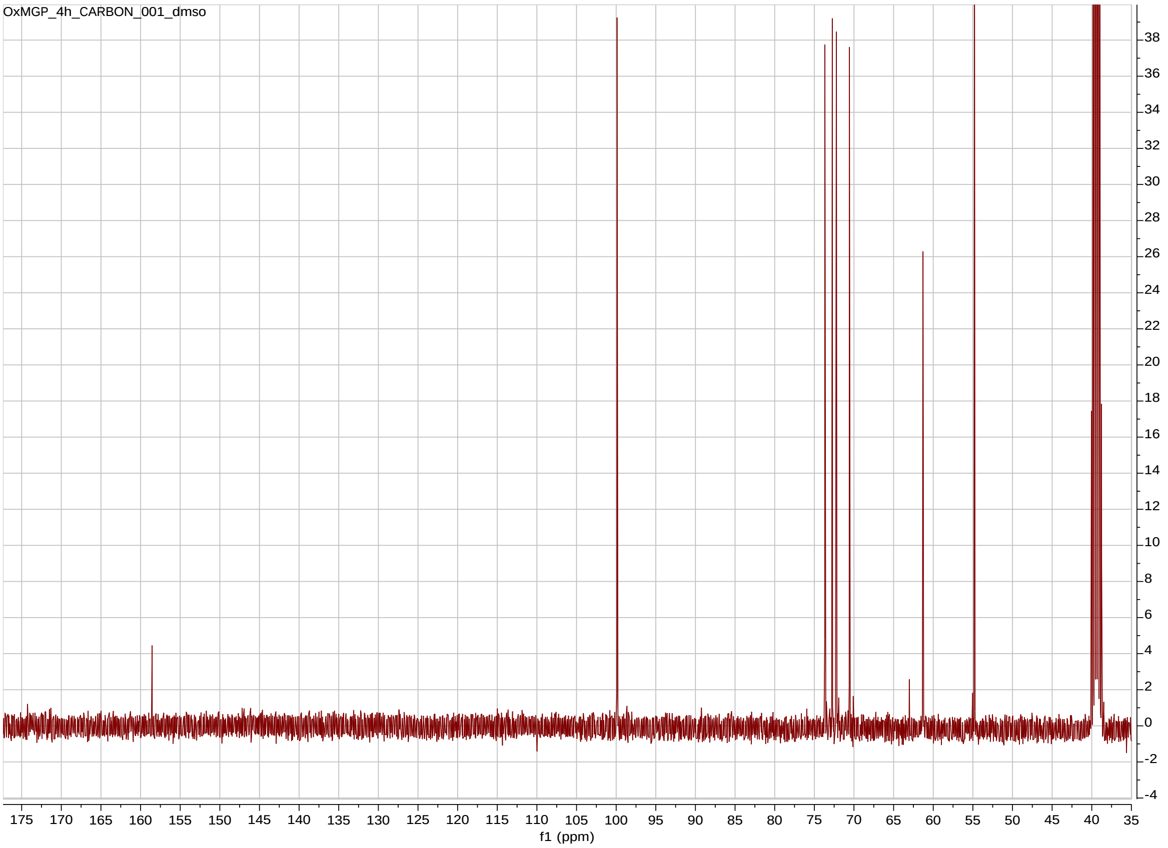

Figure 16: ^{13}**C-NMR on E13 in DMSO.**

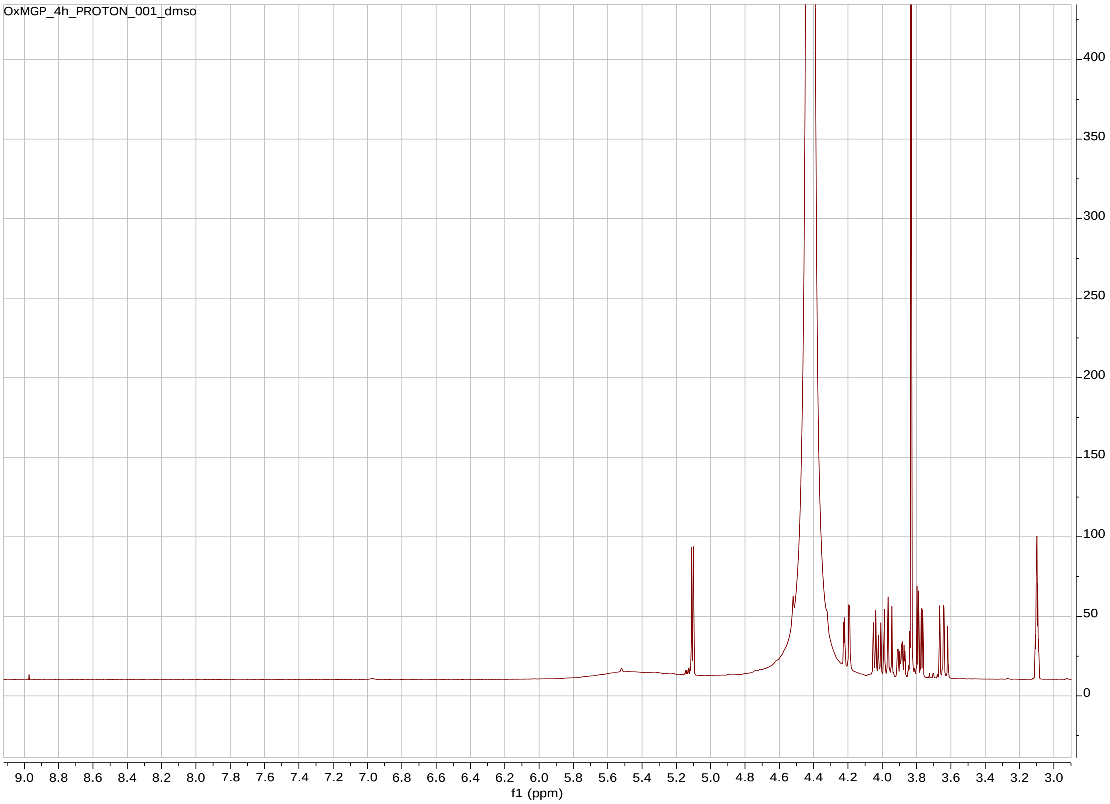

Figure 17: ^{1}**H-NMR on E13 in DMSO.**

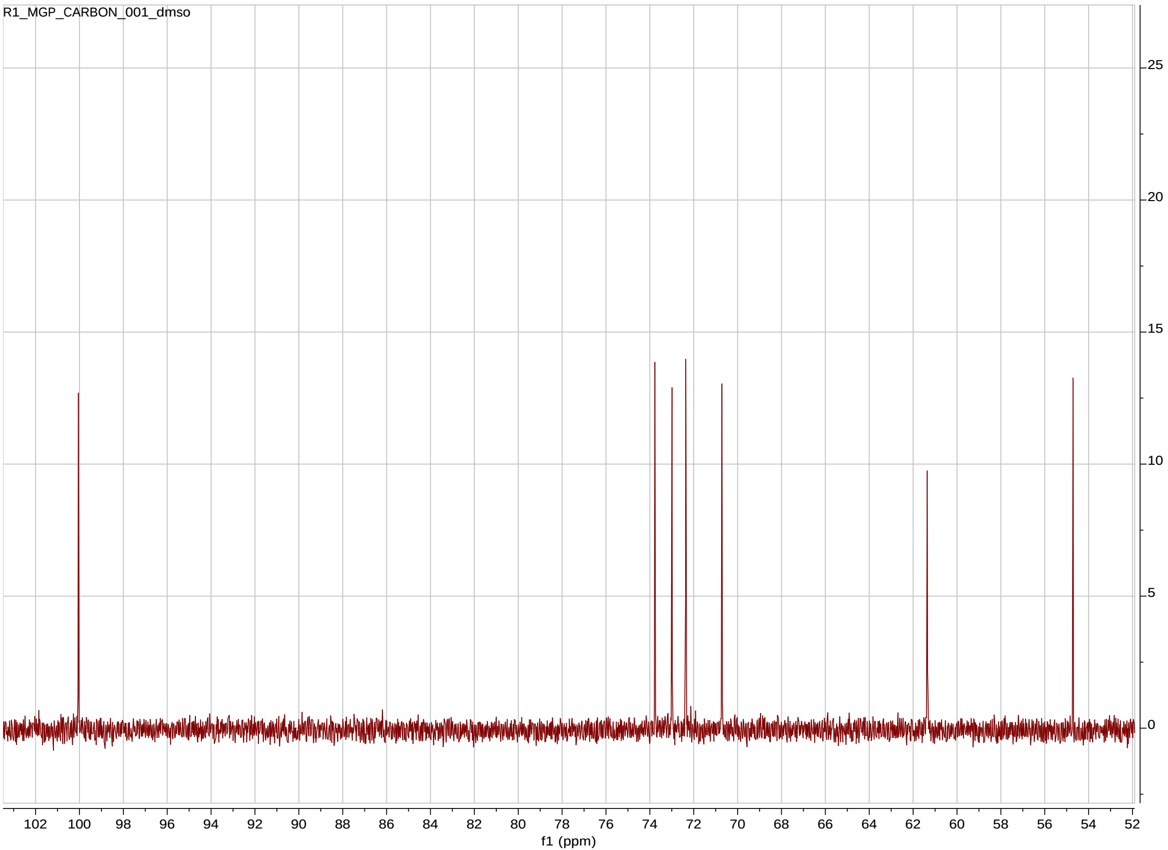

Figure 18: ^{13}C-NMR on R1 in DMSO

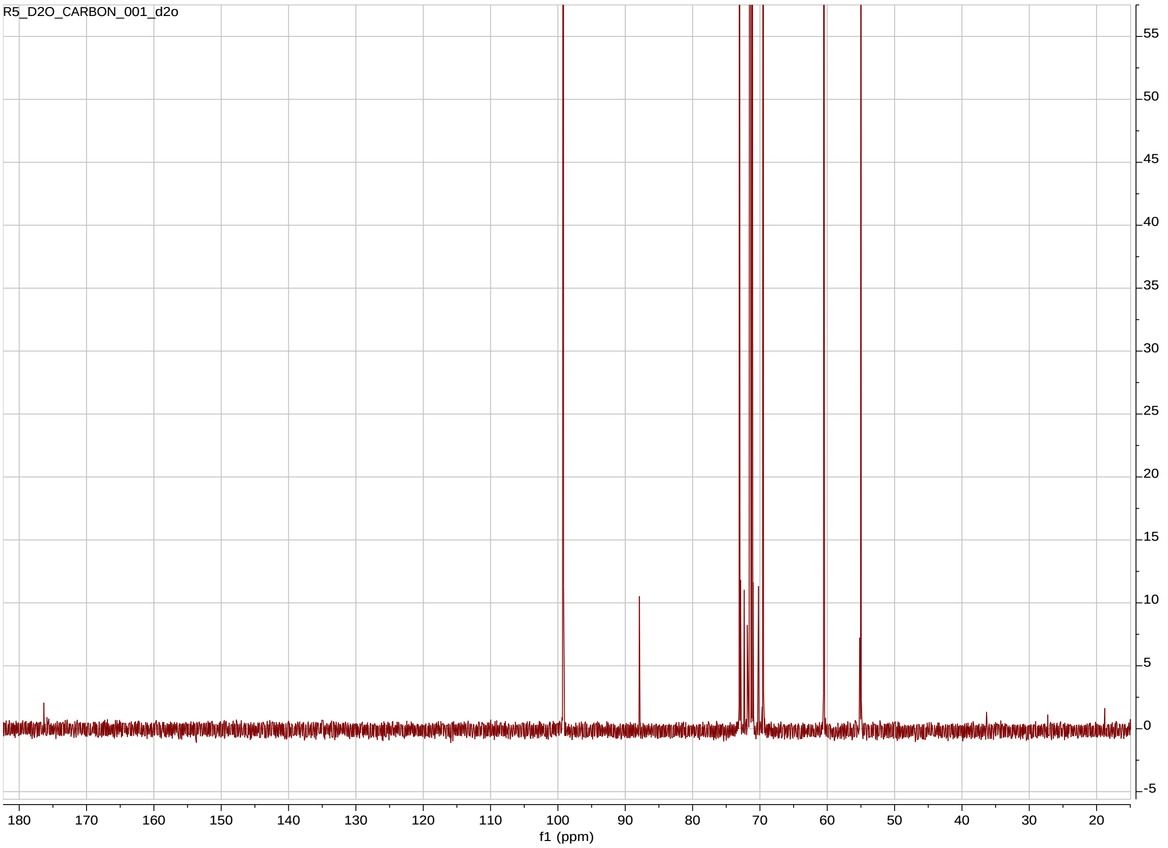

Figure 19: ^{13}C-NMR on R5 in D2O, showing an oxidation peak at 177 ppm.

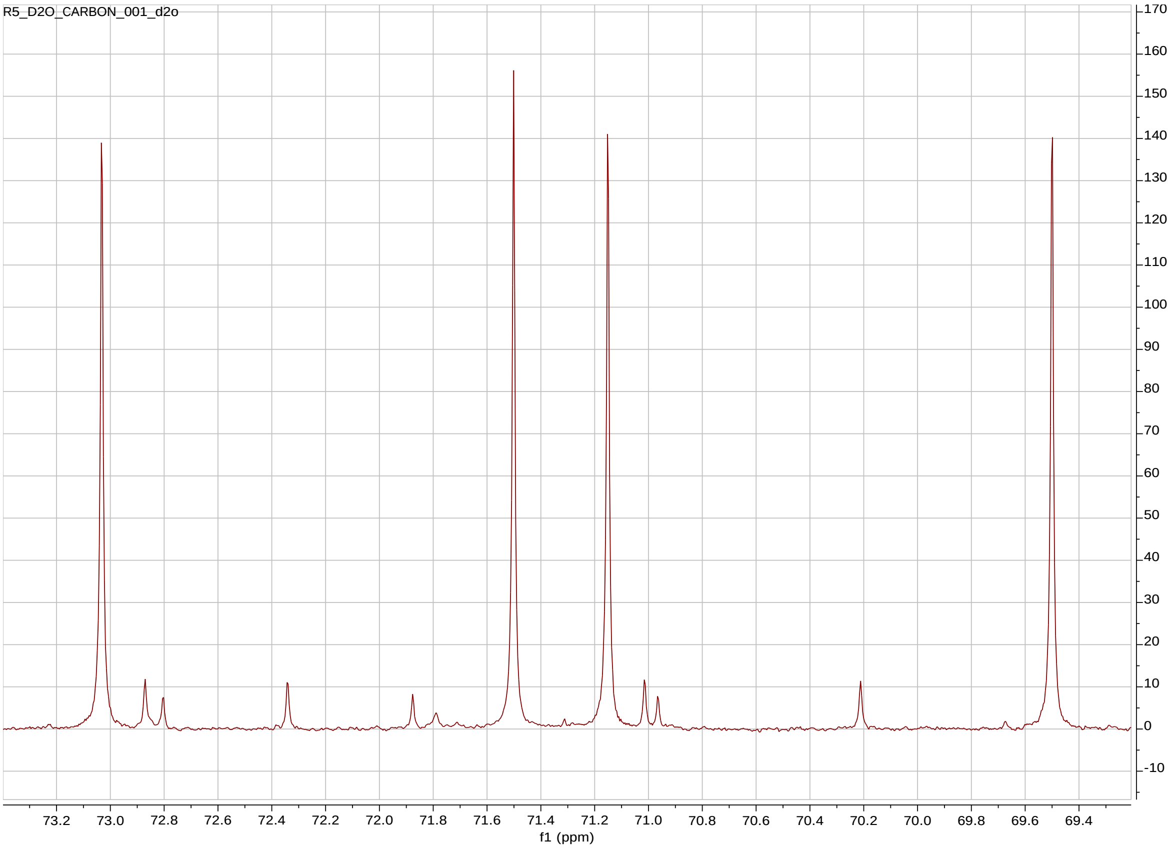

Figure 20: ^{13}C-NMR on R5 In D2O, showing many small new peaks.

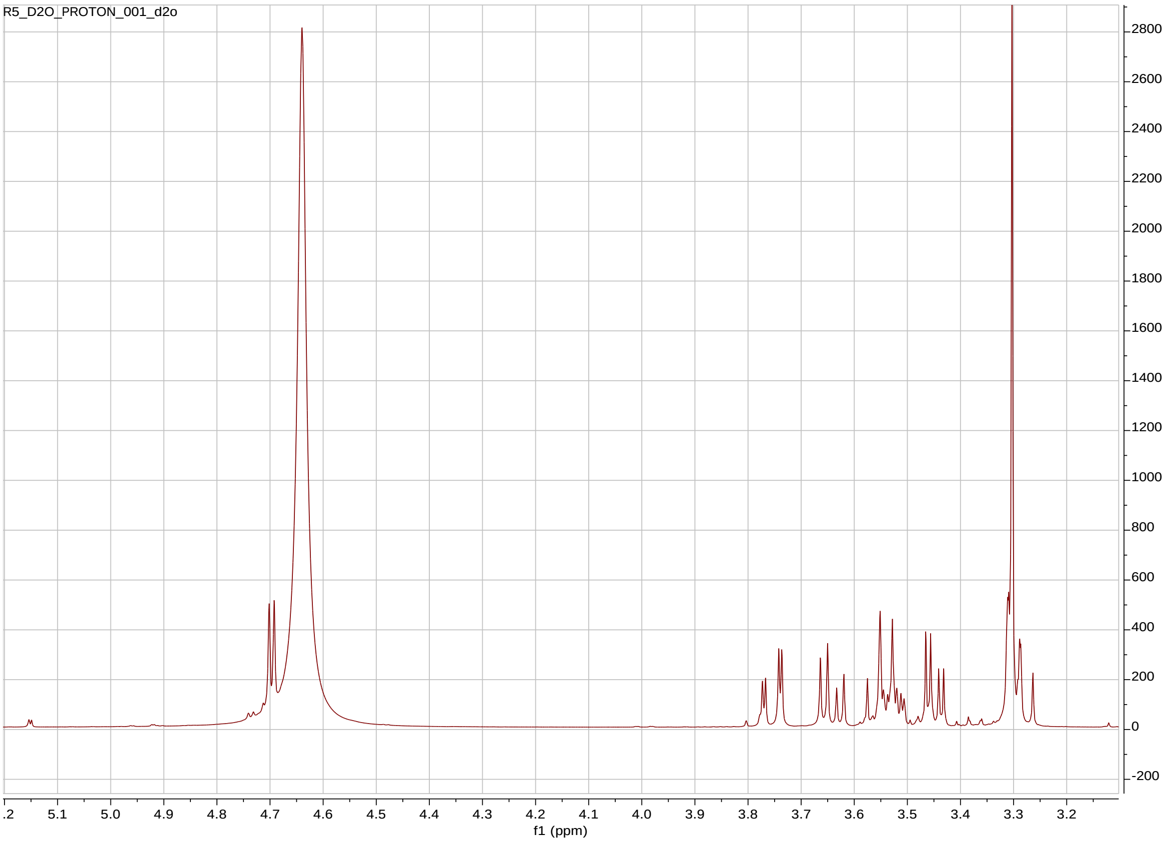

Figure 21: ^{1}H NMR for R5.

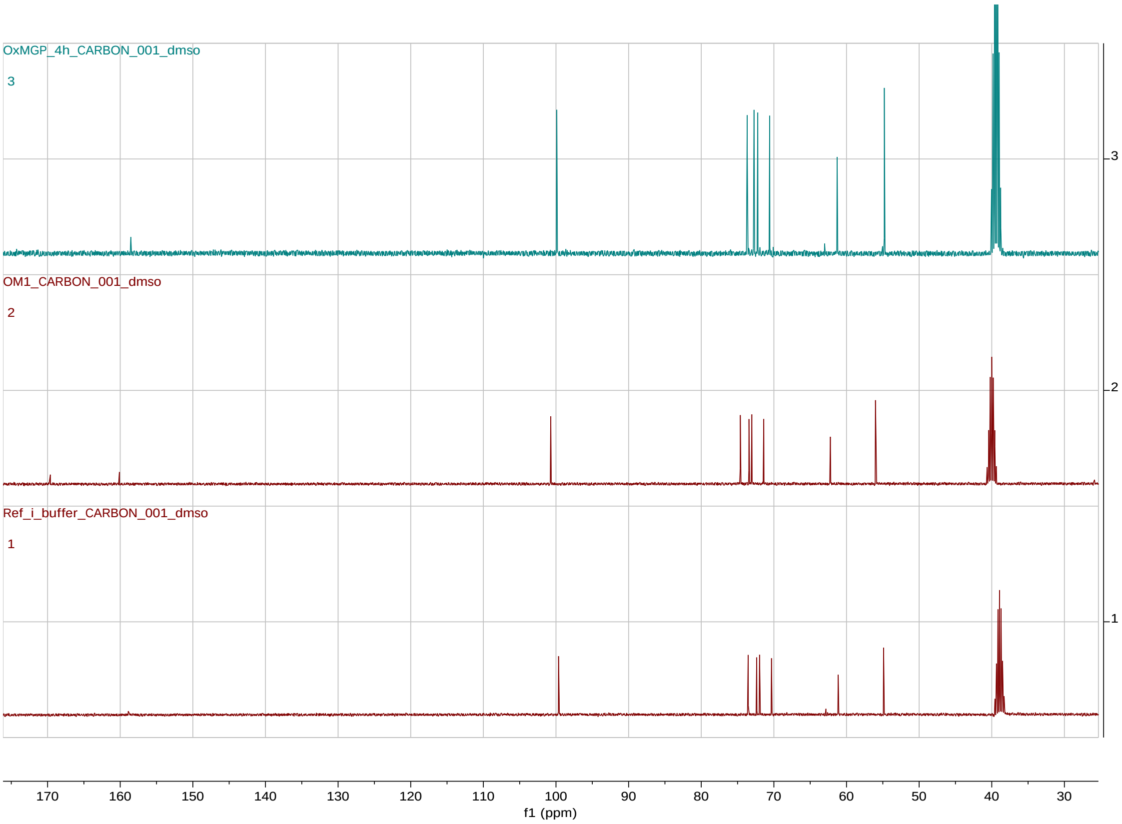

Figure 22: Comparison spectras of ^{13}C-NMR on E13 and E12 with reference, showing an oxidation peak at 170 ppm for E12 only.

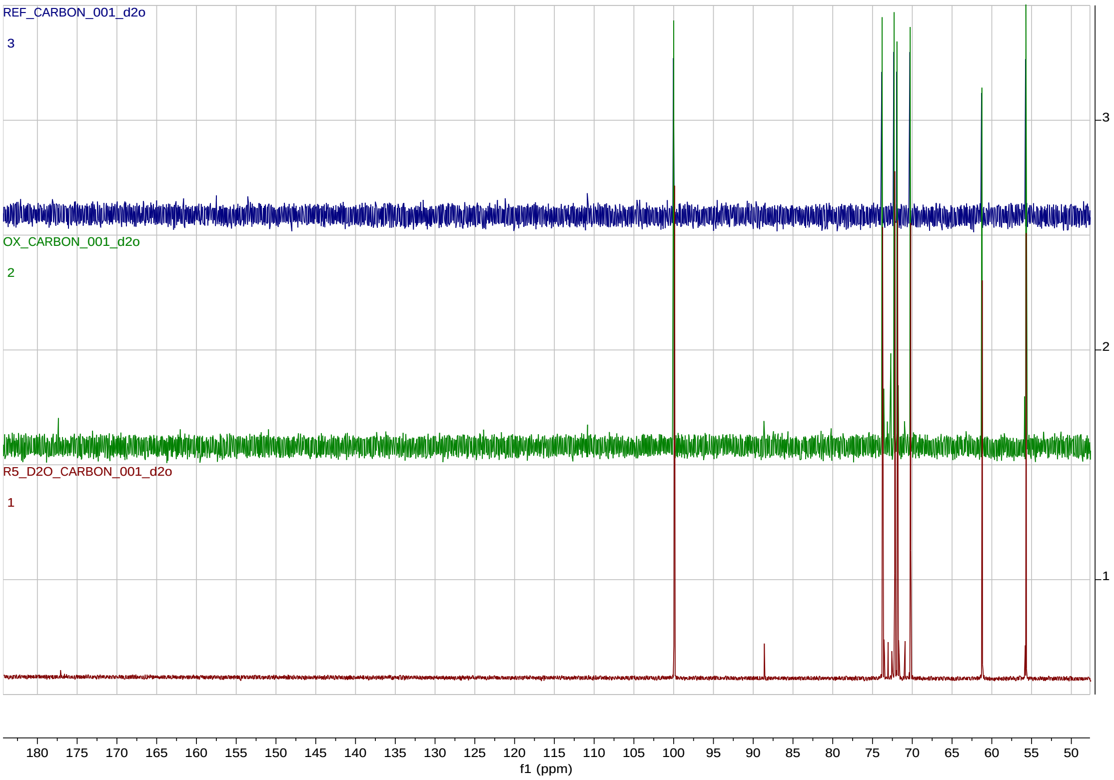

Figure 23: Comparison spectras of ^{13}C-NMR on reference, E4 and R5, showing an oxidation peak at 177 ppm and also many new peaks in the lower area of 70-90 ppm, for the oxidized samples.

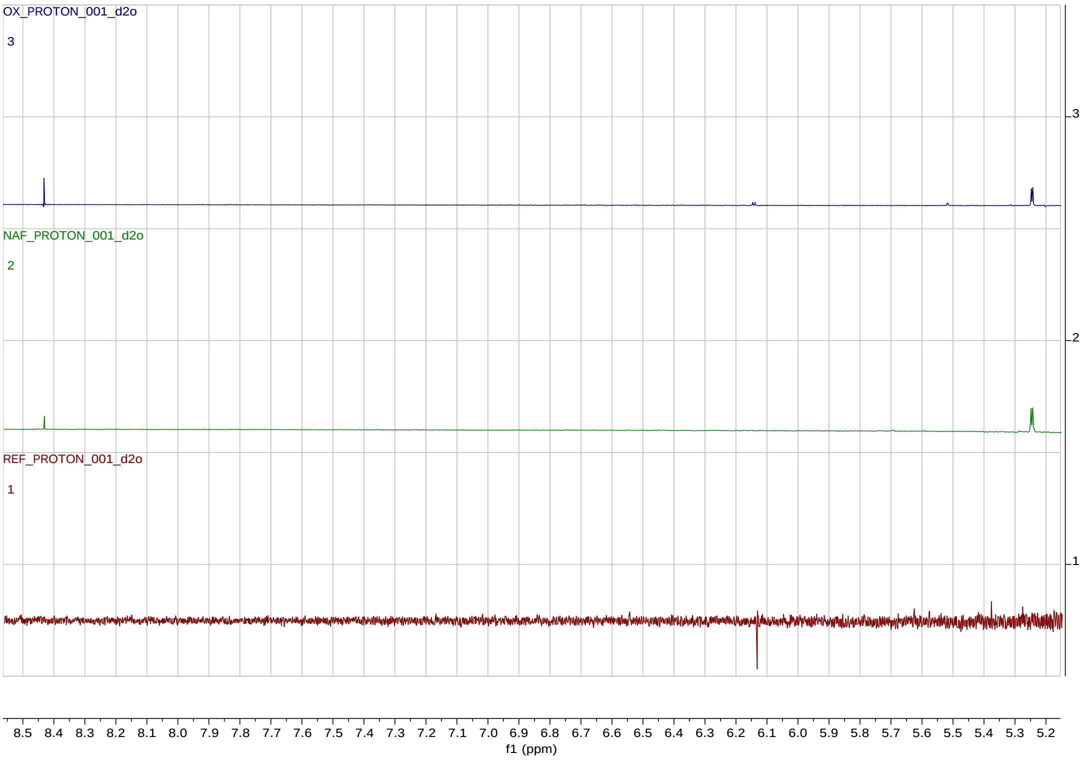

Figure 24: Comparison of ^{1}H NMR for E4 and E6 with reference, showing a new peak at 8.43 ppm.